January 2009

Aggregation & Localization of a Disease-Associated Prion Protein (PrP) Mutant

Andrea Rhonda Medrano
Washington University in St. Louis

WASHINGTON UNIVERSITY SCHOOL OF MEDICINE

Division of Biology and Biomedical Sciences

Molecular Genetics and Genomics

Dissertation Examination Committee:
David Harris, MD, PhD, Chair
Guojun Bu, PhD
Mark Goldberg, MD
Phyllis Hanson, PhD
James Skeath, PhD
Heather True-Krob, PhD

AGGREGATION AND LOCALIZATION OF A DISEASE-ASSOCIATED PRION

PROTEIN MUTANT

by

Andrea Rhonda Zaragoza Medrano

A dissertation presented to the
Graduate School of Arts and Sciences
of Washington University in
partial fulfillment of the
requirements for the degree
of Doctor of Philosophy

August 2009

Saint Louis, Missouri

ACKNOWLEDGEMENTS

Behind every success story is a team of people whose encouragement and support are so crucial that without them, success may not have been realized. The completion of my graduate work is no exception, and I would like to thank the many people who cheered me on when I was frustrated with experiments and who celebrated with me each milestone of progress.

First, to the One who created the world. Science is beautiful. Second, to my parents, Ben and Rhoda Medrano, who fostered my curiosity at a young age by buying my siblings and me a complete set of the Encyclopedia Britannica and for giving me my first toy microscope. Third, to my siblings BJ, Mika, Jackie, & Robert, along with my in-laws Caroline and Joe, who by conversation and by company made me laugh and reminded me that school isn't everything.

I would also like to thank my roommates through the years: Elizabeth Sitati, Courtney Cannon, Evelyne Mayer, and especially Jax, for making home a welcoming place to relax with friends after hard days at the lab. Thanks also to the many friends at WashU and the CSC who helped me balance life with a good dose of fun throughout the years. Thanks also to my new family-in-law, especially Joe & Sharon Behlmann, for being behind me all the way and for encouraging studiousness by giving the gift of an espresso machine, which greatly helped me through the day.

Special thanks to David Harris, for being not only a great boss, but also a great mentor. Your didactic approach to students helped me learn how to navigate the research field, and from your example I picked up a few things about what it takes to be a good teacher for others. Thanks.

Thanks also to the rest of the Harris lab 'family' that have made work an exceptionally positive place to be, people-wise. To Cheryl Adles, our 'lab mom,' who shows support for us in lab and in life. To the post-docs who I relied on for endless technical assistance and intellectual direction—Emiliano Biasini, Aimin Li, Rich Stewart, Leanne Stewart, Tania Massignan, and more recently Ursula Unterberger and Oriol Nicolas—thank you! Thanks also to Cheryl and Su Deng for amazing work keeping the lab running extremely efficiently, we could not do what we do without you. Many, many thanks to my fellow graduate students in the lab: Laura Westergard, Jessie Schepker, Isaac Solomon, and PhD grads Sami Barmada and Heather Christensen, for all the encouragement and understanding that only other graduate students can offer. The people in the Harris Lab have truly been an amazing group to work with, and I appreciate the opportunity to have learned and worked right alongside each person.

Lastly, to Josh Behlmann, my husband of three weeks, who I met at the Cell Biology retreat in '04. He has been with me on this ride for the last four years and knows more than anyone what it took for me to get here, because he was right beside me through it all. Thanks babe.

TABLE OF CONTENTS

LIST OF FIGURES

Chapter 1: Introduction

Chapter 2: GFP-tagged mutant prion protein forms intra-axonal aggregates in transgenic mice

Chapter 3: The role of the GPI anchor in the cellular behavior of a disease-associated familial prion protein mutant

Chapter 4: Discussion

Appendix 1: WT PrP-EGFP does not bind PG14 aggregates

Appendix 2: WT PrP-EGFP is resistant to conversion to PrP^{Sc}

Appendix 3: PrP-EGFP axonal transport studies

LIST OF TABLES

CHAPTER 1

Introduction

1.1 Prion Protein (PrP) & Disease

Structural rearrangement or genetic mutation of the cellular prion protein (PrP^C) is implicated in several human diseases, including kuru, Creutzfeldt-Jakob Disease (CJD), Fatal Familial Insomnia (FFI), and Gerstman-Straussler-Sheinker disease (GSS). These neurological disorders are pathologically characterized by intracerebral spongiform change, neuronal loss, PrP deposition, and astrogliosis (Figure 1). Dementia and ataxia are present as general features in all of these disorders, with each disease exhibiting distinctive clinical markers. Symptoms for CJD include memory loss, weakness, involuntary muscle contraction or muscle paralysis, and pseudo-periodic discharges on electroencephalogram. GSS patients display many of the same clinical features as CJD, but are defined neuropathologically by widespread multicentric amyloid plaques (Collins *et al.* 2001). FFI patients are marked by severe insomnia, hallucinogenic episodes, and a strong family history of the same disease (Schenkein and Montagna 2006).

Prion diseases extend to the animal domain, and are significant in light of the possible transmissibility of these diseases into humans. Sheep, cattle, elk, rodents, and non-human primates are also affected by prion disorders, which are grouped under the title of transmissible spongiform encephalopathies (TSEs). The most newsworthy example of transmission in recent decades includes the Bovine Spongiform Encephalopathy (BSE), or Mad Cow Disease, epidemic in England in the mid-1990's. A new variant of CJD was introduced into the human population by ingestion of BSE-infected meat, stimulating drastic modifications in the practice of large-scale cattle production and the governmental safety policies and regulations on the beef industry not only in Britain, but across the globe. More recently, chronic wasting disease (CWD) has
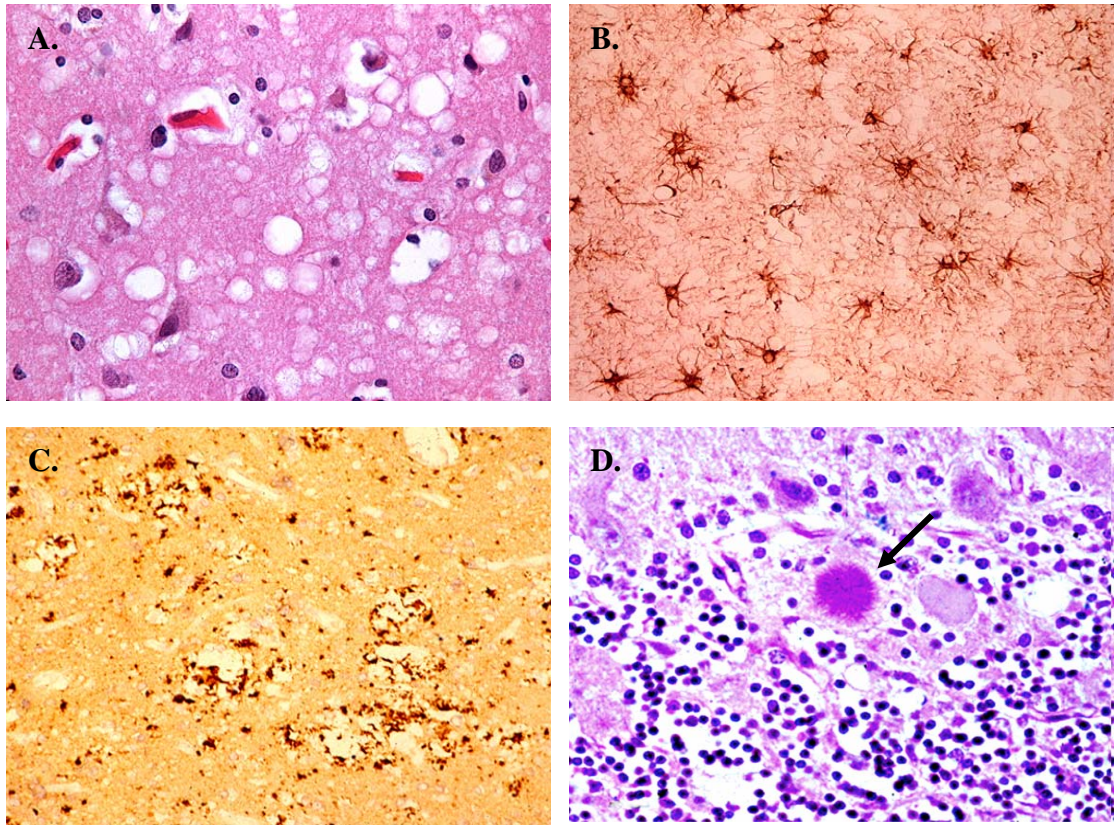
2

Figure 1. Prion Disease Neuropathology. Brain sections from a CJD patient reveal the typical hallmarks of prion disease, including spongiform degeneration (A), glial cell proliferation (B), and PrP deposition (C). In some cases, like kuru, PrP may also form florid plaques (D, arrow).

been detected in elk and deer in the Midwest and northern regions of the United States, generating a healthy concern amongst hunters, venison eaters, and the Center for Disease Control, who fear consumption of meat from infected game may expose humans to yet another variant of prion disease.

In addition to digestion, prion exposure may also occur iatrogenically. Several cases of CJD transmission have occurred through human growth hormone transplants, dura mater grafts, and infected cranio-surgical instruments. Clinical reports from the UK and France have demonstrated the development of prion disease in human patients who received blood transfusions from subclinical CJD patients (Wroe *et al.* 2006; Turner and Ludlam 2009), confirming previous reports in animals that infectivity is possible via blood transfer (Mathiason *et al.* 2006; Houston *et al.* 2008).

Prion disease acquired by ingestion or exposure to infected material account for only a small fraction of known prion disease patients. Many cases cannot be traced to a source of infectivity and are thought to occur spontaneously, with one person per million per year diagnosed with prion disease. Sporadic cases of prion disorders account for the majority of prion illness, and predominantly affect those in the sixth or seventh decade of life. The remaining number of prion disease cases are attributed to inheritance of autosomal dominant mutations in the PrP gene, PRNP, located on human chromosome 21. Over 50 distinct mutations have been identified as causative agents of familial CJD (fCJD), FFI, and GSS.

All prion diseases are associated with aberrations in the prion protein (PrP). Infectious and sporadic prion diseases are correlated with the post-translational conversion of cellular prion protein (PrP^C) to an alternate, more β-sheet rich

conformation, named scrapie prion protein (PrP^{Sc}), which has the ability to bind PrP^C molecules and replicate itself by conferring its rogue conformation onto endogenous PrP^C templates. In familial disorders, it is speculated that PrP mutants are inherently predisposed to adopt pathogenic PrP^{Sc}-like conformations, which induce spontaneous neurodegenerative disease.

Despite intense investigation since the discovery of PrP's association with infectious disease in the 1980's (Prusiner 1982; Prusiner *et al.* 1982), the mechanisms defining prion toxicity are ambiguous, whether the disorder is acquired sporadically, through infectious material, or through genetic inheritance. Thus, attempts to find effective therapeutics for prion disorders are limited. The anti-malarial quinacrine held great potential when studies demonstrated inhibition of PrP^{Sc} conversion in scrapie-infected neuroblastoma cells (Korth *et al.* 2001; Klingenstein *et al.* 2006) and in mice (Spilman *et al.* 2008). When applied to patients, the drug was able to restore voluntary movement in response to verbal cues in some patients during the first month of enteric administration (Nakajima *et al.* 2004). Although quinacrine is tolerated reasonably well, continued treatment fails to significantly altar clinical progression in patients affected with sporadic, iatrogenic, or familial prion diseases (Collinge *et al.* 2009). Alternative candidates for therapy include pentosan polysulphate and flupirtine, but the impact of these at the patient level have not been robust (Gilch *et al.* 2008). Given the severe lack of therapeutics for prion diseases, further studies are necessary to dissect the cellular, molecular, and neurophysiological components involved with prion pathogenesis. Investigations into prion disorders may prove insightful for other more common neurodegenerative diseases, such as Alzheimer's, Parkinson's, and Huntington's Disease,

given that all share the common characteristic of protein aggregation associated with dementia and kinetic impairment.

1.2 The cellular prion protein (PrP^C)

A. Synthesis & Cellular Trafficking

PrP^C expression begins early in embyrogenesis, and is expressed in many tissue types, including heart, kidney, and testes. The highest expression levels are found within the central nervous system in adults, specifically in neuronal cells. Murine PrP^C is synthesized as a 254 amino acid polypeptide by ribosomal translation (Figure 2A). Upon translocation into the endoplasmic reticulum, both the amino-terminal signal peptide and carboxy-terminal GPI attachment sequence are cleaved. A GPI anchor is subsequently attached while high-mannose carbohydrate structures are appended onto two asparagines that serve as N-linked glycosylation sites. These underdeveloped oligosaccharide chains are sensitive to Endoglycosidase H until further modification and processing. In the Golgi, mannose structures are trimmed, and fructose and sialic acid moieties are added to yield more complex oligosaccharide branches (Caughey *et al.* 1989). Over 50 unique antennary structures have been associated with PrP^C, and these are sensitive to deglycosylation by enzyme PNGase F (Rudd *et al.* 1999; Stimson *et al.* 1999). The GPI anchor core structure is modified by addition of mannose, ethanolamine, and sialic acid residues, and is susceptible to cleavage when treated with bacterial enzyme phosphatidylinositol-specific phospholipase C (PIPLC) (Stahl *et al.* 1992). PrP^C is then organized into cholesterol and sphingolipid-rich detergent-resistant membrane (DRM) microdomains, or "lipid rafts" (Taylor and Hooper 2006). PrP transits via the secretory

pathway to the plasma membrane, where the protein establishes itself on the extracellular face of the lipid bilayer, attached by its GPI anchor. After delivery to the surface, PrP^C can transfer from DRMs to clathrin-coated pits, where it is constitutively endocytosed and recycled back onto the plasma membrane (Shyng *et al.* 1993).

The mature PrP protein contains a flexible N-terminal end, which encompasses a series of five proline- and glycine-rich repeating octapeptide motifs that are able to bind copper (Figure 2B). The C-terminal end of PrP is globular in structure, and contains a highly conserved hydrophobic segment, two glycosylation sites, and a carboxy-terminal glycophosphatidylinositol (GPI) anchor. NMR studies demonstrate that the globular domain also carries two anti-parallel β-sheet sub-structures and three α-helical arrangements (Riek *et al.* 1997; Zahn *et al.* 2000). A disulfide bond linking amino acids 178 and 213 further enhances structural stability of the C-terminal end.

B. PrP Function

PrP is a membrane-bound glycoprotein that can be found in almost all vertebrate species, and prion-like proteins that have similar sequence homology have been identified in several species of birds and zebrafish (Gabriel *et al.* 1992; Miesbauer *et al.* 2006). Across species, PrP displays comparable structural features, including repeating motifs able to bind copper, N-linked glycosylation, α-helical and β-sheet arrangements, and a notably well-conserved hydrophobic domain (Cotto *et al.* 2005; Shields and Franklin 2007; Blinov *et al.* 2009). Together, these observations suggest that the prion protein provides a significant function that merits both genetic and structural conservation through evolution.

A.

B.
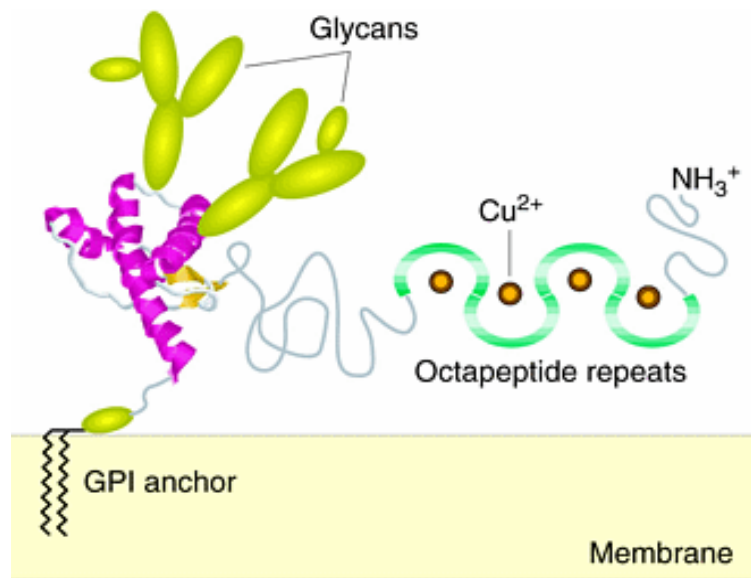
Figure 2. Cellular Prion Protein (PrP^C). (A) The structural features of murine PrP^C include an N-terminal signal peptide (white), five endogenous octapeptide repeats (yellow), two N-linked glycosylation sites (CHO), a disulfide bond (S-S), and a C-terminal end GPI anchor attachment signal (orange.) Numbers indicate amino acid positions. (B) A PrP^C protein schematic reveals that the N-terminal portion of the protein, which is able to bind copper, is mostly flexible. The C-terminal end forms a globular structure composed of three alpha helices (pink) and two beta sheet strands (yellow). The GPI anchor (black) is embedded at the extracellular face of the plasma membrane.

PrP$^{o/o}$ Knockout Mice

In order to dissect the physiological purpose of PrP *in vivo*, several lines of PrP knockout mice have been independently generated. Genetic ablation of coding sequences within the open reading frame (ORF) of the murine PrP gene, *Prn-p*, has been accomplished by homologous recombination (Bueler *et al.* 1992; Manson *et al.* 1994). ORF disruption led to abolition of mRNA transcripts, which completely abrogated prion protein synthesis in mice. Interestingly, mice homozygous for the inactivated gene (*Prn-p$^{o/o}$*) were born in expected Mendelian ratios, completed development with no grossly abnormal physical defects, and continued to live normal life spans without any indication of prion disease. Additionally, null mice performed equally well compared with their wild-type counterparts when challenged with a battery of neurological tests for behavior, spatial learning, and memory (Bueler *et al.* 1992; Lipp *et al.* 1998). Collectively, these studies strongly argue that PrP holds a non-essential function in development or adulthood. It was speculated that redundant proteins could compensate for the lack of PrP at the early stages of biogenesis and then uphold this function into adulthood. Mallucci and colleagues utilized Cre-LoxP technology to test this theory and induced genetic *Prn-p* deletion in a time- and cell-specific manner, abrogating PrP protein synthesis in neurons of mice only at adulthood (Mallucci *et al.* 2002). The post-natal deletion strategy resulted in no significant neurophysiological changes, arguing against the idea that independent factors substitute for, and then sustain, PrP function (Mallucci *et al.* 2002).

Several additional lines of PrP$^{o/o}$ mice were generated by deleting an extended stretch of DNA that encompassed not only the ORF but portions of the flanking regions

as well. These mice also developed normally, but displayed severe ataxia and Purkinje

cell loss as they aged (Sakaguchi *et al.* 1996). It was later found that neurodegeneration

in these mice was not due to loss of PrP, but of upregulation of the *Prnd* gene that lies

downstream of *Prn-p* (Moore *et al.* 1999; Rossi *et al.* 2001). As a result of the extended

genetic deletion, *Prnd* expression was placed in control of the *Prn-p* promoter, leading to

novel expression of PrP-like protein Doppel in brain and other tissues where PrP is

detected. Doppel is structurally similar to the C-terminal end of PrP, and is usually

expressed mainly in the testes. When expressed in brain, it is capable of producing

spontaneous neurodegeneration in transgenic mice. Thus, expression of Doppel, and not

loss of PrP, was the cause of disease in these mice. Because several lines of PrP$^{o/o}$ mice

carrying the shorter ORF deletion show a lack of any grossly abnormal phenotype, it is

reasonable to conclude that PrP holds no essential function for development or viability.

Putative Functions for PrP

There is wide-ranging evidence implicating the involvement of PrP in a variety of

biological activities, including neuronal defense against apoptosis, cellular protection

from oxidative stress, copper homeostasis, transmembrane signaling, and synaptic

operation. PrP function in each of these pathways has been studied *in vivo* in knockout

and transgenic mice and *in vitro* in primary neurons and immortalized cell culture

systems. A general overview of investigations is provided below, highlighting that the

strongest evidence thus far connects PrP function with a role in neuroprotectivity and

synaptic activity.

In several cell culture systems, PrP expression protects against pro-apoptotic cellular stresses. In human primary neurons and in yeast, cells microinjected or transfected with a plasmid encoding pro-apoptotic factor Bax succumbed to cell death (Bounhar *et al.* 2001; Li and Harris 2005). However, PrP expression rescued cells from Bax-mediated cell death in both cell models, in a manner that was found to be independent of anti-apoptotic factor Bcl-2 in yeast (Bounhar *et al.* 2006). Additional protective effects of PrP expression have been reported in MCF-7 cells treated with apoptosis-inducing tumor necrosis factor (TNF-α) (Diarra-Mehrpour *et al.* 2004), and in immortalized hippocampal neurons susceptible to serum deprivation-triggered cell death (Kuwahara *et al.* 1999; Sakudo *et al.* 2003). Although these latter studies reported robust anti-apoptotic PrP activity, a more recent article attempting to reproduce these experiments showed only modest, if any, PrP-mediated rescue (Christensen and Harris 2008).

Indeed, the strongest arguments for PrP as a neuroprotective agent lie mainly in *in vivo* studies that demonstrate PrP alleviation from mutation-induced neurological prion disease. For example, Doppel mice (described above) spontaneously develop late-onset ataxia and Purkinje cell degeneration when expressed on a PrP-null background (Sakaguchi *et al.* 1996). These symptoms can be relieved by co-expression of WT PrP in a dose-dependent manner. Similarly, transgenic mice expressing PrP harboring large deletions at the N-terminus ("F35", Δ32-134) or within the highly conserved transmembrane domain ("ΔCR", Δ105-125) display severe ataxia, as well as cerebellar granule loss and white matter vacuolation (Shmerling *et al.* 1998; Li *et al.* 2007). Re-introduction of PrP by crossing transgenic animals with WT PrP^{+/+} mice significantly

11

delays disease onset and progression as well as neuropathological defects. PrP can also rescue effects from disease-associated PrP mutants in transgenic mice, such as GSS mutant P101L (Telling *et al.* 1996). Collectively, these examples reveal that WT PrP protects neurons at the cellular level and prevents mutation-induced toxicity.

Consistent with its localization at the cell surface, some evidence suggests that PrP^C acts as a receptor for transmembrane signaling. Although specific mechanisms of activation have not yet been detailed, antibody-mediated crosslinking of PrP^C was found to trigger tyrosine kinase fyn signaling, mainly at neurites, which lead to downstream activation of extracellular-regulated kinases (ERKs) and NADPH oxidase and the production of reactive oxidative species (ROS) (Mouillet-Richard *et al.* 2000; Schneider *et al.* 2003). Confirmation of fyn activation was demonstrated in studies showing that PrP binding with neuronal cell adhesion molecule (NCAM) led to fyn stimulation and PrP/NCAM-dependent neuritic outgrowth (Santuccione *et al.* 2005). Several other investigations have implicated PrP-induced signaling of several kinases, which was associated with neuronal development and survival in cultured neurons (Chen *et al.* 2003; Kanaani *et al.* 2005). Given that PrP lies entirely at the extracellular face of the lipid bilayer, one or more transmembrane adaptor proteins, such as NCAM, would presumably be necessary to fulfill this function. It is also speculated that PrP localization to lipid rafts may facilitate such interactions, as signal transduction molecules, such as Fyn and Src kinases, cluster within lipid rafts (Taylor and Hooper 2006).

Recent evidence implicates PrP as a mediator of cell-to-cell adhesion, either by itself or in conjunction with another factor. PrP-overexpressing neuroblastoma cells incubated in single cell suspension increased cation-independent aggregation, which was

disrupted by PIPLC-mediated PrP release from the cell surface and by PrP antibody preincubation (Mange *et al.* 2002). Additionally, PrP-null zebrafish are arrested in the gastrulation phase due to loss of embryonic cell adhesion. This phenotype can be rescued by expression of both zebrafish and mouse PrP, arguing for a conserved function in cell adhesion (Malaga-Trillo *et al.* 2009). Interactions with N-CAM may mediate this function (Schmitt-Ulms *et al.* 2001). Evidence for PrP involvement with cellular adhesion is preliminary, and the mechanisms underlying PrP-mediated cell-to-cell contact have yet to be elucidated.

Some data suggest that PrP may help regulate copper homeostasis, perhaps by acting as a receptor or transporter for cupric ions. The octapeptide repeat region of PrP contains histidine, and is able to bind up to four Cu^{2+} ions in a pH-dependent manner with an affinity as high as 0.1 nanomolar both *in vitro* and *in vivo* (Brown *et al.* 1997; Jackson *et al.* 2001; Kramer *et al.* 2001; Walter *et al.* 2006), with PrP residues 96 and 111 also acting as additional binding sites (Jackson *et al.* 2001). Copper binding causes conformational changes in the N-terminal tail of PrP and stimulates the exit of cell-surface PrP from lipid rafts and into clathrin-coated pits for endocytosis (Pauly and Harris 1998; Brown and Harris 2003; Taylor *et al.* 2005). In support for PrP regulation of metal ions, early investigations demonstrated a decrease in copper content within brains of $PrP^{o/o}$ mice (Brown *et al.* 1997; Herms *et al.* 1999). However, subsequent studies were unable to authenticate a significant correlation between cerebral copper activity and PrP expression level in transgenic mice (Waggoner *et al.* 2000). Further investigations have not yet yielded substantial evidence directly connecting PrP function with copper regulation.

Accumulating evidence suggests that PrP mediates synaptic development or transmission. Localization studies at the light and electron microscope level indicate that PrP is highly enriched along axonal tracts and in pre-synaptic terminals in developing and mature neurons *in vivo* (Moya *et al.* 2000; Laine *et al.* 2001; Ford *et al.* 2002; Sales *et al.* 2002). PrP can also be transported via fast axonal transport mechanisms in the retrograde and anterograde directions (Borchelt *et al.* 1994; Rodolfo *et al.* 1999; Moya *et al.* 2004). In cell culture studies, exposure of rat hippocampal neurons to recombinant prion protein resulted in rapid polarization, axonal extension, and an increase in synapse formations (Kanaani *et al.* 2005), indicating PrP participation in synaptic development.

Several lines of evidence also exist associating PrP with synaptic maintenance. PrP crosslinking also modulates activity of several G protein-coupled serotonin receptors (Mouillet-Richard *et al.* 2005; Mouillet-Richard *et al.* 2007), suggesting that PrP may aid in serotonergic transmission (Schneider *et al.* 2003). Other examples indicating *in vivo* PrP involvement in neurophysiological regulation include the increase of glutamatergic transmission in hippocampi of PrP-overexpressing mice (Carleton *et al.* 2001) and disrupted calcium-activated potassium currents in PrP$^{o/o}$ hippocampus and in cerebellar Purkinje cells (Colling *et al.* 1996; Herms *et al.* 2001). More recently, it was also found that Alzheimer's disease-associated amyloid-beta oligomers can bind to PrP^{C} molecules, which then act as receptors mediating oligomer-induced synaptic dysfunction (Lauren *et al.* 2009). These data argue strongly for a PrP function regulating neuronal excitability at the synapse.

Subtle behavioral anomalies have been identified in PrP knockout mice, many of which correlate with abnormal neuronal physiology, thus indirectly supporting a role for

PrP in synaptic function. For instance, alterations in circadian rhythm activity are associated with sleep pattern irregularities in PrP-null animals (Tobler *et al.* 1996). PrP$^{o/o}$ mice also display decreased olfactory sensitivity compared with PrP$^{+/+}$ animals when challenged with odor-guidance tasks, and reveal correlating aberrations in synaptic transmission between olfactory bulb granule and mitral cells (Le Pichon *et al.* 2009). Both behavioral and neurophysiological irregularities were rescued by re-introduction of PrP protein expression. In juvenile PrP KO mice, altered synaptic plasticity and neuronal excitability affected performance on rotarod and movement tests, although these were corrected when animals reached 50 days of age (Prestori *et al.* 2008). Additionally, PrP null mice demonstrate increased susceptibility to pentylenetetrazol- or kainic acid-induced seizures (Walz *et al.* 1999). These data *in vivo* cumulatively support a role for PrP in synaptic homeostasis in neurons, although the molecular details underlying these phenotypes have yet to be clarified.

This summary of potential functions for PrP demonstrates that the prion protein is an elusive molecule that is associated with a wide variety of cellular activities, which vary depending on assay type and model system used in each study. Although several hypotheses regarding function have been presented, the most frequently observed and most convincing evidence implicates PrP as having a role in neuroprotectivity or synaptic formation or maintenance. The proposed roles for PrP may not be mutually exclusive, as many studies have discovered multiple consequences of PrP loss, mutation, or overexpression.

1.3 PrP^{Sc} & Infectious Prion Disease

A. History of PrP^{Sc} and the Prion Hypothesis

Transmissibility of scrapie was demonstrated in the 1940s when 10% of a flock of Scottish sheep developed neurological disease after injection with a vaccine created from infected sheep brain extract (Gordon 1946). Continued investigation on scrapie revealed that brain homogenate containing the infectious agent was resistant to UV irradiation (Alper *et al.* 1967), suggesting that nucleic acids were not necessary for disease transmission. In the 1980's, Stanley Prusiner and colleagues further isolated the source of scrapie infectivity through the fractionation of diseased golden Syrian hamsters (Bolton *et al.* 1982; Prusiner *et al.* 1982). They confirmed that the infectious agent resisted inactivation by irradiation, as well as DNAse and RNAse treatments, providing support for a non-nucleic acid-based mode of infection. Furthermore, they found that infectivity was reduced when purified scrapie components were subjected to conditions that disrupt and degrade proteins, such as denaturing detergent sodium dodecyl sulfate (SDS) (Prusiner *et al.* 1980; Prusiner 1982).

This led Prusiner and colleagues to support a protein-only hypothesis, whereby scrapie transmission was due exclusively to the actions of an *in*fectious *pr*otein, or '*prion*' (Griffith 1967; Prusiner 1982), capable of infecting similar protein molecules. This novel concept was initially met with mockery from fellow investigators at a time when scientific dogma stipulated that only pathogens with nucleic acids, such as bacteria and viruses, were capable of communicating disease. However, to date there is a very conspicuous lack of convincing evidence supporting a role for nucleic-acid based pathogens that are specific for prion disease transmission, despite persistent efforts to

detect them (Safar *et al.* 2005). Although the hypothesis was first ridiculed,

investigations eventually revealed a single protein that was recognized as the main

infectious agent and named "PrP^{Sc}", for *pr*ion *p*rotein in *sc*rapie-infected animals

(McKinley *et al.* 1983). Subsequent studies identified a PrP gene as the template which

encoded PrP^{Sc}. PrP gene expression was also confirmed in healthy, non-infected animals,

generating an endogenous cellular isoform, PrP^{C} (Oesch *et al.* 1985; Basler *et al.* 1986).

The prion hypothesis postulates that PrP^{Sc} self-propagates by converting native

PrP^{C} molecules into PrP^{Sc}. Consistent with this theory, knockout mice deficient for PrP

are unable to sustain infectious PrP^{Sc} propagation and do not contract neurological

disease when inoculated with scrapie prions (Bueler *et al.* 1993; Prusiner *et al.* 1993;

Sailer *et al.* 1994; Weissmann *et al.* 1994). Additionally, a murine 89-231 PrP fragment

synthesized and polymerized *in vitro* is able to cause neurological dysfunction when

inoculated into transgenic animals expressing similar PrP fragments. Analysis of brain

homogenates derived from these animals revealed the presence of aggregated and

infectious PrP^{Sc}, demonstrating the generation of the first infectious synthetic mammalian

prion (Legname *et al.* 2004). Stronger support for the prion hypothesis was exhibited by

the genesis of full-length hamster PrP^{Sc} in a biochemical system that utilized protein

misfolding cyclic amplification (PMCA) reactions. In a PCR-like manner, aggregated

PrP^{Sc} "seeds" are fragmented through a series of sonication steps, with each cycle of

sonication generating new PrP^{Sc} templates to serve as scaffolds for PrP^{C} conversion

(Kocisko *et al.* 1994). Using this system, investigators isolated PrP^{Sc} synthesized *de*

novo, injected the material into wild-type hamsters, and demonstrated that their

artificially constructed PrP^{Sc} induces neurological illness and replicates itself *in vivo*

(Castilla *et al.* 2005; Barria *et al.* 2009). Data from these studies and others collected over the past decades have established the prion hypothesis as the most widely accepted model of prion transmission.

The primary structures of PrP^{Sc} and PrP^{C} are identical. However, their tertiary conformations and biochemical properties are distinct (Figure 3). NMR studies of recombinant PrP^{C} demonstrate the presence of three α-helices and a short anti-parallel β-sheet (Riek *et al.* 1997; Zahn *et al.* 2000). In contrast, pathogenic PrP^{Sc} exhibits 45% β-sheet content and reduced α-helical content (Pan *et al.* 1993). These conformational disparities likely account for the unique PrP^{Sc} biochemical properties that allow distinction from PrP^{C}. PrP^{Sc} has a protease-resistant core, encompassing residues 89-231, that resists digestion by proteinase K (Bolton *et al.* 1982; McKinley *et al.* 1983). PrP^{Sc} is also insoluble in non-ionic detergents, and has a propensity to form aggregate structures both *in vivo*, in cells, and in biochemical preparations (Prusiner 1989). Additionally, the majority of antibodies traditionally used to detect PrP^{C} are unable to recognize PrP^{Sc} in non-denaturing conditions, indicating recognition of epitopes that are exposed in the endogenous, but not infectious, aggregated PrP isoforms. Reciprocally, there are several antibodies able to bind PrP^{Sc} conformers, but not PrP^{C} (Korth *et al.* 1997; Moroncini *et al.* 2004).

A. PrP^C   **B. PrP^{Sc}**
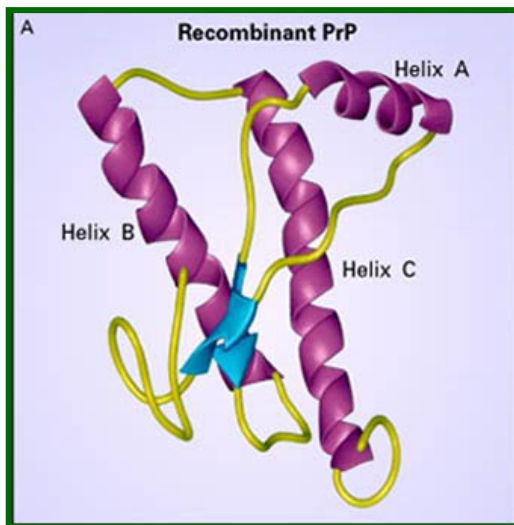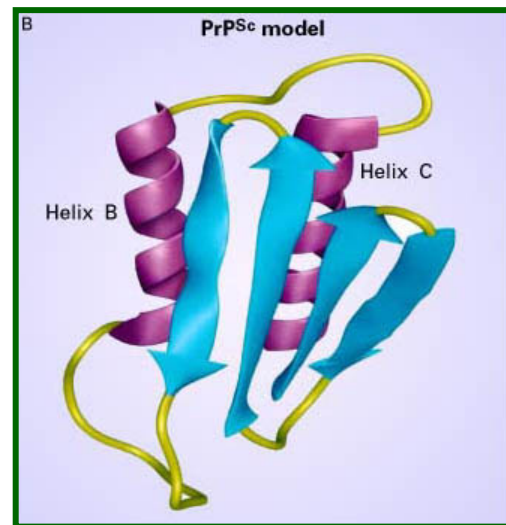
C. Biochemical Properties

PrP^C	PrP^{Sc}
α-helix rich	β-sheet rich
Soluble	Insoluble
PK-sensitive	PK-resistant
Not aggregated	Aggregated

Figure 3. PrP^C and Scrapie Prion (PrP^{Sc}). (A) Recombinant PrP^C is mostly alpha-helical by nature.   Upon conversion to PrP^{Sc} (B), PrP adopts a more beta-sheet rich conformation. (C) Structural rearrangement of PrP results in alterations of the biochemical nature of the protein.

B. PrP^{Sc} Propagation

It is generally accepted that PrP^{Sc} is able to replicate itself by stimulating a post-translational conformational change in PrP^C molecules within the host organism, wherein PrP^C is structurally rearranged to adopt the infectious conformation. Two main model mechanisms offer explanations for molecular PrP^{Sc} replication through direct physical interaction with PrP^C (Figure 4).

In the template-centered refolding model, PrP^{Sc} is able to bind PrP^C post-translationally, starting a catalytic reaction that converts a single PrP^C molecule to a protease-resistant entity, which is capable of binding to and converting yet another molecule (Figure 4A) (Griffith 1967). Presumably, PrP^C rearrangement is normally inhibited by a high activation energy barrier, which may be decreased upon the formation of a PrP^{Sc} / PrP^C heterodimer (Aguzzi *et al.* 2008). Sporadic cases of CJD, which occur with a frequency of approximately one case per million people per year, are thought to arise from rare spontaneous conversions of PrP^C to PrP^{Sc} due to stochastic fluctuations in protein conformation (Kahana *et al.* 1974). Mutations in the PRNP gene in humans may also destabilize PrP protein conformation such that conversion to the PrP^{Sc} form requires less activation energy as well (Surewicz *et al.* 2006).

A second model proposes that conversions between PrP^C and PrP^{Sc} are reversible, but that nucleated "seeds" of oligomeric PrP^{Sc} recruit monomeric PrP^C molecules that then convert to PrP^{Sc} upon introduction into the PrP^{Sc} aggregate (Figure 4B) (Jarrett and Lansbury 1993). Acceleration of monomer incorporation, and hence PrP^{Sc} conversion, occurs only in the presence of oligomeric, fibrillar, or aggregated PrP^{Sc}. In this model, the PrP^{Sc} conformation is only stabilized in the form of multimers, with individual PrP^{Sc}

A. Template-Centered Model
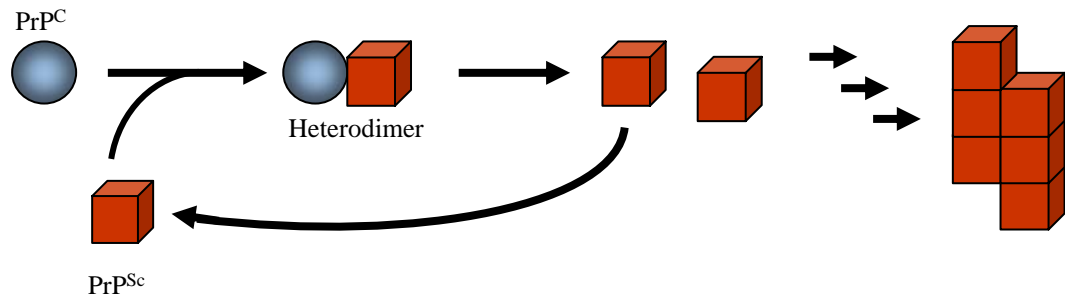
B. Nucleation-Polymerization Model
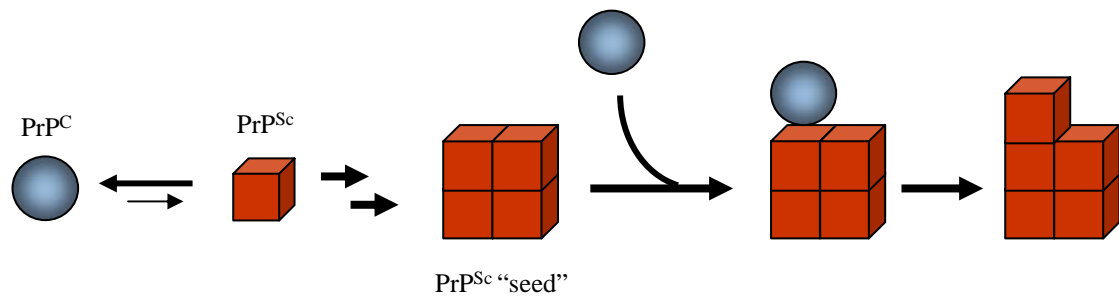
Adapted from Soto, C. (2004) Nature Reviews Microbiology 2:809-819.

Figure 4. Models of PrP^{Sc} Replication. In the template-centered refolding model (A), PrP^C and PrP^{Sc} molecules bind and form a heterodimer, which stimulates conversion of PrP^C to PrP^{Sc}. Increased concentrations of PrP^{Sc} lead to aggregate formation. In the nucleation-polymerization model (B), PrP^C molecules can convert to PrP^{Sc}, but the reaction is unfavorable. PrP^{Sc} "seeds" are slow to develop, but once formed, catalyze PrP^{Sc} conversion by recruiting PrP^C molecules.

monomers posing little threat of infectivity until seed formation with other PrP molecules of similar conformation. Breakage of aggregates may explain the exponential increase of PrP^{Sc} during infection (Orgel 1996), and the success of *in vitro* generation of PrP^{Sc} through PMCA reactions (described above) demonstrates that PrP^{Sc} can be produced by this mode of nucleated polymerization (Castilla *et al.* 2005; Barria *et al.* 2009).

In both of these models, direct physical interaction between PrP^{Sc} and PrP^{C} is assumed. Antibodies directed against PrP fragments 96-104 and 133-158 interfere with scrapie replication in infected neuroblastoma cells, supporting this postulation (Peretz *et al.* 2001). Additionally, separate antibody scaffolds displaying murine PrP fragments composed of sequences 89-112 and 136-158 are able to recognize and bind PrP^{Sc}, but not PrP^{C}, suggesting that these areas are interfaces for murine PrP^{Sc} interaction (Moroncini *et al.* 2004; Moroncini *et al.* 2006).

Successful conversion of PrP^{C} to PrP^{Sc} depends largely on the homology of host and template PrPs. The most efficient conversions occur when both the PrP^{Sc} seed and PrP^{C} target are of identical amino acid sequence. Variation of even a single amino acid may alter the PrP structure, and although the structural difference may be slight, disruption of the PrP^{C} / PrP^{Sc} interface can produce a negative effect on the rate of PrP recognition and binding (Priola *et al.* 2001). Additionally, some PrP^{C}'s bind heterologous PrP^{Sc}, but resist conversion to the infectious form (Horiuchi *et al.* 2000; Barmada and Harris 2005), indicating that subsequent reactions are necessary for complete rearrangement to the PrP^{Sc} conformation after the initial binding step.

Indeed, PrP heterology accounts for the "species barrier" effect observed in interspecies transmission of TSE infection. The species barrier is a phenomenon

whereby incubation time increases and attack rate decreases when prion disease is transmitted from one species to another. For example, inoculation of prions derived from mice into hamsters results in prolonged time to appearance of clinical symptoms and decreased proportion of animals affected by disease (Prusiner *et al.* 1990). In some cases, the species barrier can be overcome by successive passaging of the original inoculum through the target species, resulting in prion adaptation (Kimberlin and Walker 1979). In others, infection may be abrogated altogether, as is the case with wild type mice inoculated with prions from mule deer infected with chronic wasting disease (CWD) (Raymond *et al.* 2007). This effect is abolished in transgenic mice carrying the PrP gene from mule deer (Tamguney *et al.* 2006) because PrP^{Sc} from inocula and PrP^{C} targets are then identical in amino acid sequence. Parallel experiments demonstrate that murine-PrP null mice transgenic for bovine, ovine, and human PrP genes easily succumb to scrapie prions prepared from cognate donors (Scott *et al.* 1999; Crozet *et al.* 2001; Mastrianni *et al.* 2001).

Within species of animals, there exist "strains" of prions that are distinguished by their incubation times and PrP^{Sc} deposition patterns, despite having identical primary structures. For example, distinct human PrP^{Sc} types associated with different CJD neuropathologies have unique glycoform ratios and proteolytic fragment size patterns after digestion with protease K. One group has been able to demonstrate that PrP^{Sc} molecules from eight different hamster prion strains retain distinct conformations, supporting the idea that strain properties are enciphered solely within protein structure (Safar *et al.* 1998). Furthermore, several murine PrP^{Sc} conformations are faithfully maintained and propagated in cell-free PMCA reactions, and these *in vitro*-generated

PrP^{Sc} molecules maintain their specific strain properties when inoculated into mice, arguing against the influence of other cellular factors in determining biological properties associated with strains (Castilla *et al.* 2008).

C. PrP^{Sc} Localization

Investigation of intracellular PrP^{Sc} localization is essential for understanding the nature of transmission and disease pathology. However, localization by visualization in fixed samples show varied results, depending on cell type and detection protocol. In scrapie-infected neuroblastoma cells, PrP^{Sc} mainly localizes intracellularly within lysosomes, but not the cell surface (McKinley *et al.* 1991). *In vivo*, mice inoculated with 87V scrapie displayed prion aggregation in the form of plaques and amyloid fibrils at the extracellular face of the plasmalemma along neurites (Jeffrey *et al.* 1994). Recently, one group of investigators conducted a series of experiments in infected neuronal cell lines where protein trafficking was selectively impaired at different points (Marijanovic *et al.* 2009). Marijanovic *et al.* determined that PrP^{C} → PrP^{Sc} conversion occurred in specific endosomal recycling compartments, but not early or late endosomes.

The variable conclusions from each of these experiments may partially stem from the different techniques used to overcome the technical difficulties associated with recognizing aggregated PrP. The majority of antibodies commonly used to detect PrP^{C} are rendered ineffective for PrP^{Sc} detection, likely due to the inaccessibility of epitopes that become hidden or buried within the rogue folding pattern of aggregated PrP^{Sc} (Williamson *et al.* 1998). Thus, antigen retrieval (AR) techniques are necessary to denature PrP^{Sc} molecules, leading to epitope exposure and allowing subsequent antibody

recognition. Procedures such as hydrolytic autoclaving or treatment with high concentrations of guanidine thiocyanate are successful at denaturing PrP^{Sc} (Van Everbroeck *et al.* 1999), but at the expense of sometimes severe and irreversible cellular damage and at the risk of PrP redistribution or antigen loss (Moroncini *et al.* 2006).

Several studies have been able to bypass the use of AR and identify PrP^{Sc} aggregates with the use of fluorescence technology. Genetically engineered Tg(WT-EGFP) mice express a murine PrP protein fused with an enhanced jellyfish-derived green fluorescent protein (EGFP). Although unable to convert to the infectious form, WT-EGFP was able to bind PrP^{C}-derived infectious prions *in vivo*. In brain sections of prion-inoculated mice co-expressing both WT-EGFP and endogenous PrP, PrP^{Sc} aggregates are visualized in the form of fluorescent puncta in the neuropil, axonal regions, and Golgi apparatus of neurons (Barmada and Harris 2005). In another study involving scrapie-infected neuroblastoma cells, PrP^{C} containing a tetracysteine (TC) tag was expressed, then able to convert into a PK-resistant form (Taguchi *et al.* 2009). Upon addition of a biarsenical fluorophore derivative, tagged PrP^{Sc} was identified at the cell surface. In SN56 neuronal cell lines, Magalhaes *et al.* labeled PK-resistant PrP, derived from brain homogenate of prion-infected animals, by covalent linkage with a primary amine-reactive analog of Alexa Fluor 568 (PrP-res^{A568}). Non-infected cells exposed to PrP-res^{A568} were able to internalize the aggregates, which subsequently colocalized with late endosomes and lysosomes. PrP-res^{A568} aggregates also traveled along neurites to points of contact with other cells, suggesting a direct cell-to-cell mode of transfer and propagation (Magalhaes *et al.* 2005). These studies set a good foundation for PrP^{Sc} visualization, and further clarification of PrP^{Sc} localization and transfer at the cellular and anatomical

levels will greatly facilitate understanding key concepts of disease pathogenesis, transmission, and possible therapeutics.

D. Possible Mechanisms of Infectious Prion Disease Toxicity

Prion diseases are usually defined in part by the presence and propagation of PrP^{Sc} within the central nervous system. There are many examples that associate PrP^{Sc} accumulation with neurodegeneration, suggesting that PrP^{Sc} is not only infectious, but also causes disease toxicity directly. In support of this, immunohistochemical studies in infected brain show PrP^{Sc} aggregates before symptom onset and within or near areas of CNS degeneration, including neuronal loss and neuropil vacuolation (Jeffrey *et al.* 2001; Ersdal *et al.* 2004). PrP^{C} (subsequently converted to PrP^{Sc}) is absolutely necessary for disease toxicity, as demonstrated by the lack of susceptibility in PrP knockout mice exposed to PrP^{Sc} by intracerebral inoculation (Bueler *et al.* 1993; Sailer *et al.* 1994; Weissmann *et al.* 1994). Additionally, synthetically-derived PrP^{Sc} molecules generated *in vitro* are capable of inducing prion disease when inoculated into mice (Castilla *et al.* 2005), supporting the idea of direct PrP^{Sc} toxicity. However, these latter studies are accomplished within brain homogenates, and the influence of other unknown CNS factors on toxicity cannot be excluded.

Although PrP^{Sc} was initially thought to be the prime candidate for prion disease pathogenicity, there are a number of examples that reveal a large discrepancy between the amount of PrP^{Sc} and the extent of neurodegeneration and brain damage, arguing that the model of PrP^{Sc}-only toxicity is oversimplified. Tga20 transgenic mice express 10X the amount of endogenous PrP^{C}, and display highly accelerated disease progression

compared to WT mice, but accumulate only ~50% of PrP^{Sc} material (Fischer *et al.* 1996).

Additionally, inoculation of mice with bovine spongiform encephalopathy (BSE) resulted

in 100% transmission of disease, but over 55% of clinically symptomatic animals did not

display protease-resistant PrP^{Sc} (Lasmezas *et al.* 1997). These models illustrate that

toxicity exists even in the absence, or limited accumulation, of PrP^{Sc}.

Reciprocally, there are examples of animals ridden with PrP^{Sc} in the absence of

clinical symptoms of prion disease. RML-inoculated transgenic mice expressing an

anchorless form of PrP accumulate massive PrP^{Sc} deposition within the cerebellum,

hippocampus, and cortex, but remain free of neurological illness for the duration of their

lifetimes (Chesebro *et al.* 2005). Additionally, brain extracts from a human GSS patient

carrying the P102L mutation were able to induce PrP^{Sc} amyloid deposition when

inoculated into mice carrying the murine form of the same mutation, but failed to

transmit clinical disease (Piccardo *et al.* 2007). In another stunning example,

neurotoxicity and spongiosis in inoculated animals were abrogated and reversed by

depleting PrP^{C} expression post-natally, despite the accumulation of PrP^{Sc} to intensities

observed in terminally ill wild-type animals (Mallucci *et al.* 2003). These investigations

strongly argue that PrP^{Sc} as conventionally defined cannot account for prion

neurotoxicity.

What then, is the toxic species (PrP^{toxic}) involved with prion disease? There is an

emerging viewpoint implicating small oligomeric complexes in the induction of toxicity

in several neurodegenerative diseases, including prion disorders (Caughey and Lansbury

2003; Haass and Selkoe 2007). In this model, transient oligomeric PrP^{Sc} intermediates,

or protofibrils, are the active components of cellular interaction and neurotoxicity.

Consistent with this hypothesis, small soluble or partially PK-resistant PrP oligomers have displayed toxicity in cell culture and in primary neurons from $PrP^{+/+}$ mice (Novitskaya *et al.* 2006; Simoneau *et al.* 2007). In principal, continuous PrP^C expression would be necessary to maintain the pool of transitory oligomers, and large PrP^{Sc} aggregates could serve as reservoirs of these toxic intermediates upon disassembly.

Interestingly, membrane attachment seems to play a role in PrP^{Sc} aggregation and toxicity. In cells, proper GPI anchorage of PrP to the extracellular face of the plasma membrane is necessary for efficient PrP^{Sc} conversion (Caughey and Raymond 1991; Borchelt *et al.* 1992). Deletion or substitution of the anchor with a transmembrane domain in scrapie-infected neuroblastoma cell lines leads to impaired PrP^{Sc} formation and accumulation (Rogers *et al.* 1993). In transgenic mice that express a C-terminally truncated PrP lacking the GPI anchor signal sequence, inoculation with scrapie results in extensive plaque formation. These plaques are larger and more dense than plaques found in scrapie-inoculated wild-type counterparts. Surprisingly, inoculated Tg(PrPΔGPI) animals exhibit no clinical symptoms for the duration of their lifetimes, while inoculated wild-type mice typically survive only five months. PrP^{Sc} derived from brain homogenates of prion-infected Tg(PrPΔGPI) mice is less infectious when sequentially passaged, despite its extensive accumulation in the brain (Chesebro *et al.* 2005; Trifilo *et al.* 2008). Collectively, these data reveal that the GPI anchor affects PrP^{Sc} conversion, aggregation, toxicity, and transmissibility.

1.4 PrP^M & Inherited Prion Disease

A. Genetic Mutations in the PrP Gene and PrP^M

Ten to fifteen percent of reported cases of prion diseases in humans are caused by mutations in the PRNP gene on chromosome 20 (Mead 2006). Mutations result in dominantly inherited neurodegenerative disorders, categorized either as familial CJD (fCJD), Fatal Familial Insomnia (FFI), or Gerstman-Straussler-Sheinker disease (GSS). There is high phenotypic variability between patients, even by those carrying the same mutations within the same family (Young *et al.* 1999). Ages of onset have been observed from mid-twenties to late into the eighties, with the majority of cases reported in the fourth and fifth decades of life (Mead 2006). Disease severity can also range from mild to fatal, likely depending on as-of-yet unidentified genetic, epigenetic, and environmental factors.

Over 50 PRNP mutations have been associated with prion disease (Figure 5A). These include point mutations that lead to amino acid substitutions, amber mutations that cause truncated PrP transcripts, and insertions of the N-terminal octapeptide (OR) motifs result in repeat collapses or expansions. Mutations are found throughout the PRNP coding sequence, suggesting that instead of having primary sites of functional activity that are disrupted by mutation, structural integrity of the entire protein is necessary to maintain non-pathologic behavior.

Several non-pathogenic polymorphisms exist within the PRNP locus, including four that result in single amino acid substitutions. Of significant note, a common polymorphism at codon 129 determines whether methionine (M) or valine (V) is present at this position. Although neither variant causes disease by itself, the codon 129

genotype plays a critical role in susceptibility, severity, and incubation period of prion

diseases, both familial and infectious (Mead 2006). For example, codon 129 specifies the

disease phenotype of the D178N mutation: patients with a 129V allele display familial

CJD, while those with the 129M allele result in FFI (Kong *et al.* 2004). In transfected

cells and in patient brain samples, D178N displays different glycoform ratios and

cleavage products after protease K digestion, dependent on the codon 129 polymorphism,

indicating that phenotypic heterogeneity of the mutant is due to conformational effects of

the M/V 129 polymorphism (Petersen *et al.* 1996). Additionally, new variant CJD, which

affects only a subset of people who have ingested BSE-infected beef, has thus far only

been detected in individuals homozygous for the 129M allele (Mead 2006).

B. Molecular Basis for PrP^{M} Toxicity

Point mutations in the prion protein gene are thought to encourage spontaneous

PrP conversion to pathogenic PrP^{Sc}-like conformations (Figure 5B). Misfolding of

mutated PrP (PrP^{M}) may lead to decreased stability of endogenous PrP^{C} conformation,

thus increasing the likelihood of conversion to a pathological PrP^{Sc}-like malconformer

over time (Kong *et al.* 2004).

The highly variable biochemical and cell biological properties between different

mutations render it difficult to understand the exact molecular mechanism of PrP^{M}

toxicity. PrP^{Sc} from infectious disease is defined by resistance to protease digestion,

insolubility in nonionic detergents, and ability to form aggregate structures. However,

mutant PrPs, designated PrP^{M}, are not as easily categorized. Biochemically, some

mutations such as D197N, V179I, and V209I resemble endogenous PrP^{C} more than PrP^{Sc}

A.
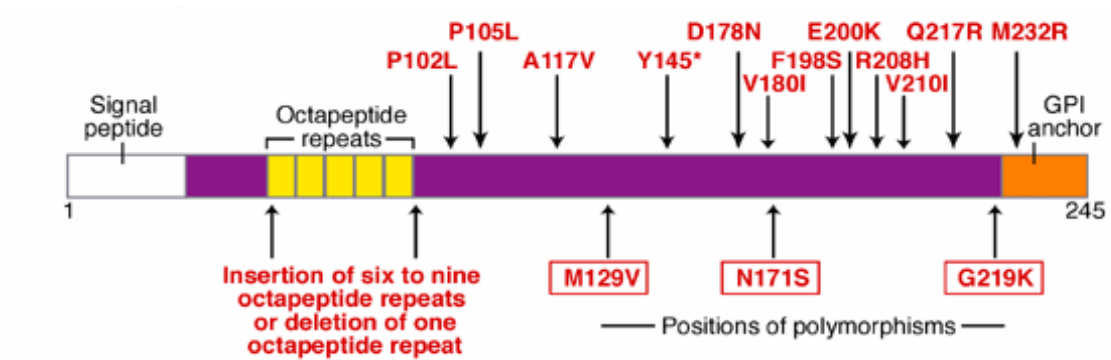
B.
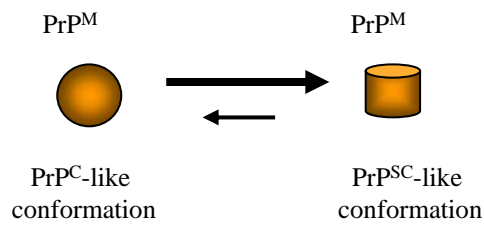
Figure 5. Genetic PrP mutants (PrP^M). (A) Over 50 pathological mutations are associated with familial prion disease, a subset of which are indicated along a schematic representation of human PrP. Several polymorphisms that do not inherently cause disease are also listed. (B) PrP mutants may not be stable in PrP^C-like conformations, thus increasing the likelihood of adopting a more PrP^{Sc}-like structural arrangement .

because they are sensitive to degradation by protease K (PK), remain soluble in detergents, and display correct PrP localization. Others, like PG14, D177N, and E199K exhibit PK resistance, are partially insoluble in detergent, and present aberrant PrP trafficking patterns, but are not infectious (Ivanova *et al.* 2001; Chiesa *et al.* 2003; Biasini *et al.* 2008).

Adding to the variability, there is a wide range of phenotypic inconsistency in patients carrying the same mutation. Even within the same families, symptoms can extend from mild to severe. In at least one case, phenotypic variability in patients sharing the same mutation can be explained by conformational differences in PrP^M structure. One particular GSS-associated mutant PrP, 102L, can fold into at least two different pathogenic conformers in human patients, with each variant correlating with the presence or absence of spongiform degeneration (Piccardo *et al.* 1998). Mice inoculated with brain homogenates carrying either conformation displayed variable pathologies (Piccardo *et al.* 2007). Thus, like prion "strains" in infectious disease, some speculate that differential mutant conformations may contribute to the clinical and neuropathological variability observed in patients (Piccardo *et al.* 2007).

C. Mouse Models of Inherited Prion Disease

In an effort to comprehend the pathogenic mechanisms underlying familial prion disorders, several transgenic mouse models have been generated to express disease-associated genetic PrP mutants.

Transgenic mice overexpressing the mouse version of GSS-associated PrP mutant P102L, MoPrP-P101L spontaneously develop neurological disease, as evidenced by the

presence of PrP plaques and spongiform degeneration (Telling *et al.* 1996). This phenomenon was dependent on expression level, as mice expressing lower levels of the mutation remained healthy. Although P101L in diseased animals is sensitive to PK digestion, the mutant protein accumulates as aggregates in sick mice, as demonstrated by its reactivity with PrP aggregate-specific antibody 15B3 (Nazor *et al.* 2005). Interestingly, inoculation of P101L brain homogenate from spontaneously sick animals to transgenic mice expressing the same mutation accelerated disease (Nazor *et al.* 2005), consistent with the nucleated polymerization model of prion replication (Figure 2B) whereby aggregate seeds increase the rate of PrP^C polymerization and conversion to disease-associated PrP^M. Like other artificial mutations such as ΔCR or F35, P101L disease can be abrogated by coexpression with WT PrP (Telling *et al.* 1996).

The GSS phenotype is also recapitulated in another transgenic mouse expressing disease-associated *Prn-p* mutation A117V (Hegde *et al.* 1998). Spongiosis and astrocytic gliosis were prominent features in sick animals, although brain homogenates contained no PK-resistant, infectious material. In transfected cells and in brain homogenates of Tg(A117) mice, the mutation demonstrated a unique characteristic whereby a subpopulation of PrPs adopted a transmembrane form of PrP (^{Ctm}PrP) post-translationally within the ER (Hegde *et al.* 1998). To investigate whether the altered transmembrane topology was responsible for disease induction, a separate, yet similar, line of Tg(L9R/3AV) mice were created. These expressed a mutant PrP containing several nonconservative amino acid changes within the transmembrane region to produce a homogenous population of ^{Ctm}PrP molecules. In mice, ^{Ctm}PrP developed progressively fatal ataxia and demonstrated hippocampal atrophy and cerebellar granule loss, leading to

the notion that ^{Ctm}PrP may be the neurotoxic intermediate that induces neurodegeneration universally in prion disorders (Stewart *et al.* 2001). However, several other disease-associated PrP mutants did not adopt the transmembrane formation (Stewart and Harris 2001), and inoculation of Tg(L9R/3AV) mice with scrapie did not shorten PrP^{Sc} incubation times. Together these data argue against ^{Ctm}PrP playing a major role in prion pathogenesis.

Mutations resulting in the addition of more than three extra octapeptide repeats are associated with prion disease, with age of onset negatively correlating with increasing numbers of ORs (Yu *et al.* 2007). The PG14 mutation, which adds an additional nine ORs, is the largest disease-associated insertion reported thus far in cases of CJD. Tg(PG14) animals expressing the murine form of PG14 develop spontaneous disease at around 270 days. Diseased mice display cerebellar atrophy, massive apoptosis of cerebellar granule cells, and extensive intracerebral PG14 deposition (Chiesa *et al.* 1998) (Figure 6A-C), which are likely due in part to intracellular retention and aggregation of the mutant PrP (Lehmann and Harris 1996; Ivanova *et al.* 2001).

Investigations in cultured cells and in primary neurons show that PG14 has distinct trafficking patterns and biochemical properties compared with PrP^C. PG14 accumulates intracellularly, showing delayed progression through the ER and hindered ability to localize to the cell surface. A subset of molecules, named PG14^{agg}, spontaneously becomes PK-resistant, detergent insoluble, and 15B3-reactive while in transit through the secretory pathway. However, a fraction of molecules remain soluble (PG14^{sol}) and have biochemical properties similar to PrP^C (Biasini *et al.* 2008) (Figure 6D). Although PG14^{sol} is readily detectable by standard immunohistochemistry, PG14^{agg}

localization, like PrP^{Sc}, is difficult to detect because of its aggregate nature and is not easily recognized by traditional PrP antibodies without antigen retrieval (Chiesa *et al.* 1998; Medrano *et al.* 2008).

Unlike PrP^{Sc}, PG14 is not infectious. When co-expressed with endogenous PrP in Tg(PG14) PrP$^{+/+}$ mice, PG14 does not convey its PK-resistant conformation onto WT PrP, indicating that PG14 serves as a prion mutant model where infectivity and toxicity are distinct (Chiesa *et al.* 2003). Not surprisingly then, PG14 pathogenesis in transgenic mice begins and proceeds at the same rate of neurodegeneration in the presence or absence of PrP^{C}, indicating a lack of interaction with, and neuroprotective effect from, WT PrP. Interestingly, infectivity can be introduced into PG14 molecules through inoculation of Tg(PG14) animals with RML scrapie prions (Biasini *et al.* 2008). The resulting PG14^{RML} molecules are both toxic and infectious, suggesting that RML is able to bind and rearrange PG14 molecules to a more PrP^{Sc}-like configuration (Figure 6E).

The most recently generated transgenic mice are those that express the fCJD mutant D178N with the V129 polymorphism (Dossena *et al.* 2008). In addition to motor dysfunction and PrP deposition, Tg(D178N/V129) mice also displayed abnormal EEG patterns and memory impairment, similar to symptoms found in D178N/V129 CJD patients. GABAergic neuronal loss, a distinctive feature in CJD, was also noted in transgenic animals. Electron microscopy of cerebella in sick animals revealed gross dilation of the endoplasmic reticulum, indicating that ER dysfunction may contribute or underlie cellular pathogenesis. Coexpression of WT PrP also failed to rescue symptoms in this mouse model, suggesting a lack of interaction with endogenous PrPs.

A. WT PG14

B. WT

C. PG14

D.

PG14^{sol} PG14^{agg}

E.

PrP^{Sc} PG14

PG14^{RML}
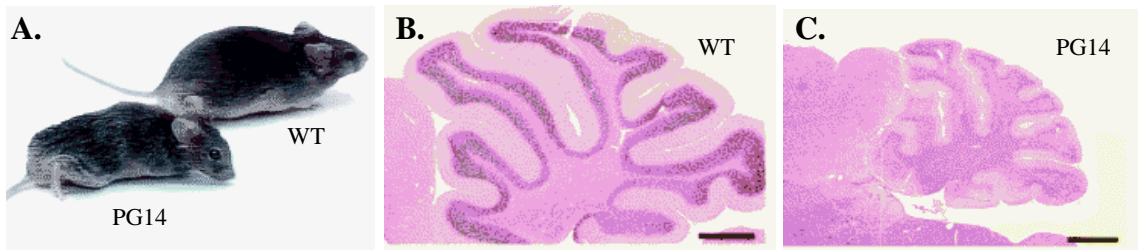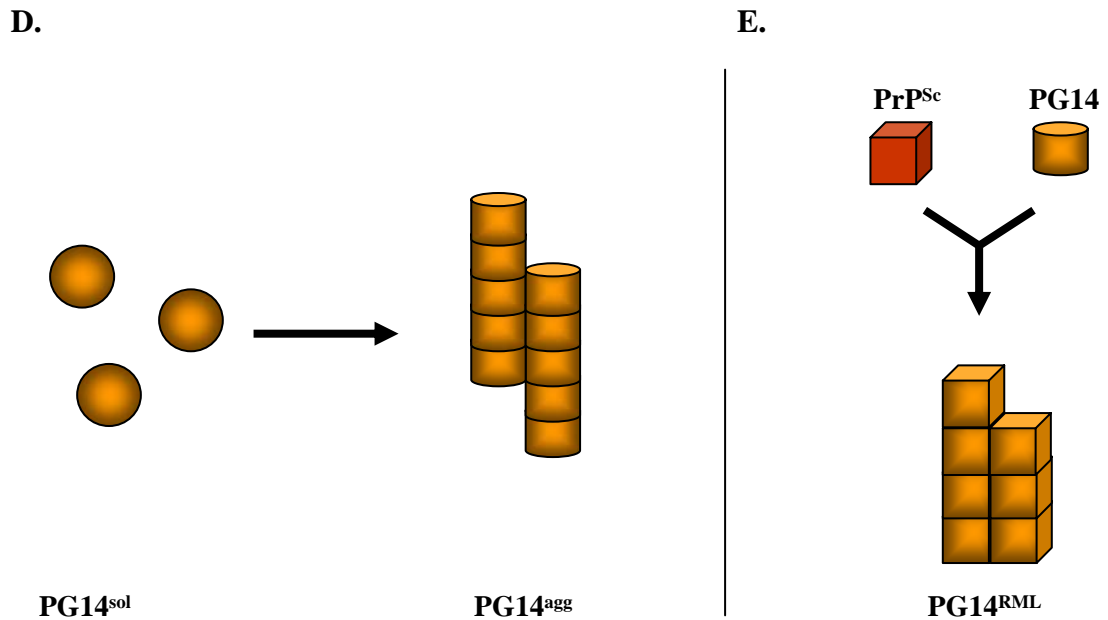
Figure 6. The PG14 mutation. (A) Transgenic mice expressing PrP with the PG14 mutation develop kyphosis and ataxia, while wild-type (WT) counterparts remain healthy. (B) H&E-stained cerebellum derived from a WT mouse demonstrates a full cerebellar granule layer (dark purple), while cerebellum from a Tg(PG14) mouse (C) shows severe atrophy and massive loss of cerebellar granule neurons. (D) PG14 is synthesized as a soluble molecule, which over time spontaneously aggregates into a toxic, but not infectious, form. (E) Tg(PG14) mice inoculated with RML scrapie prions produce PG14^{RML}, which is both toxic and infectious. RML prions likely convert PG14 molecules into adopting more RML-like conformations.

Transgenic mice expressing prion mutations mimic the toxicity and disease phenotypes observed in human illness. Collectively, these models demonstrate that prion toxicity can occur in the absence of PrP^{Sc}, and that the biochemical properties, trafficking patterns, and infectivity of PrP^{M} vary depending on mutation type.

D. Possible Mechanisms of Familial Prion Disease Toxicity

Like infectious PrP^{Sc}, the molecular, cellular, and physiological details underlying inherited prion disease remains ambiguous. It is generally thought that the root of inherited mutant prion disease stems from PrP misfolding. PrPs are synthesized and immediately translocated into the lumen of the ER, where protein folding occurs. Several genetic PrP mutants, including PG14 and ^{Ctm}PrP, have displayed delayed exit from the ER when transfected into cells (Singh *et al.* 1997; Ivanova *et al.* 2001), supporting the idea that the ER quality control is capable of recognizing and retaining misfolded PrPs. The ER has several systemic mechanisms to correct any improperly folded protein products, including chaperone assistance, ER-associated degradation (ERAD), and unfolded protein response (UPR) pathways (Scheper and Hoozemans 2009).

For this reason, several groups have investigated the role of possible ER stress and dysfunction in prion pathology. Cultured cells challenged with chemicals that induce ER stress, such as tunicamycin, produce protease-resistant mature PrPs. Further investigation prompted authors to postulate that the unfolded protein response (UPR) was activated in these cells, inducing PrP retrotranslocation into the cytosol where it formed a PrP^{Sc} –like infectious molecule (Ma *et al.* 2002). The same group demonstrated that transgenic mice expressing a cytosolic form of PrP developed severe ataxia and

cerebellar neurodegeneration (Ma *et al.* 2002). However, multiple reports from several

other investigators contend that only a small portion of PrP molecules, mutant and wild-

type, are degraded by the proteasome and that these represent transcripts that had never

been translocated in the ER. Pharmacological inhibition of proteasome activity in cells

expressing wild-type and several mutant PrPs retained within the ER affects neither

maturation nor turnover of these proteins, and does not decrease cell viability (Drisaldi *et*

al. 2003; Fioriti *et al.* 2005), refuting the hypothesis that proteasomal degradation plays a

major role in prion pathogenesis. Additionally, no activation of UPR-related signal

proteins, such as PERK or eIF2α, were detected in brains from patients with inherited

prion disease (Unterberger *et al.* 2006), and no upregulation of UPR-associated genes,

including Grp78/Bip, have been identified in Tg(D178N/V129), Tg(PG14), and

Tg(^{Ctm}PrP) mice compared with wild-type controls (Dossena *et al.* 2008) (and Stewart &

Harris, unpublished). These data argue against a significant role for proteasomal

dysfunction as a causative agent for familial prion disease. However, other ER-stress

induced neurodegenerative effects cannot be excluded. It is possible that mutant protein

accumulation within the ER interferes with ER-mediated calcium signaling necessary for

basic neuronal function (Mattson *et al.* 2000). Alternatively, PrP^M aggregation at the

lipid bilayer may interfere with assembly and transportation of other membrane proteins,

for example transmembrane receptors or interlocking ion channel subunits, thus

interfering with cell signaling or synaptic transmission (Schwappach 2008).

PG14 aggregation and massive apoptosis in cerebellar granule neurons are

hallmark pathologies described in transgenic mice, prompting the investigation for a pro-

apoptotic pathway involved in neuronal death (Chiesa *et al.* 1998; Chiesa *et al.* 2000).

PG14 animals bred onto a Bax knockout background resulted in a rescue of the neuronal apoptosis phenotype, but did not inhibit clinical presentation of prion disease, indicating that Bax-dependent signaling pathways were not involved with the inherited disorder. Synaptic abnormalities were evident in PG14 mice on both $Bax^{+/+}$ and $Bax^{o/o}$ backgrounds, but not in controls, indicating that impaired neuronal excitability could account for dysfunction, with apoptosis being a secondary effect (Chiesa *et al.* 2005). Additionally, Bax deletion does not abrogate or delay clinical disease or Purkinje cell degeneration in Tg(Doppel) mice, suggesting that Bax-dependent pro-apoptotic pathways are unlikely major players in prion toxicity (Dong *et al.* 2007).

Recently, another group has proposed that the expression of PrP^M interferes with proper PrP^C localization within detergent-resistant membrane microdomains (DRMs), which may be involved with disease progression (Schiff *et al.* 2008). Association of WT PrP^C and several GSS-associated PrP mutants (A117V, E200K, or T182A) was increased when WT and PrP^M mutants were co-expressed in Fischer Rat Thyroid (FRT) cells, and the ratio of intracellular vs. surface PrPs was altered as well. Authors postulate that mislocalization of mutant and wild-type PrPs may alter membrane equilibrium in lipid rafts, thus leading to a toxic effect in neurons by an unknown mechanism.

Collectively, these data show that ER retention and Bax-dependent apoptotic pathways are features of some familial prion disease mutants, but are not the main causative agents of toxicity. PrP^M DRM mislocalization may provide some clues as to pathogenicity, but many more investigations using other PrP mutants will be necessary to substantiate whether the phenomenon is common between PrP^M models and whether it is contributory to disease.

One major difficulty in studying familial prion disease and attempting to find a universal explanation for pathogenicity is the wide range of biochemical properties and cellular properties that exist between the 50+ different PrP^M mutations. Molecular and cellular variables such as increased β-sheet structure, aggregation, infectivity, abnormal glycosylation, PK resistance, and aberrant trafficking behavior can influence PrP^M toxicity (Prusiner 1998). Given the extensive assortment of cellular and biochemical characteristics of disease-associated PrP mutants, none of these factors alone are sufficient to cause the clinical and neurodegenerative pathologies observed in all familial prion disorders. Thus, the main mode of PrP^M toxicity, like PrP^{Sc}, remains unknown.

Whether familial and infectious prion diseases are governed by the same mechanism(s) is indefinite. It is possible that PrP^M and PrP^{Sc} induce pathology by differential mechanisms. The lack of infectious PrP^M in some mutants indicates that infectivity is not inherently linked with pathogenicity in familial prion disease. This is distinct from PrP^{Sc}, which by definition is transmissible. PrP^M can also be soluble or partially insoluble, suggesting that these forms may represent misfolded PrP^{Sc} intermediates capable of toxicity. Alternatively, PrP^M may increase formation of PrP oligomers, causing toxicity in a manner similar to that described in the emerging "oligomeric toxicity" hypothesis for infectious disease. However, because the mode of pathogenicity is equally ambiguous for PrP^M and PrP^{Sc}, further study in both fields is necessary for understanding disease toxicity.

1.5 Focus of Thesis Research

Mechanisms underlying sporadic, infectious, and inherited prion diseases remain ambiguous. Further exploration of PrP^M especially is necessary to understand genetic prion pathogenesis and any mechanisms that distinguish inherited versus infectious toxicity. Thus, the objectives of my thesis work revolve around the study of PrP mutant PG14 and the role of aberrant trafficking and accumulation in disease. Localization of aggregated mutant PrP is essential for elucidating the pathological mechanisms at the physiological and neuronal levels. In Chapter 2, I describe experiments characterizing the clinical and neuropathological progression of disease in transgenic mice expressing fluorescently-tagged PG14. Tg(PG14-EGFP) mice allow the *in vivo* examination of PG14 aggregate localization, which clarifies PG14 distribution in primary neurons and in brain section without the use of antigen retrieval techniques. PG14 was observed for the first time in axon-dense regions of the brain, suggesting that PrP^M may interfere with neuronal signaling or synaptic transmission by blocking axonal transport mechanisms.

I also initiate investigation into the role of membrane attachment in PG14 aggregation, cell behavior, and toxicity. Previous work has demonstrated that GPI-mediated membrane attachment plays a significant role in PrP^{Sc} aggregation, transmission, and disease pathogenesis. Because PrP^{Sc} and PrP^M can differ in their cellular and biochemical characteristics, the significance of GPI anchorage in aggregated PrP^M cell trafficking, behavior, and toxicity are unknown. In Chapter 3, I investigate the function of the GPI anchor in PG14 cell localization, glycosylation, and aggregation in cells. These experiments set the foundation for parallel studies to be continued *in vivo*.

Tg(PG14ΔGPI) mice are currently being generated to study the effect of GPI anchor loss

in PG14 aggregation and disease in a physiologically relevant setting.

Finally, in the appendices, I present continued attempts to visualize both

aggregated mutant PG14 and infectious PrP^{Sc} in cells and in mice using green fluorescent

protein (GFP) technology. Live imaging of fluorescently labeled mutant PG14 within

neurites in cell culture would give greater insight into how and when PG14 aggregates,

and how axon-specific accumulation influences cellular behavior. Similarly, the GFP-

tagged PrP^{Sc} would permit imaging of intra- and inter-cellular transfer of the infectious

protein, thus facilitating visualization of PrP^{Sc} transmission.

1.6 References

Aguzzi, A., C. Sigurdson, *et al.* (2008). "Molecular mechanisms of prion pathogenesis." Annu Rev Pathol **3**: 11-40.

Alper, T., W. A. Cramp, *et al.* (1967). "Does the agent of scrapie replicate without nucleic acid?" Nature **214**(5090): 764-6.

Barmada, S. J. and D. A. Harris (2005). "Visualization of prion infection in transgenic mice expressing green fluorescent protein-tagged prion protein." J Neurosci **25**(24): 5824-32.

Barria, M. A., A. Mukherjee, *et al.* (2009). "De novo generation of infectious prions in vitro produces a new disease phenotype." PLoS Pathog **5**(5): e1000421.

Basler, K., B. Oesch, *et al.* (1986). "Scrapie and cellular PrP isoforms are encoded by the same chromosomal gene." Cell **46**(3): 417-28.

Biasini, E., A. Z. Medrano, *et al.* (2008). "Multiple biochemical similarities between infectious and non-infectious aggregates of a prion protein carrying an octapeptide insertion." J Neurochem **104**(5): 1293-308.

Biasini, E., M. E. Seegulam, *et al.* (2008). "Non-infectious aggregates of the prion protein react with several PrP(Sc)-directed antibodies." J Neurochem.

Blinov, N., M. Berjanskii, *et al.* (2009). "Structural domains and main-chain flexibility in prion proteins." Biochemistry **48**(7): 1488-97.

Bolton, D. C., M. P. McKinley, *et al.* (1982). "Identification of a protein that purifies with the scrapie prion." Science **218**(4579): 1309-11.

Borchelt, D. R., V. E. Koliatsos, *et al.* (1994). "Rapid anterograde axonal transport of the cellular prion glycoprotein in the peripheral and central nervous systems." J Biol Chem **269**(20): 14711-4.

Borchelt, D. R., A. Taraboulos, *et al.* (1992). "Evidence for synthesis of scrapie prion proteins in the endocytic pathway." J Biol Chem **267**(23): 16188-99.

Bounhar, Y., K. K. Mann, *et al.* (2006). "Prion protein prevents Bax-mediated cell death in the absence of other Bcl-2 family members in Saccharomyces cerevisiae." FEMS Yeast Res **6**(8): 1204-12.

Bounhar, Y., Y. Zhang, *et al.* (2001). "Prion protein protects human neurons against Bax-mediated apoptosis." J Biol Chem **276**(42): 39145-9.

Brown, D. R., K. Qin, *et al.* (1997). "The cellular prion protein binds copper in vivo." Nature **390**(6661): 684-7.

Brown, L. R. and D. A. Harris (2003). "Copper and zinc cause delivery of the prion protein from the plasma membrane to a subset of early endosomes and the Golgi." J Neurochem **87**(2): 353-63.

Bueler, H., A. Aguzzi, *et al.* (1993). "Mice devoid of PrP are resistant to scrapie." Cell **73**(7): 1339-47.

Bueler, H., M. Fischer, *et al.* (1992). "Normal development and behaviour of mice lacking the neuronal cell-surface PrP protein." Nature **356**(6370): 577-82.

Carleton, A., P. Tremblay, *et al.* (2001). "Dose-dependent, prion protein (PrP)-mediated facilitation of excitatory synaptic transmission in the mouse hippocampus." Pflugers Arch **442**(2): 223-9.

Castilla, J., R. Morales, *et al.* (2008). "Cell-free propagation of prion strains." Embo J **27**(19): 2557-66.

Castilla, J., P. Saa, *et al.* (2005). "In vitro generation of infectious scrapie prions." Cell **121**(2): 195-206.

Caughey, B. and P. T. Lansbury (2003). "Protofibrils, pores, fibrils, and neurodegeneration: separating the responsible protein aggregates from the innocent bystanders." Annu Rev Neurosci **26**: 267-98.

Caughey, B., R. E. Race, *et al.* (1989). "Prion protein biosynthesis in scrapie-infected and uninfected neuroblastoma cells." J Virol **63**(1): 175-81.

Caughey, B. and G. J. Raymond (1991). "The scrapie-associated form of PrP is made from a cell surface precursor that is both protease- and phospholipase-sensitive." J Biol Chem **266**(27): 18217-23.

Chen, S., A. Mange, *et al.* (2003). "Prion protein as trans-interacting partner for neurons is involved in neurite outgrowth and neuronal survival." Mol Cell Neurosci **22**(2): 227-33.

Chesebro, B., M. Trifilo, *et al.* (2005). "Anchorless prion protein results in infectious amyloid disease without clinical scrapie." Science **308**(5727): 1435-9.

Chiesa, R., B. Drisaldi, *et al.* (2000). "Accumulation of protease-resistant prion protein (PrP) and apoptosis of cerebellar granule cells in transgenic mice expressing a PrP insertional mutation." Proc Natl Acad Sci U S A **97**(10): 5574-9.

Chiesa, R., P. Piccardo, *et al.* (2005). "Bax deletion prevents neuronal loss but not neurological symptoms in a transgenic model of inherited prion disease." Proc Natl Acad Sci U S A **102**(1): 238-43.

Chiesa, R., P. Piccardo, *et al.* (1998). "Neurological illness in transgenic mice expressing a prion protein with an insertional mutation." Neuron **21**(6): 1339-51.

Chiesa, R., P. Piccardo, *et al.* (2003). "Molecular distinction between pathogenic and infectious properties of the prion protein." <u>J Virol</u> **77**(13): 7611-22.

Christensen, H. M. and D. A. Harris (2008). "Prion protein lacks robust cytoprotective activity in cultured cells." <u>Mol Neurodegener</u> **3**: 11.

Colling, S. B., J. Collinge, *et al.* (1996). "Hippocampal slices from prion protein null mice: disrupted Ca(2+)-activated K+ currents." <u>Neurosci Lett</u> **209**(1): 49-52.

Collinge, J., M. Gorham, *et al.* (2009). "Safety and efficacy of quinacrine in human prion disease (PRION-1 study): a patient-preference trial." <u>Lancet Neurol</u> **8**(4): 334-44.

Collins, S., C. A. McLean, *et al.* (2001). "Gerstmann-Straussler-Scheinker syndrome,fatal familial insomnia, and kuru: a review of these less common human transmissible spongiform encephalopathies." <u>J Clin Neurosci</u> **8**(5): 387-97.

Cotto, E., M. Andre, *et al.* (2005). "Molecular characterization, phylogenetic relationships, and developmental expression patterns of prion genes in zebrafish (Danio rerio)." <u>Febs J</u> **272**(2): 500-13.

Crozet, C., F. Flamant, *et al.* (2001). "Efficient transmission of two different sheep scrapie isolates in transgenic mice expressing the ovine PrP gene." <u>J Virol</u> **75**(11): 5328-34.

Diarra-Mehrpour, M., S. Arrabal, *et al.* (2004). "Prion protein prevents human breast carcinoma cell line from tumor necrosis factor alpha-induced cell death." <u>Cancer Res</u> **64**(2): 719-27.

Dong, J., A. Li, *et al.* (2007). "Doppel induces degeneration of cerebellar Purkinje cells independently of Bax." <u>Am J Pathol</u> **171**(2): 599-607.

Dossena, S., L. Imeri, *et al.* (2008). "Mutant prion protein expression causes motor and memory deficits and abnormal sleep patterns in a transgenic mouse model." <u>Neuron</u> **60**(4): 598-609.

Drisaldi, B., R. S. Stewart, *et al.* (2003). "Mutant PrP is delayed in its exit from the endoplasmic reticulum, but neither wild-type nor mutant PrP undergoes retrotranslocation prior to proteasomal degradation." <u>J Biol Chem</u> **278**(24): 21732-43.

Ersdal, C., M. M. Simmons, *et al.* (2004). "Relationships between ultrastructural scrapie pathology and patterns of abnormal prion protein accumulation." <u>Acta Neuropathol</u> **107**(5): 428-38.

Fioriti, L., S. Dossena, *et al.* (2005). "Cytosolic prion protein (PrP) is not toxic in N2a cells and primary neurons expressing pathogenic PrP mutations." <u>J Biol Chem</u> **280**(12): 11320-8.

Fischer, M., T. Rulicke, *et al.* (1996). "Prion protein (PrP) with amino-proximal deletions restoring susceptibility of PrP knockout mice to scrapie." Embo J **15**(6): 1255-64.

Ford, M. J., L. J. Burton, *et al.* (2002). "A marked disparity between the expression of prion protein and its message by neurones of the CNS." Neuroscience **111**(3): 533-51.

Gabriel, J. M., B. Oesch, *et al.* (1992). "Molecular cloning of a candidate chicken prion protein." Proc Natl Acad Sci U S A **89**(19): 9097-101.

Gilch, S., C. Krammer, *et al.* (2008). "Targeting prion proteins in neurodegenerative disease." Expert Opin Biol Ther **8**(7): 923-40.

Gordon, W. S. (1946). "Advances in veterinary research--looping ill, tick-borne fever and scrapie." Veterinarian Records **58**: 516-20.

Griffith, J. S. (1967). "Nature of the Scrapie Agent: Self-replication and Scrapie." Nature **215**: 1043-44.

Haass, C. and D. J. Selkoe (2007). "Soluble protein oligomers in neurodegeneration: lessons from the Alzheimer's amyloid beta-peptide." Nat Rev Mol Cell Biol **8**(2): 101-12.

Hegde, R. S., J. A. Mastrianni, *et al.* (1998). "A transmembrane form of the prion protein in neurodegenerative disease." Science **279**(5352): 827-34.

Herms, J., T. Tings, *et al.* (1999). "Evidence of presynaptic location and function of the prion protein." J Neurosci **19**(20): 8866-75.

Herms, J. W., T. Tings, *et al.* (2001). "Prion protein affects Ca2+-activated K+ currents in cerebellar purkinje cells." Neurobiol Dis **8**(2): 324-30.

Horiuchi, M., S. A. Priola, *et al.* (2000). "Interactions between heterologous forms of prion protein: binding, inhibition of conversion, and species barriers." Proc Natl Acad Sci U S A **97**(11): 5836-41.

Houston, F., S. McCutcheon, *et al.* (2008). "Prion diseases are efficiently transmitted by blood transfusion in sheep." Blood **112**(12): 4739-45.

Ivanova, L., S. Barmada, *et al.* (2001). "Mutant prion proteins are partially retained in the endoplasmic reticulum." J Biol Chem **276**(45): 42409-21.

Jackson, G. S., I. Murray, *et al.* (2001). "Location and properties of metal-binding sites on the human prion protein." Proc Natl Acad Sci U S A **98**(15): 8531-5.

Jarrett, J. T. and P. T. Lansbury, Jr. (1993). "Seeding "one-dimensional crystallization" of amyloid: a pathogenic mechanism in Alzheimer's disease and scrapie?" Cell **73**(6): 1055-8.

Jeffrey, M., C. M. Goodsir, *et al.* (1994). "Infection-specific prion protein (PrP) accumulates on neuronal plasmalemma in scrapie-infected mice." <u>Ann N Y Acad Sci</u> **724**: 327-30.

Jeffrey, M., S. Martin, *et al.* (2001). "Onset of accumulation of PrPres in murine ME7 scrapie in relation to pathological and PrP immunohistochemical changes." <u>J Comp Pathol</u> **124**(1): 20-8.

Kahana, E., M. Alter, *et al.* (1974). "Creutzfeldt-jakob disease: focus among Libyan Jews in Israel." <u>Science</u> **183**(4120): 90-1.

Kanaani, J., S. B. Prusiner, *et al.* (2005). "Recombinant prion protein induces rapid polarization and development of synapses in embryonic rat hippocampal neurons in vitro." <u>J Neurochem</u> **95**(5): 1373-86.

Kimberlin, R. H. and C. A. Walker (1979). "Pathogenesis of scrapie: agent multiplication in brain at the first and second passage of hamster scrapie in mice." <u>J Gen Virol</u> **42**(1): 107-17.

Klingenstein, R., S. Lober, *et al.* (2006). "Tricyclic antidepressants, quinacrine and a novel, synthetic chimera thereof clear prions by destabilizing detergent-resistant membrane compartments." <u>J Neurochem</u> **98**(3): 748-59.

Kocisko, D. A., J. H. Come, *et al.* (1994). "Cell-free formation of protease-resistant prion protein." <u>Nature</u> **370**(6489): 471-4.

Kong, Q., W. K. Surewicz, *et al.* (2004). Inherited Prion Diseases. <u>Prion Biology and Diseases</u>. S. B. Prusiner. Cold Spring Harbor, Cold Spring Harbor Laboratory Press**:** 673-776.

Korth, C., B. C. May, *et al.* (2001). "Acridine and phenothiazine derivatives as pharmacotherapeutics for prion disease." <u>Proc Natl Acad Sci U S A</u> **98**(17): 9836-41.

Korth, C., B. Stierli, *et al.* (1997). "Prion (PrPSc)-specific epitope defined by a monoclonal antibody." <u>Nature</u> **390**(6655): 74-7.

Kramer, M. L., H. D. Kratzin, *et al.* (2001). "Prion protein binds copper within the physiological concentration range." <u>J Biol Chem</u> **276**(20): 16711-9.

Kuwahara, C., A. M. Takeuchi, *et al.* (1999). "Prions prevent neuronal cell-line death." <u>Nature</u> **400**(6741): 225-6.

Laine, J., M. E. Marc, *et al.* (2001). "Cellular and subcellular morphological localization of normal prion protein in rodent cerebellum." <u>Eur J Neurosci</u> **14**(1): 47-56.

Lasmezas, C. I., J. P. Deslys, *et al.* (1997). "Transmission of the BSE agent to mice in the absence of detectable abnormal prion protein." <u>Science</u> **275**(5298): 402-5.

Lauren, J., D. A. Gimbel, *et al.* (2009). "Cellular prion protein mediates impairment of synaptic plasticity by amyloid-beta oligomers." <u>Nature</u> **457**(7233): 1128-32.

Le Pichon, C. E., M. T. Valley, *et al.* (2009). "Olfactory behavior and physiology are disrupted in prion protein knockout mice." <u>Nat Neurosci</u> **12**(1): 60-9.

Legname, G., I. V. Baskakov, *et al.* (2004). "Synthetic mammalian prions." <u>Science</u> **305**(5684): 673-6.

Lehmann, S. and D. A. Harris (1996). "Mutant and infectious prion proteins display common biochemical properties in cultured cells." <u>J Biol Chem</u> **271**(3): 1633-7.

Li, A., H. M. Christensen, *et al.* (2007). "Neonatal lethality in transgenic mice expressing prion protein with a deletion of residues 105-125." <u>Embo J</u> **26**(2): 548-58.

Li, A. and D. A. Harris (2005). "Mammalian prion protein suppresses Bax-induced cell death in yeast." <u>J Biol Chem</u> **280**(17): 17430-4.

Lipp, H. P., M. Stagliar-Bozicevic, *et al.* (1998). "A 2-year longitudinal study of swimming navigation in mice devoid of the prion protein: no evidence for neurological anomalies or spatial learning impairments." <u>Behav Brain Res</u> **95**(1): 47-54.

Ma, J., R. Wollmann, *et al.* (2002). "Neurotoxicity and neurodegeneration when PrP accumulates in the cytosol." <u>Science</u> **298**(5599): 1781-5.

Magalhaes, A. C., G. S. Baron, *et al.* (2005). "Uptake and neuritic transport of scrapie prion protein coincident with infection of neuronal cells." <u>J Neurosci</u> **25**(21): 5207-16.

Malaga-Trillo, E., G. P. Solis, *et al.* (2009). "Regulation of embryonic cell adhesion by the prion protein." <u>PLoS Biol</u> **7**(3): e55.

Mallucci, G., A. Dickinson, *et al.* (2003). "Depleting neuronal PrP in prion infection prevents disease and reverses spongiosis." <u>Science</u> **302**(5646): 871-4.

Mallucci, G. R., S. Ratte, *et al.* (2002). "Post-natal knockout of prion protein alters hippocampal CA1 properties, but does not result in neurodegeneration." <u>Embo J</u> **21**(3): 202-10.

Mange, A., O. Milhavet, *et al.* (2002). "PrP-dependent cell adhesion in N2a neuroblastoma cells." <u>FEBS Lett</u> **514**(2-3): 159-62.

Manson, J. C., A. R. Clarke, *et al.* (1994). "129/Ola mice carrying a null mutation in PrP that abolishes mRNA production are developmentally normal." <u>Mol Neurobiol</u> **8**(2-3): 121-7.

Marijanovic, Z., A. Caputo, *et al.* (2009). "Identification of an intracellular site of prion conversion." <u>PLoS Pathog</u> **5**(5): e1000426.

Mastrianni, J. A., S. Capellari, *et al.* (2001). "Inherited prion disease caused by the V210I mutation: transmission to transgenic mice." <u>Neurology</u> **57**(12): 2198-205.

Mathiason, C. K., J. G. Powers, *et al.* (2006). "Infectious prions in the saliva and blood of deer with chronic wasting disease." <u>Science</u> **314**(5796): 133-6.

Mattson, M. P., F. M. LaFerla, *et al.* (2000). "Calcium signaling in the ER: its role in neuronal plasticity and neurodegenerative disorders." <u>Trends Neurosci</u> **23**(5): 222-9.

McKinley, M. P., D. C. Bolton, *et al.* (1983). "A protease-resistant protein is a structural component of the scrapie prion." <u>Cell</u> **35**(1): 57-62.

McKinley, M. P., A. Taraboulos, *et al.* (1991). "Ultrastructural localization of scrapie prion proteins in cytoplasmic vesicles of infected cultured cells." <u>Lab Invest</u> **65**(6): 622-30.

Mead, S. (2006). "Prion disease genetics." <u>Eur J Hum Genet</u> **14**(3): 273-81.

Medrano, A. Z., S. J. Barmada, *et al.* (2008). "GFP-tagged mutant prion protein forms intra-axonal aggregates in transgenic mice." <u>Neurobiol Dis</u> **31**(1): 20-32.

Miesbauer, M., T. Bamme, *et al.* (2006). "Prion protein-related proteins from zebrafish are complex glycosylated and contain a glycosylphosphatidylinositol anchor." <u>Biochem Biophys Res Commun</u> **341**(1): 218-24.

Moore, R. C., I. Y. Lee, *et al.* (1999). "Ataxia in prion protein (PrP)-deficient mice is associated with upregulation of the novel PrP-like protein doppel." <u>J Mol Biol</u> **292**(4): 797-817.

Moroncini, G., N. Kanu, *et al.* (2004). "Motif-grafted antibodies containing the replicative interface of cellular PrP are specific for PrPSc." <u>Proc Natl Acad Sci U S A</u> **101**(28): 10404-9.

Moroncini, G., M. Mangieri, *et al.* (2006). "Pathologic prion protein is specifically recognized in situ by a novel PrP conformational antibody." <u>Neurobiol Dis</u> **23**(3): 717-24.

Mouillet-Richard, S., M. Ermonval, *et al.* (2000). "Signal transduction through prion protein." <u>Science</u> **289**(5486): 1925-8.

Mouillet-Richard, S., M. Pietri, *et al.* (2005). "Modulation of serotonergic receptor signaling and cross-talk by prion protein." <u>J Biol Chem</u> **280**(6): 4592-601.

Mouillet-Richard, S., B. Schneider, *et al.* (2007). "Cellular prion protein signaling in serotonergic neuronal cells." <u>Ann N Y Acad Sci</u> **1096**: 106-19.

Moya, K. L., R. Hassig, *et al.* (2004). "Enhanced detection and retrograde axonal transport of PrPc in peripheral nerve." <u>J Neurochem</u> **88**(1): 155-60.

Moya, K. L., N. Sales, *et al.* (2000). "Immunolocalization of the cellular prion protein in normal brain." <u>Microsc Res Tech</u> **50**(1): 58-65.

Nakajima, M., T. Yamada, *et al.* (2004). "Results of quinacrine administration to patients with Creutzfeldt-Jakob disease." <u>Dement Geriatr Cogn Disord</u> **17**(3): 158-63.

Nazor, K. E., F. Kuhn, *et al.* (2005). "Immunodetection of disease-associated mutant PrP, which accelerates disease in GSS transgenic mice." <u>Embo J</u> **24**(13): 2472-80.

Novitskaya, V., O. V. Bocharova, *et al.* (2006). "Amyloid fibrils of mammalian prion protein are highly toxic to cultured cells and primary neurons." <u>J Biol Chem</u> **281**(19): 13828-36.

Oesch, B., D. Westaway, *et al.* (1985). "A cellular gene encodes scrapie PrP 27-30 protein." <u>Cell</u> **40**(4): 735-46.

Orgel, L. E. (1996). "Prion replication and secondary nucleation." <u>Chem Biol</u> **3**(6): 413-4.

Pan, K. M., M. Baldwin, *et al.* (1993). "Conversion of alpha-helices into beta-sheets features in the formation of the scrapie prion proteins." <u>Proc Natl Acad Sci U S A</u> **90**(23): 10962-6.

Pauly, P. C. and D. A. Harris (1998). "Copper stimulates endocytosis of the prion protein." <u>J Biol Chem</u> **273**(50): 33107-10.

Peretz, D., R. A. Williamson, *et al.* (2001). "Antibodies inhibit prion propagation and clear cell cultures of prion infectivity." <u>Nature</u> **412**(6848): 739-43.

Petersen, R. B., P. Parchi, *et al.* (1996). "Effect of the D178N mutation and the codon 129 polymorphism on the metabolism of the prion protein." <u>J Biol Chem</u> **271**(21): 12661-8.

Piccardo, P., S. R. Dlouhy, *et al.* (1998). "Phenotypic variability of Gerstmann-Straussler-Scheinker disease is associated with prion protein heterogeneity." <u>J Neuropathol Exp Neurol</u> **57**(10): 979-88.

Piccardo, P., J. C. Manson, *et al.* (2007). "Accumulation of prion protein in the brain that is not associated with transmissible disease." <u>Proc Natl Acad Sci U S A</u> **104**(11): 4712-7.

Prestori, F., P. Rossi, *et al.* (2008). "Altered neuron excitability and synaptic plasticity in the cerebellar granular layer of juvenile prion protein knock-out mice with impaired motor control." J Neurosci **28**(28): 7091-103.

Priola, S. A., J. Chabry, *et al.* (2001). "Efficient conversion of normal prion protein (PrP) by abnormal hamster PrP is determined by homology at amino acid residue 155." J Virol **75**(10): 4673-80.

Prusiner, S. B. (1982). "Novel proteinaceous infectious particles cause scrapie." Science **216**(4542): 136-44.

Prusiner, S. B. (1989). "Scrapie prions." Annu Rev Microbiol **43**: 345-74.

Prusiner, S. B. (1998). "Prions." Proc Natl Acad Sci U S A **95**(23): 13363-83.

Prusiner, S. B., D. C. Bolton, *et al.* (1982). "Further purification and characterization of scrapie prions." Biochemistry **21**(26): 6942-50.

Prusiner, S. B., D. Groth, *et al.* (1993). "Ablation of the prion protein (PrP) gene in mice prevents scrapie and facilitates production of anti-PrP antibodies." Proc Natl Acad Sci U S A **90**(22): 10608-12.

Prusiner, S. B., D. F. Groth, *et al.* (1980). "Molecular properties, partial purification, and assay by incubation period measurements of the hamster scrapie agent." Biochemistry **19**(21): 4883-91.

Prusiner, S. B., M. Scott, *et al.* (1990). "Transgenetic studies implicate interactions between homologous PrP isoforms in scrapie prion replication." Cell **63**(4): 673-86.

Raymond, G. J., L. D. Raymond, *et al.* (2007). "Transmission and adaptation of chronic wasting disease to hamsters and transgenic mice: evidence for strains." J Virol **81**(8): 4305-14.

Riek, R., S. Hornemann, *et al.* (1997). "NMR characterization of the full-length recombinant murine prion protein, mPrP(23-231)." FEBS Lett **413**(2): 282-8.

Rodolfo, K., R. Hassig, *et al.* (1999). "A novel cellular prion protein isoform present in rapid anterograde axonal transport." Neuroreport **10**(17): 3639-44.

Rogers, M., F. Yehiely, *et al.* (1993). "Conversion of truncated and elongated prion proteins into the scrapie isoform in cultured cells." Proc Natl Acad Sci U S A **90**(8): 3182-6.

Rossi, D., A. Cozzio, *et al.* (2001). "Onset of ataxia and Purkinje cell loss in PrP null mice inversely correlated with Dpl level in brain." Embo J **20**(4): 694-702.

Rudd, P. M., T. Endo, *et al.* (1999). "Glycosylation differences between the normal and pathogenic prion protein isoforms." <u>Proc Natl Acad Sci U S A</u> **96**(23): 13044-9.

Safar, J., H. Wille, *et al.* (1998). "Eight prion strains have PrP(Sc) molecules with different conformations." <u>Nat Med</u> **4**(10): 1157-65.

Safar, J. G., K. Kellings, *et al.* (2005). "Search for a prion-specific nucleic acid." <u>J Virol</u> **79**(16): 10796-806.

Sailer, A., H. Bueler, *et al.* (1994). "No propagation of prions in mice devoid of PrP." <u>Cell</u> **77**(7): 967-8.

Sakaguchi, S., S. Katamine, *et al.* (1996). "Loss of cerebellar Purkinje cells in aged mice homozygous for a disrupted PrP gene." <u>Nature</u> **380**(6574): 528-31.

Sakudo, A., D. C. Lee, *et al.* (2003). "Impairment of superoxide dismutase activation by N-terminally truncated prion protein (PrP) in PrP-deficient neuronal cell line." <u>Biochem Biophys Res Commun</u> **308**(3): 660-7.

Sales, N., R. Hassig, *et al.* (2002). "Developmental expression of the cellular prion protein in elongating axons." <u>Eur J Neurosci</u> **15**(7): 1163-77.

Santuccione, A., V. Sytnyk, *et al.* (2005). "Prion protein recruits its neuronal receptor NCAM to lipid rafts to activate p59fyn and to enhance neurite outgrowth." <u>J Cell Biol</u> **169**(2): 341-54.

Schenkein, J. and P. Montagna (2006). "Self management of fatal familial insomnia. Part 1: what is FFI?" <u>MedGenMed</u> **8**(3): 65.

Scheper, W. and J. J. Hoozemans (2009). "Endoplasmic reticulum protein quality control in neurodegenerative disease: the good, the bad and the therapy." <u>Curr Med Chem</u> **16**(5): 615-26.

Schiff, E., V. Campana, *et al.* (2008). "Coexpression of wild-type and mutant prion proteins alters their cellular localization and partitioning into detergent-resistant membranes." <u>Traffic</u> **9**(7): 1101-15.

Schmitt-Ulms, G., G. Legname, *et al.* (2001). "Binding of neural cell adhesion molecules (N-CAMs) to the cellular prion protein." <u>J Mol Biol</u> **314**(5): 1209-25.

Schneider, B., V. Mutel, *et al.* (2003). "NADPH oxidase and extracellular regulated kinases 1/2 are targets of prion protein signaling in neuronal and nonneuronal cells." <u>Proc Natl Acad Sci U S A</u> **100**(23): 13326-31.

Schwappach, B. (2008). "An overview of trafficking and assembly of neurotransmitter receptors and ion channels (Review)." <u>Mol Membr Biol</u> **25**(4): 270-8.

Scott, M. R., R. Will, *et al.* (1999). "Compelling transgenetic evidence for transmission of bovine spongiform encephalopathy prions to humans." <u>Proc Natl Acad Sci U S A</u> **96**(26): 15137-42.

Shields, S. B. and S. J. Franklin (2007). "Investigation of the affinity and selectivity of avian prion hexarepeat peptides for physiological divalent metal ions." <u>J Inorg Biochem</u> **101**(5): 783-8.

Shmerling, D., I. Hegyi, *et al.* (1998). "Expression of amino-terminally truncated PrP in the mouse leading to ataxia and specific cerebellar lesions." <u>Cell</u> **93**(2): 203-14.

Shyng, S. L., M. T. Huber, *et al.* (1993). "A prion protein cycles between the cell surface and an endocytic compartment in cultured neuroblastoma cells." <u>J Biol Chem</u> **268**(21): 15922-8.

Silveira, J. R., G. J. Raymond, *et al.* (2005). "The most infectious prion protein particles." <u>Nature</u> **437**(7056): 257-61.

Simoneau, S., H. Rezaei, *et al.* (2007). "In vitro and in vivo neurotoxicity of prion protein oligomers." <u>PLoS Pathog</u> **3**(8): e125.

Singh, N., G. Zanusso, *et al.* (1997). "Prion protein aggregation reverted by low temperature in transfected cells carrying a prion protein gene mutation." <u>J Biol Chem</u> **272**(45): 28461-70.

Spilman, P., P. Lessard, *et al.* (2008). "A gamma-secretase inhibitor and quinacrine reduce prions and prevent dendritic degeneration in murine brains." <u>Proc Natl Acad Sci U S A</u> **105**(30): 10595-600.

Stahl, N., M. A. Baldwin, *et al.* (1992). "Glycosylinositol phospholipid anchors of the scrapie and cellular prion proteins contain sialic acid." <u>Biochemistry</u> **31**(21): 5043-53.

Stewart, R. S., B. Drisaldi, *et al.* (2001). "A transmembrane form of the prion protein contains an uncleaved signal peptide and is retained in the endoplasmic Reticulum." <u>Mol Biol Cell</u> **12**(4): 881-9.

Stewart, R. S. and D. A. Harris (2001). "Most pathogenic mutations do not alter the membrane topology of the prion protein." <u>J Biol Chem</u> **276**(3): 2212-20.

Stimson, E., J. Hope, *et al.* (1999). "Site-specific characterization of the N-linked glycans of murine prion protein by high-performance liquid chromatography/electrospray mass spectrometry and exoglycosidase digestions." <u>Biochemistry</u> **38**(15): 4885-95.

Surewicz, W. K., E. M. Jones, *et al.* (2006). "The emerging principles of mammalian prion propagation and transmissibility barriers: Insight from studies in vitro." <u>Acc Chem Res</u> **39**(9): 654-62.

Taguchi, Y., Z. D. Shi, *et al.* (2009). "Specific biarsenical labeling of cell surface proteins allows fluorescent- and biotin-tagging of amyloid precursor protein and prion proteins." <u>Mol Biol Cell</u> **20**(1): 233-44.

Tamguney, G., K. Giles, *et al.* (2006). "Transmission of elk and deer prions to transgenic mice." <u>J Virol</u> **80**(18): 9104-14.

Taylor, D. R. and N. M. Hooper (2006). "The prion protein and lipid rafts." <u>Mol Membr Biol</u> **23**(1): 89-99.

Taylor, D. R., N. T. Watt, *et al.* (2005). "Assigning functions to distinct regions of the N-terminus of the prion protein that are involved in its copper-stimulated, clathrin-dependent endocytosis." <u>J Cell Sci</u> **118**(Pt 21): 5141-53.

Telling, G. C., T. Haga, *et al.* (1996). "Interactions between wild-type and mutant prion proteins modulate neurodegeneration in transgenic mice." <u>Genes Dev</u> **10**(14): 1736-50.

Tobler, I., S. E. Gaus, *et al.* (1996). "Altered circadian activity rhythms and sleep in mice devoid of prion protein." <u>Nature</u> **380**(6575): 639-42.

Trifilo, M. J., M. Sanchez-Alavez, *et al.* (2008). "Scrapie-induced defects in learning and memory of transgenic mice expressing anchorless prion protein are associated with alterations in the gamma aminobutyric acid-ergic pathway." <u>J Virol</u> **82**(20): 9890-9.

Turner, M. L. and C. A. Ludlam (2009). "An update on the assessment and management of the risk of transmission of variant Creutzfeldt-Jakob disease by blood and plasma products." <u>Br J Haematol</u> **144**(1): 14-23.

Unterberger, U., R. Hoftberger, *et al.* (2006). "Endoplasmic reticulum stress features are prominent in Alzheimer disease but not in prion diseases in vivo." <u>J Neuropathol Exp Neurol</u> **65**(4): 348-57.

Van Everbroeck, B., P. Pals, *et al.* (1999). "Antigen retrieval in prion protein immunohistochemistry." <u>J Histochem Cytochem</u> **47**(11): 1465-70.

Waggoner, D. J., B. Drisaldi, *et al.* (2000). "Brain copper content and cuproenzyme activity do not vary with prion protein expression level." <u>J Biol Chem</u> **275**(11): 7455-8.

Walter, E. D., M. Chattopadhyay, *et al.* (2006). "The affinity of copper binding to the prion protein octarepeat domain: evidence for negative cooperativity." <u>Biochemistry</u> **45**(43): 13083-92.

Walz, R., O. B. Amaral, *et al.* (1999). "Increased sensitivity to seizures in mice lacking cellular prion protein." <u>Epilepsia</u> **40**(12): 1679-82.

Weissmann, C., H. Bueler, *et al.* (1994). "PrP-deficient mice are resistant to scrapie." Ann N Y Acad Sci **724**: 235-40.

Williamson, R. A., D. Peretz, *et al.* (1998). "Mapping the prion protein using recombinant antibodies." J Virol **72**(11): 9413-8.

Wroe, S. J., S. Pal, *et al.* (2006). "Clinical presentation and pre-mortem diagnosis of variant Creutzfeldt-Jakob disease associated with blood transfusion: a case report." Lancet **368**(9552): 2061-7.

Young, K., P. Piccardo, *et al.* (1999). Prions: Molecular and Cellular Biology. Wymondham, Horizon Scientific Press.

Yu, S., S. Yin, *et al.* (2007). "Aggregation of prion protein with insertion mutations is proportional to the number of inserts." Biochem J **403**(2): 343-51.

Zahn, R., A. Liu, *et al.* (2000). "NMR solution structure of the human prion protein." Proc Natl Acad Sci U S A **97**(1): 145-50.

CHAPTER 2

GFP-tagged mutant prion protein forms intra-axonal aggregates in transgenic mice

A Medrano, S Barmada, E Biasini, & DA Harris.

2.1 Summary

A nine-octapeptide insertional mutation in the prion protein (PrP) causes a fatal neurodegenerative disorder in both humans and transgenic mice. To determine the precise cellular localization of this mutant PrP (designated PG14), we have generated transgenic mice expressing PG14-EGFP, a fluorescent fusion protein that can be directly visualized *in vivo*. Tg(PG14-EGFP) mice develop an ataxic neurological illness characterized by astrogliosis, PrP aggregation, and accumulation of a partially protease-resistant form of the mutant PrP. Strikingly, PG14-EGFP forms numerous fluorescent aggregates in the neuropil and white matter of multiple brain regions. These aggregates are particularly prominent along axonal tracts in both brain and peripheral nerve, and similar intracellular deposits are visible along the processes of cultured neurons. Our results reveal intra-axonal aggregates of a mutant PrP, which could contribute to the pathogenesis of familial prion disease by disrupting axonal transport.

2.2 Introduction

Prions are infectious proteins associated with several fatal neurodegenerative diseases in mammals (Prusiner, 2004). Prion diseases result from conversion of the cellular prion protein (PrP^C) into a conformationally altered isoform (PrP^{Sc}) that is aggregated and protease-resistant. Dominantly inherited mutations in the gene encoding PrP are responsible for familial forms of prion disease (Kong et al., 2004).   One mutant, designated PG14, harbors a nine-octapeptide repeat insertion in the N-terminal region of PrP that is associated with ataxia, dementia, and cerebellar PrP plaques in several families (Duchen et al., 1993; Krasemann et al., 1995; Owen et al., 1992). Tg(PG14) mice expressing the mouse homolog of the PG14 mutant develop an ataxic neurological illness characterized by non-amyloid PrP deposits, apoptosis of cerebellar granule neurons, and loss of synaptophysin-positive nerve terminals (Chiesa et al., 2000; Chiesa et al., 2005; Chiesa et al., 1998).

Elucidating the mechanisms by which PG14 and other mutant PrPs induce neuropathology requires information about the localization of these molecules at the anatomical and subcellular levels. However, immunolocalization of PG14 PrP deposits in brain tissue has proven to be technically challenging due to the poor antibody reactivity of the mutant protein as a result of conformational changes and/or aggregation. Like PrP^{Sc}, PG14 PrP possesses hidden epitopes that prevent antibody recognition without the use of harsh antigen retrieval techniques, such as hydrolytic autoclaving or treatment with guanidine thiocyanate (Kitamoto et al., 1987; Kitamoto et al., 1992; Van Everbroeck et al., 1999). However, these techniques, which denature or partially hydrolyze proteins, necessarily introduce a number of potential artifacts.

Our previous immunohistochemical studies identified punctate, most likely extracellular deposits of PG14 PrP in the cerebellum and other brain regions of Tg(PG14) mice (Chiesa et al., 2000; Chiesa et al., 1998). However, intracellular aggregates of the protein in neuronal cell bodies or axons were never observed. This result is surprising, given the known cellular trafficking patterns of PrP along secretory, endocytic and axonal transport pathways (Harris, 2003), as well as our own previous observation that mutant PrP molecules are partially retained in the endoplasmic reticulum of cultured cells (Ivanova et al., 2001). These considerations suggest that conventional immunohistochemical methods may be providing an incomplete picture of the localization of PG14 in brain tissue.

To overcome the limitations of immunocytochemical detection, we have developed lines of transgenic mice expressing PrP-EGFP, a fusion protein incorporating enhanced green fluorescent protein (EGFP) inserted near the C-terminal, glycolipid attachment site of PrP. In mice that express PrP-EGFP incorporating wild-type (WT) PrP, the fluorescent protein is correctly synthesized and posttranslationally modified, and is distributed in an anatomic and subcellular pattern similar to that of untagged PrP (Barmada et al., 2004). In addition, the fusion protein retains functional activity, as assayed by a genetic test (Barmada et al., 2004). We have used Tg(WT-EGFP) mice to monitor the distribution of PrP^{Sc} after scrapie inoculation (Barmada and Harris, 2005).

In the present study, we report the construction and characterization of transgenic mice expressing the PG14 version of WT-EGFP. Our results provide, for the first time, evidence for an intra-axonal localization of a mutant PrP, and they suggest that disruption of axonal transport may play a role in the phenotype of familial prion disorders.

59

2.3 Materials & Methods

Transgenic mice. The PG14-EGFP construct was generated as described by Ivanova et al. (2001) by inserting the EGFP open reading frame into the *Stu*I site (within codon 223, wild-type numbering) of a plasmid encoding murine PG14 PrP tagged with the 3F4 epitope. The PG14-EGFP open reading frame was then amplified by PCR with *Sal*I ends, and cloned initially into pGEM-T and then into the *Xho*I site of the MoPrP.XhoI transgenic vector (Borchelt et al., 1996) as described by Barmada et al. (2004). The transgene was excised with *Not*I and microinjected into the pronuclei of fertilized eggs from an F_2 cross of C57BL/6J X CBA/J F_1 parental mice. Founder animals were identified by PCR screening of tail DNA using primers P1 (AACCGAGCTGAAGCATT) and P4 (CACGAGAAATGCGAAGGAACAAGC). Tg(PG14-EGFP) lines were established by breeding transgene-positive founders to a recombinant inbred strain of C57BL/6J X CBA/J mice. All mice used in this study were bred onto a *Prn-p*$^{+/+}$ (C57BL/6J X CBA/J) background, with the exception of one (Figure 3D), which had been bred onto a *Prn-p*$^{0/0}$ (C57BL/6J x 129) background (Büeler et al., 1992). All mice were housed in a pathogen-free environment and were cared for following the guidelines set forth by the Washington University Policy on Animal Care.

The following mouse lines have been described previously: Tg(WT-EGFP) (line A) (Barmada et al., 2004), Tg(PG14) (line A2) (Chiesa et al., 1998), Tg(WT) (line E1) (Chiesa et al., 1998), and *Prn-p*$^{0/0}$ (Büeler et al., 1992).

Mice were checked weekly for symptoms of neurological dysfunction. Kyphosis, seizure, foot clasp, and hyperexcitability were determined by visual observation, while

ataxia was tested by placing mice in the center of a horizontally oriented grill (45 x 45 cm) consisting of 3 mm diameter steel rods spaced 7 mm apart. Mice unable to maneuver around the grid were scored as ataxic. Animals that exhibited at least two symptoms were scored as ill.

Paraffin sections. Mice were injected intraperitoneally with heparin anticoagulant (1,000 U/ml), then anesthetized by injection of ketamine (Fort Dodge Animal Health, Fort Dodge, IA) and xylazine (Butler Animal Health Supply, Dublin, OH). Animals were perfused intracardially with 50 ml of saline solution, followed by 40 ml of 4% paraformaldehyde in 0.1M sodium phosphate buffer (pH 7.2). Brains were removed and then post-fixed in the same solution for 48 hrs. After bisecting the brain along the mid-sagittal plane, each hemisphere was dehydrated in graded ethanol solutions, cleared in xylene, and then embedded in paraffin. Six μm sagittal sections were cut and mounted on polylysine coated glass slides.

Hematoxylin and eosin staining was performed after dewaxing sections in xylene and rehydrating them in graded ethanol solutions. For assessing astrocytosis, dewaxed and rehydrated sections were stained with anti-GFAP monoclonal antibody (DAKO, Carpinteria, CA), followed by incubation with Alexa 594-coupled goat anti-mouse IgG (Molecular Probes, Eugene, OR). Sections were imaged using a Nikon TE2000-E inverted fluorescence microscope.

Fluorescence microscopy. Animals were fixed by intracardiac perfusion as above. Brains were then removed and then post-fixed in the same solution for 2 hrs before transfer to 0.1M sodium phosphate buffer (pH 7.2) containing 0.02% sodium azide for storage at 4°C. A vibratome (The Vibratome Company, St. Louis, MO) was used to

cut the tissue into 60 μm thick sagittal sections. Sections were mounted on glass slides using Gel/Mount (Biomeda, Foster City, CA). Intrinsic EGFP fluorescence was imaged using a Zeiss LSM 510 inverted confocal microscope with an Axiovert 200 laser scanning system.

To visualize PrP, vibratome sections were stained with antibodies P45-66 (Lehmann and Harris, 1995), 3F4 (Bolton et al., 1991), or 8H4 (Zanusso et al., 1998). Some sections were stained with antibodies directed against giantin (Covance, Berkeley, CA), TRAP (Upstate, Charlottesville, VA), LAMP1 (1D4B, Developmental Studies Hybridoma Bank, Univ. of Iowa, Iowa City, IA), MAP2 (Sigma, St. Louis, MO), or GFP (gift of Maurine Linder, Washington University). Primary antibodies were visualized using Alexa 488-coupled goat anti-rabbit IgG (P45-66, GFP), Alexa 488-coupled anti-mouse IgG (3F4, 8H4), or Alexa 594-coupled goat anti-mouse IgG (giantin, TRAP, LAMP1, MAP2). Sections were then imaged as described above.

Biochemical analyses. Brain homogenates (10% w/v) were prepared in ice-cold PBS using a Teflon-glass apparatus with pestle revolving at 3,500 rpm (Wheaton Science Products, Millville, NJ). A postnuclear supernatant was obtained by centrifuging homogenates at 1,000 x g for 5 min. Protein concentration was determined using a BCA assay (Pierce, Rockford, IL). Homogenates were analyzed by SDS-PAGE followed by Western blot using anti-PrP antibodies 8H4 (Zanusso et al., 1998) or 3F4 (Bolton et al., 1991).

To quantitate protein expression levels, serial dilutions of Tg(PG14-EGFP)$^{+/o}$ mouse brain homogenate were analyzed by Western blot using Image J software

(National Institutes of Health, USA). The amount of PG14-EGFP was calibrated by comparison to the level of endogenous PrP.

To assay protease resistance, frozen brain hemispheres were homogenized in detergent buffer (DB: 10 mM Tris-HCl, pH 7.4, 0.5% sodium deoxycholate, 0.5% NP-40, 150 mM NaCl), then assayed for protein concentration as described above. Two hundred μg of total protein were diluted in DB to a final concentration of 1 μg/μl. The solution was mixed for 10 min at 4°C, then centrifuged at 1,500 x g for 5 min at 4°C. 0.5-2 μg/ml of proteinase K was added to the supernatant and the mixture was incubated at 37°C for 30 min. Phenylmethylsulfonyl fluoride (PMSF; 10 mg/ml) was added to terminate digestion. Proteins were isolated using methanol precipitation, then analyzed by SDS-PAGE and Western blotting.

To assay detergent insolubility, brain homogenates prepared in DB were diluted to 0.4 μg/μl in the presence of protease inhibitors (1 μg/ml pepstatin and leupeptin, 0.5 mM PMSF, and 2 mM EDTA), then incubated for 20 min at 4°C. The sample was centrifuged at 1,500 x g for 5 min at 4°C. The supernatant was then recovered and centrifuged for 75 min at 135,000 x g at 4°C to separate soluble and insoluble fractions. Proteins from the supernatant of this subsequent centrifugation were recovered by methanol precipitation, and then both the supernatant and pellet fractions were analyzed by SDS-PAGE.

To test sensitivity to phosphatidylinositol-specific phospholipase C (PIPLC), 200 μg of postnuclear supernatant was centrifuged at 16,000 x g at 4°C for 5 min to collect membranes. Membrane pellets were resuspended in PBS with *B. thuringiensis* PIPLC (prepared as described in Shyng et al. (1995)) at a final concentration of 1 unit/ml, then

incubated on ice for 2.5 hrs. Membranes were then collected again by centrifugation at

16,000 $x g$, and proteins released into the supernatant were precipitated with methanol.

Membrane pellets and proteins precipitated from the supernatant were resuspended in gel

loading buffer and analyzed by SDS-PAGE and Western blotting.

To immunoprecipitate aggregated PrP with antibody 15B3, we followed the

procedure recommended by Prionics (Zurich, Switzerland), utilizing the buffers supplied

by them. First, a 100 µl aliquot of mouse anti-IgM Dynabeads (Dynal, Carlsbad, CA)

was coated with 20 µg of mAb 15B3. Ten µl of 15B3-coated Dynabeads were then

added to 200 µg of total protein from brain homogenates. Samples were incubated on a

rotating wheel for 2 hr at 25°C, after which beads were washed three times with 1 ml of

15B3 Wash Buffer (Prionics, Zurich, Switzerland). Washed beads were suspended in 40

µl of 2X 15B3 Loading Buffer (Prionics) and heated for 5 min at 96°C.

Immunoprecipitated proteins were resolved by SDS-PAGE followed by Western blotting

with 6D11 antibody (Pankiewicz et al., 2006).

Neuronal cell culture and transfection. Cerebellar granule neurons (CGNs) were

isolated from 4 day old mouse pups according to methods described previously (Miller

and Johnson, 1996). Neurons were plated in CGN medium (basal medium Eagle's with

Earle's salts, 10% fetal calf serum, 2 mM glutamine, 25 mM KCl, 0.1 mg/ml

gentamycin). Cells were plated at a density of 375,000-450,000/cm^2 onto 35 mm glass-

bottom dishes pre-coated with poly-D-lysine. Cultures were stained with FM 4-64

(Invitrogen) according to the manufacturer's directions.

EGFP-WT and EGFP-PG14 constructs (in which EGFP is inserted near the N-

terminus of PrP) were generated by first cleaving the EGFP open reading frame from the

pEGFP-C1 plasmid (Clontech, Mountain View, CA) using restriction enzymes *Nco*I and

*EcoR*I. Both ends were blunted, then ligated into the *AgeI* site (within codon 33) of a

pcDNA3 plasmid encoding murine WT or PG14 PrP tagged with the 3F4 epitope. The

resulting plasmids were introduced into CGNs cultured from non-transgenic mice by

transfection using Lipofectamine 2000 (Invitrogen, Carlsbad, CA). Cells were analyzed

24 hrs after transfection.

Primary neurons were imaged in the living state using a Zeiss LSM 510 inverted

confocal microscope with an Axiovert 200 laser scanning system using LSM Image

Browser software. For kymograph analysis, we used a Nikon TE-2000E inverted

fluorescence microscope, and images were captured and analyzed with Metamorph

imaging software.

2.4 Results

Weak immunostaining of native PG14 PrP in brain sections. In all of our

previous studies using immunostaining to localize PG14 PrP in paraffin-embedded brain

sections from Tg(PG14) mice, antigen retrieval treatments (guanidine thiocyanate plus

hydrolytic autoclaving) were applied to partially denature the mutant PrP and so enhance

its immunoreactivity (Chiesa et al., 2000; Chiesa et al., 2005; Chiesa et al., 1998; Chiesa

et al., 2003). To test the reactivity of PG14 PrP in the native state, we immunostained

vibratome sections without pre-treatment. We observed that, while brain sections from

Tg(WT) mice (expressing wild-type PrP) stained strongly with antibodies directed

against three different regions of the PrP molecule (supplemental Figure 1A, D, G),

sections from Tg(PG14) mice produced only a low level of fluorescence (supplemental

Figure 1B, E, H). Western blots confirmed that the expression levels of PG14 and WT

PrP are similar (Chiesa et al., 1998). We noted that, although the fluorescence signal

observed in Tg(PG14) brains was low with all three antibodies, it was detectably above

the background level seen in $Prn-p^{0/0}$ mice that do not express any PrP (supplemental

Figure 1C, F, I). This residual signal is most likely due to the presence of a sub-

population of PG14 PrP molecules (designated PG14^{Sol}) that are soluble and that possess

all of the biochemical properties of PrP^C, including reactivity with antibodies that

recognize PrP^C-accessible epitopes (Biasini et al., manuscript submitted).

Construction of Tg(PG14-EGFP) mice. To allow antibody-independent

localization of PG14 PrP, we generated transgenic mice expressing PG14-EGFP, a fusion

protein in which the EGFP moiety is inserted near the C-terminal glycolipid attachment

site of PrP harboring the PG14 mutation (Figure 1A). For comparison, we used Tg(WT-

EGFP) mice expressing the wild-type version of PrP-EGFP, which have been described

previously (Barmada et al., 2004) (Figure 1A). Both WT-EGFP and PG14-EGFP were

constructed with an epitope tag for the 3F4 antibody (Bolton et al., 1991), which allows

discrimination of transgenically encoded PrP from endogenous PrP. The PG14-EGFP

fusion construct was cloned into the MoPrP.XhoI vector (Borchelt et al., 1996), which

contains a partial promoter sequence from the endogenous PrP gene. This promoter

drives protein expression in a developmental and tissue-specific pattern comparable to

that of endogenous PrP, with the exception that the transgene is not expressed in Purkinje

cells (Barmada et al., 2004; Fischer et al., 1996).

Four separate lines of Tg(PG14-EGFP) mice were established (D, X1, X3, and X4). Anatomical localization of PG14-EGFP within the brain was unusual in line D, which showed preferential expression of the fluorescent protein in the mossy fibers, alveus, and stratum lacunosum moleculare, but low expression elsewhere (supplemental Figure 2B). This unusual expression pattern is likely due to the site of transgene integration. In contrast, the gross neuroanatomical distribution of fluorescent protein in the X1, X3 and X4 lines was similar to that of WT-EGFP (Barmada et al., 2004) (supplemental Figure 2D-O), and to the known distribution of endogenous PrP^C (Moya et al., 2000; Salès et al., 1998). However, only the X4 line expressed PG14-EGFP at a sufficiently high level to be detected by fluorescence microscopy without the aid of anti-GFP labeling (supplemental Figure 2). Although the X4 line served as the primary source of data for the experiments described below, the subcellular distribution of PG14-EGFP (including the presence of axonal aggregates, see results) was confirmed in the D line using the intrinsic fluorescence of EGFP and in the X1 and X3 lines by staining with anti-GFP antibody (supplemental Figure 2, and data not shown).

Western blot analysis of brain homogenates confirmed expression of PG14-EGFP protein in transgenic animals. PG14-EGFP migrates at approximately 85 kDa, larger than WT-EGFP which migrates at 60-70 kDa (Figure 1B,C). Antibody 8H4 recognizes both endogenous and transgenic PrPs (Figure 1C), whereas 3F4 identifies only transgenically encoded PrP molecules (PG14, WT-EGFP and PG14-EGFP), each of which carries the 3F4 epitope tag (Figure 1B). Based on quantitative Western blotting, we determined that expression of PG14-EGFP in animals of the X4 line was ~0.15X that
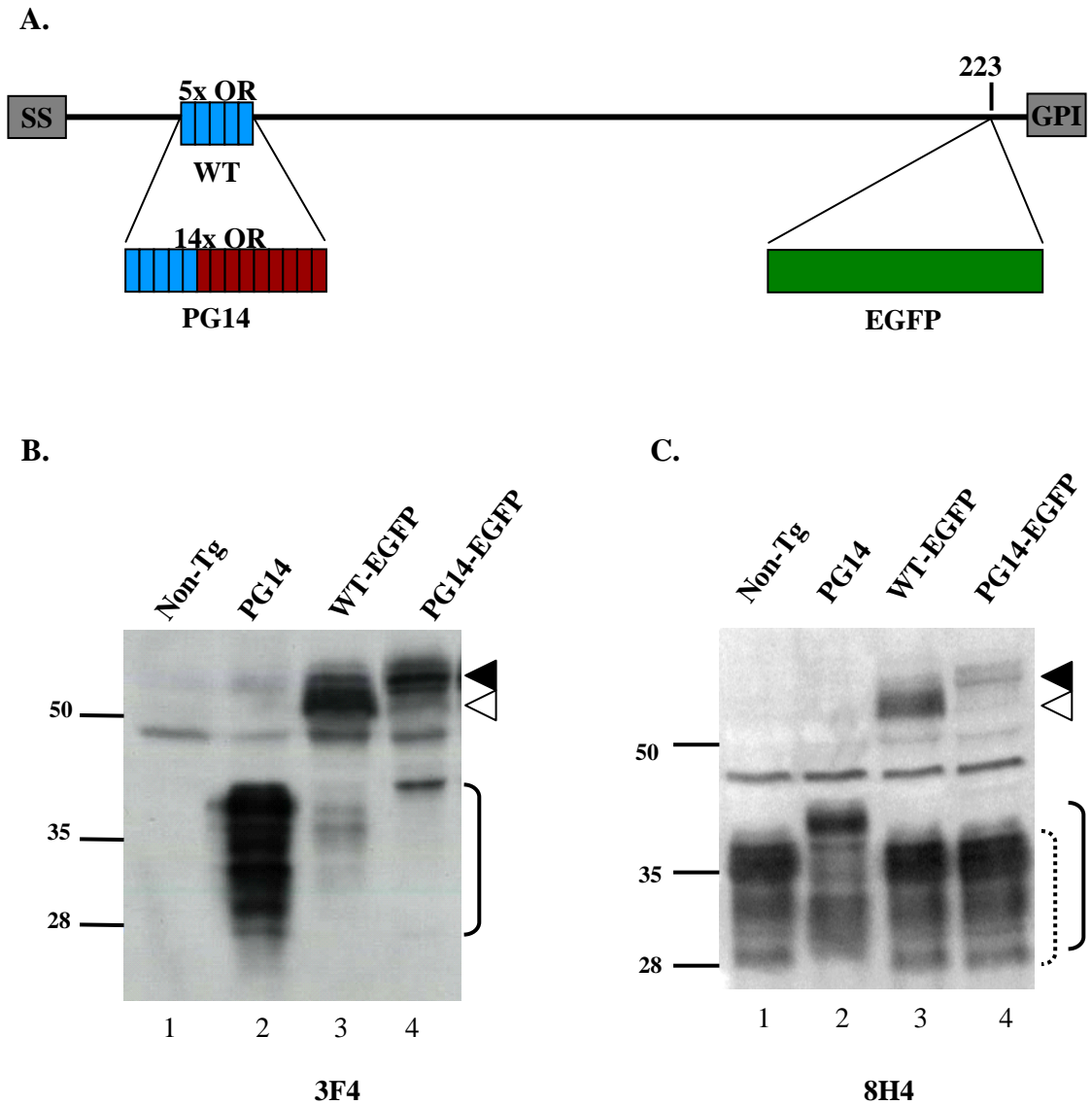
FIGURE 1. Structure and expression of WT-EGFP and PG14-EGFP in transgenic mice. (A) Schematic of the structures of WT-EGFP and PG14-EGFP. WT-EGFP contains an N-terminal signal sequence (SS), five octapeptide repeats (OR, blue), and a C-terminal GPI addition signal (GPI). The EGFP tag is inserted at codon 223. PG14-EGFP is similar to WT-EGFP, but contains nine additional octapeptide repeats (OR, red), resulting in a total of 14 repeats. (B, C) Expression of WT-EGFP and PG14-EGFP. Brain homogenates from non-transgenic (lane 1), Tg(PG14) (lane 2), Tg(WT-EGFP) (lane 3), and Tg(PG14-EGFP) (lane 4) mice were analyzed by Western blotting using anti-PrP antibodies 3F4 (B) and 8H4 (C). All mice were on the *Prn-p*$^{+/+}$ background. ▲, PG14-EGFP; △, WT-EGFP; solid bracket, PG14 PrP; dotted bracket, endogenous WT PrP. Molecular size markers are given in kilodaltons.

of endogenous PrP in mice carrying a hemizygous transgene array, and ~0.3X in those

carrying a homozygous transgene array (data not shown).

Tg(PG14-EGFP) mice develop a spontaneous neurological illness. Tg(PG14-

EGFP) mice that were homozygous for the transgene array developed spontaneous

neurological disease at 391 ± 54 days (Table 1). Symptoms in these animals included

kyphosis, ataxia, foot clasp, poor grooming, hyperexcitability, and seizures. The same

clinical features were also present in approximately 10% of Tg(PG14-EGFP)

hemizygotes, but they appeared only at much later ages (~630 days).   All Tg(WT-EGFP)

mice remained healthy (Table 1), as reported previously (Barmada et al., 2004).

Histological analysis revealed prominent astrogliosis in the cerebella and

hippocampi of homozygous Tg(PG14-EGFP) mice compared with Tg(WT-EGFP)

controls (Figure 2A, C, D, F). Healthy Tg(PG14-EGFP) heterozygotes exhibited some

astrogliosis, although of a lesser severity than their homozygote counterparts (Figure 2B,

E). Cerebellar sections from either homozygous or heterozygous Tg(PG14-EGFP) mice

stained with hematoxylin and eosin did not show significant granule cell loss or other

obvious histological abnormalities (Figure 2G-I). Consistent with these observations, we

did not detect positive staining in the cerebellum by the TUNEL method, which reveals

dying cells undergoing DNA fragmentation (data not shown).

PG14-EGFP possesses PrP^{Sc}-like biochemical properties. To investigate

whether PG14-EGFP displays abnormal biochemical properties like untagged PG14 PrP,

Table 1. Disease onset in Tg(PG14-EGFP) animals

Genotype	Age of Onset
WT-EGFP[+/o]	>600 (0/7)
PG14-EGFP^{+/+}	391 ± 54 (6/7)
PG14-EGFP[+/o]	$630d \pm 43$ (2/27)
PG14[+/o]	235 ± 10 (61/61)[a]

Age of onset is recorded in days. Numbers in parentheses indicate the number of ill mice over the total number of animals observed. [a] Data taken from Chiesa et. al. (2000).
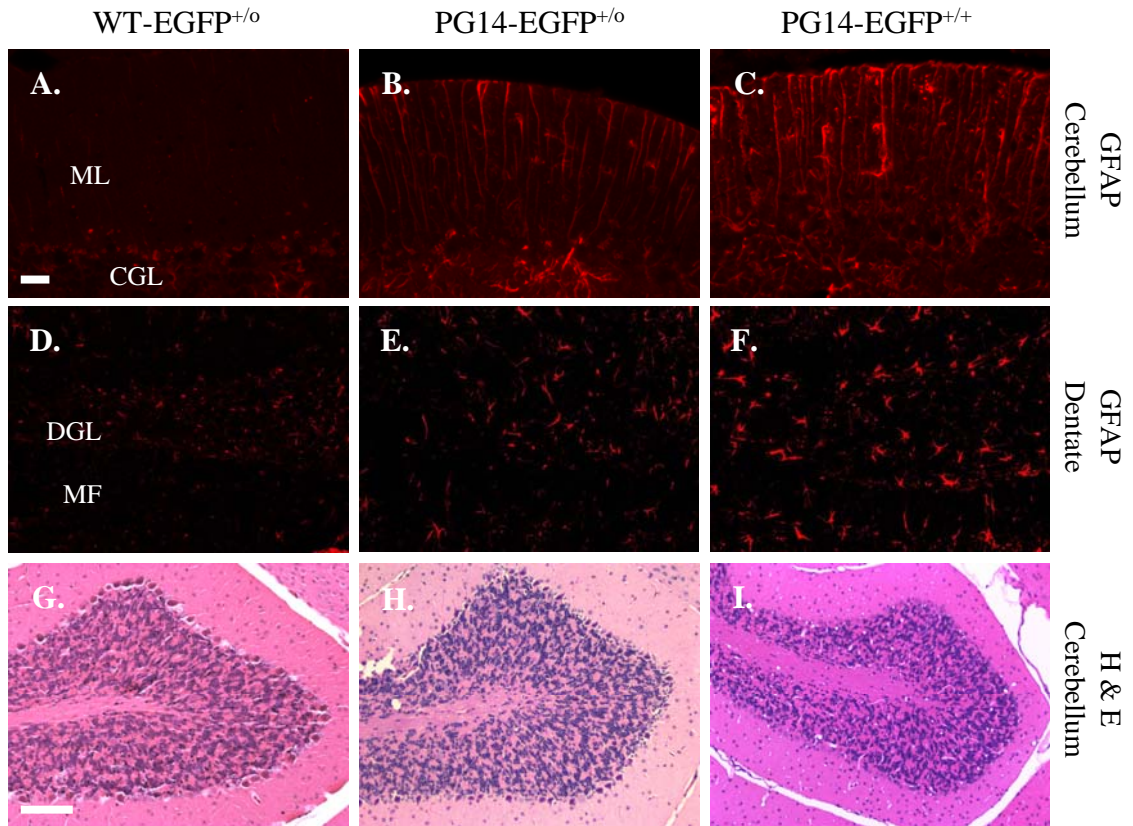
FIGURE 2. Tg(PG14-EGFP) mice exhibit astrogliosis but not loss of cerebellar granule cells.
Paraffin sections from cerebellum (A-C, G-I) and dentate gyrus (D-F) were stained with an antibody against GFAP (A-F), or with hematoxylin and eosin (G-I). Sections were obtained from age-matched healthy Tg(WT-EGFP$^{+/0}$) mice (A, D, G), healthy Tg(PG14-EGFP$^{+/0}$) mice (B, E, H), and clinically ill Tg(PG14-EGFP$^{+/+}$) mice (C, F, I). The abbreviations are: ML, molecular layer; CGL, cerebellar granule cell layer; DGL, dentate granule cell layer; MF, mossy fibers. Scale bars are 20 μm for A-F and 200 μm for G-I.

we performed assays for protease resistance, detergent insolubility, phospholipase

sensitivity, and immunoprecipitation by the PrP^{Sc}-reactive antibody 15B3.

Like untagged PG14 PrP, PG14-EGFP is weakly protease resistant, producing a

PrP 27-30 core fragment when subjected to digestion with proteinase K (PK)

concentrations of 0.5-2 μg/ml (Figure 3A, lanes 1-4, 9). In contrast, WT-EGFP was

completely digested by PK under the same conditions (Figure 3A, lanes 5-8).

To test detergent insolubility, detergent lysates of brain were subjected to

ultracentrifugation to separate soluble from insoluble protein fractions. As expected,

WT-EGFP is recovered almost entirely in the supernatant (S, soluble) fraction in this

assay (Figure 3B, lanes 5, 6). In contrast, PG14-EGFP, like untagged PG14 PrP, was

found in both supernatant and pellet (P, insoluble) fractions (Figure 3B, lanes 1-4). In

multiple experiments, the proportion of insoluble PG14-EGFP varied from 25-50% (data

not shown).

PIPLC is a bacterial enzyme that cleaves the glycosylphosphatidylinositol (GPI)

anchor that attaches PrP to cellular membranes, thereby releasing the protein into the

extracellular medium. PG14 PrP is partially resistant to the action of PIPLC, probably

due to aggregation and/or conformational changes at the C-terminus of the protein, as

opposed to aberrant GPI anchor incorporation (Chiesa et al., 1998; Lehmann and Harris,

1995; Narwa and Harris, 1999). After PIPLC treatment of brain membranes,

approximately half of the total amount of WT-EGFP shifts into the supernatant (S)

fraction, indicating partial release of the protein (Figure 3C, lanes 1, 2, 5, 6). Incomplete

release of WT PrP from brain membranes has been observed previously (Chiesa et al.,

1998; Ivanova et al., 2001), and is probably attributable to the mixed topology of the

membranous vesicles produced by homogenization. In contrast, the majority of PG14-EGFP remains associated with the membrane (P) fraction, demonstrating that the protein is partially resistant to PIPLC cleavage, like untagged PG14 (Figure 3C, lanes 3, 4, 7, 8). Also similar to untagged PG14, a small fraction of PG14-EGFP is found to be PIPLC-sensitive (Figure 3C, lane 7), demonstrating that the protein contains a functional GPI anchor. Thus, the presence of the EGFP tag does not interfere with GPI anchoring of either WT or PG14 PrP.

15B3 is a monoclonal antibody that was originally reported to react specifically with PrP^{Sc} and not PrP^{C} (Korth et al., 1997). Recently, we have shown that this antibody recognizes multiple forms of aggregated PrP, both infectious and non-infectious, including PG14 PrP from both transfected cells and transgenic mouse brain (Biasini et al., manuscript submitted). The antibody shows no reactivity with monomeric PrP^{C}, even when present in vast excess. We found that 15B3 immunoprecipitated both PG14-EGFP and untagged PG14 PrP, but did not recognize wild-type PrP from both Tg(WT) and non-transgenic mice (Figure 3D). Thus, PG14-EGFP and PG14 PrP share aggregation-specific, 15B3-reactive epitopes.

Collectively, these results show that PG14-EGFP behaves like untagged PG14 in four different assays that measure PrP^{Sc}-like biochemical properties.

PG14-EGFP forms aggregates in multiple brain regions. To compare the distributions of PG14-EGFP and WT-EGFP in brain tissue, vibratome sections from transgenic mice were examined using fluorescence microscopy. Consistent with our previous analysis (Barmada et al., 2004), we found that WT-EGFP was concentrated
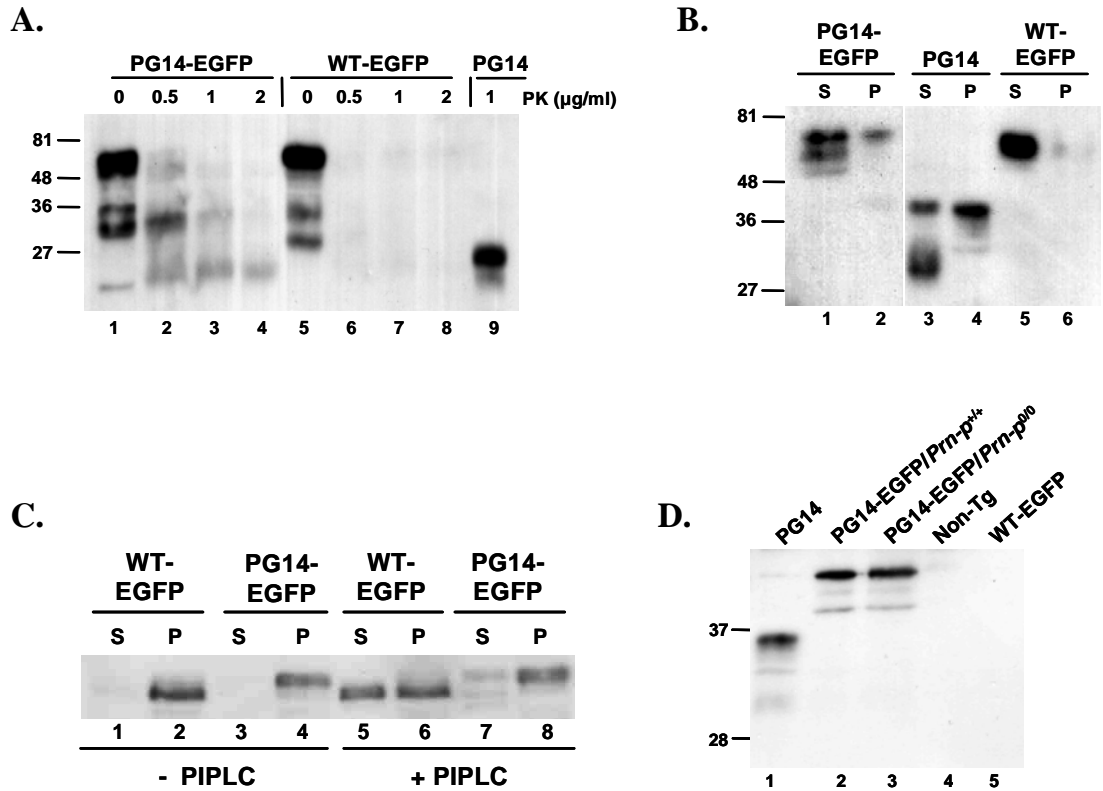
FIGURE 3. PG14-EGFP displays abnormal biochemical properties like untagged PG14 PrP. (A) Assay for protease resistance. Brain homogenates from Tg(PG14-EGFP) mice (lanes 1-4), Tg(WT-EGFP) mice (lanes 5-8) and Tg(PG14) mice (lane 9) were treated with the indicated concentrations of PK, and then subjected to Western blotting with 3F4 antibody. PG14-EGFP and PG14, but not WT-EGFP, give rise to PrP 27-30 fragments. (B) Assay for detergent insolubility. Brain homogenates from Tg(PG14-EGFP) mice (lanes 1, 2), Tg(PG14) mice (lanes 3, 4) and Tg(WT-EGFP) mice (lanes 5, 6) were subjected to ultracentrifugation, followed by Western blotting of supernatant (S lanes) and pellet fractions (P lanes) using 3F4 antibody. PG14-EGFP and PG14 PrP, but not WT-EGFP, are partially detergent insoluble. (C) Assay for PIPLC release. Brain membranes from Tg(WT-EGFP) mice (lanes 1, 2, 5, 6) and Tg(PG14-EGFP) mice (lanes 3, 4, 7, 8) were incubated without (lanes 1-4) or with (lanes 5-8) PIPLC. Membranes were then collected by centrifugation, and PrP in pellets (P lanes) and supernatants (S lanes) was analyzed by Western blotting with 8H4 antibody. WT-EGFP, but not PG14-EGFP, is partially released by PIPLC. (D) Test of reactivity with antibody 15B3. Brain homogenates from the following mice were subjected to immunoprecipitation with 15B3, followed by Western blotting with 6D11 antibody: Tg(PG14)/*Prn-p*[0/0] (lane 1); Tg(PG14-EGFP)/*Prn-p*^{+/+} (lane 2); Tg(PG14-EGFP)/*Prn-p*[0/0] (lane 3); non-Tg (lane 4); and Tg(WT-EGFP) (lane 5). One-fifth as much brain homogenate was used as starting material in lane 1 as in the other lanes. All Tg(PG14-PrP) mice were hemizygous for the transgene array, and all had a *Prn-p*^{+/+} genetic background unless otherwise stated.

primarily in neuropil areas that are rich in synapses as well as along axon tracts, and was present only at low levels in dendrites and neuronal somata. In the hippocampus, for example, fluorescence was distributed in the stratum oriens and stratum radiatum of the CA1 region (Figure 4A). Mossy fibers in the dentate gyrus were also fluorescent (Figure 4C). In the cerebellum, WT-EGFP was present in the molecular layer, as well as in neuropil of the granule cell layer (Figure 4E). In these three brain regions, the fluorescence signal had a relatively uniform distribution, with the exception of fluorescent puncta in the cell bodies of pyramidal and granule neurons, corresponding to the location of the Golgi apparatus in these cells (Barmada et al., 2004) (arrows in Figure 4A, C, E).

The distribution PG14-EGFP was markedly different from that of WT-EGFP. In Tg(PG14-EGFP) mice, bright, intensely fluorescent aggregates were visible in multiple brain areas. In the CA1 region of the hippocampus, PG14-PrP aggregates were found in the stratum oriens, and to a lesser extent in the stratum radiatum and the pyramidal cell layer (Figure 4B). Intensely fluorescent aggregates of PG14-EGFP were also evident along mossy fibers of the hippocampus (Figure 4D, K, L), as well as in the molecular layer of the cerebellum (Figure 4F), the neocortex (Figure 4G. H), and the striatum (Figure 4I, J). In general, PG14-EGFP aggregates were concentrated in the same brain regions that displayed high levels of WT-EGFP in Tg(WT-EGFP) mice (Barmada et al., 2004). The aggregates were often distributed in a linear pattern that seemed to correspond to the course of individual neuronal processes (arrowheads in Figure 4D, J). Although much of the PG14-EGFP signal was present in the form of discrete fluorescent aggregates, these aggregates were superimposed on a more uniform, but less intense
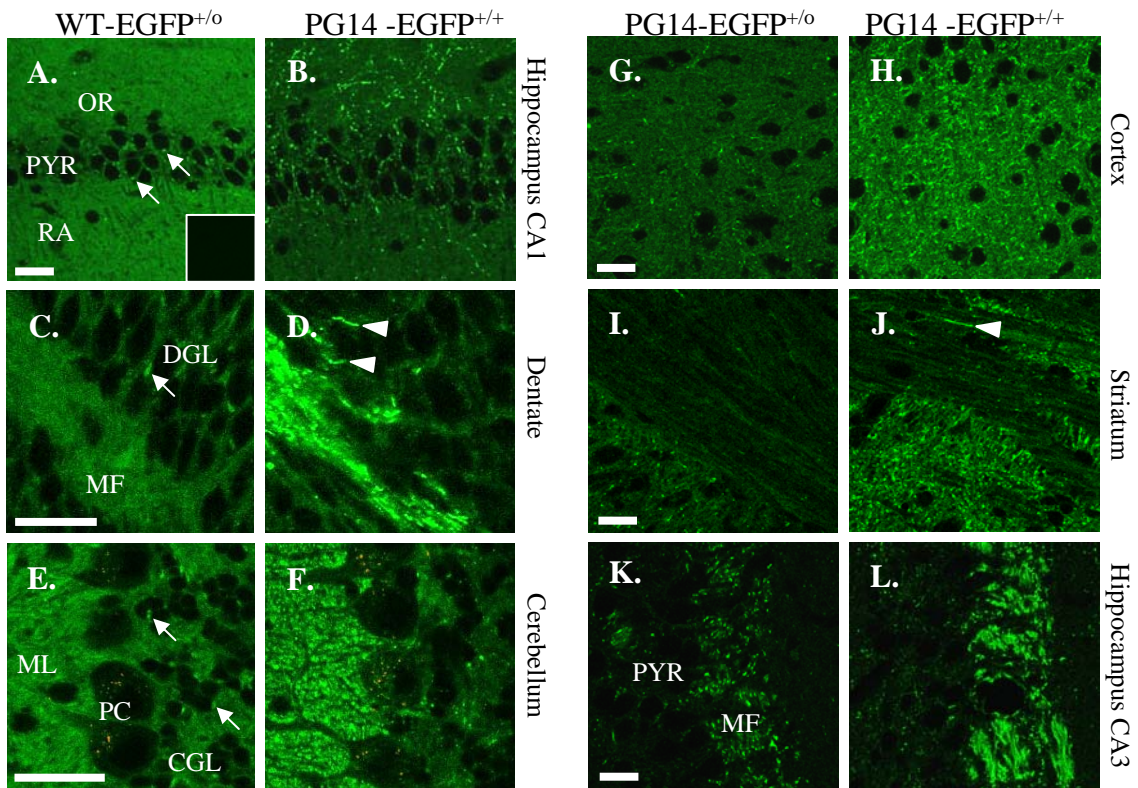
FIGURE 4. PG14-EGFP forms aggregates in multiple brain regions. (A-F) Comparison of the distributions of WT-EGFP and PG14-EGFP in brain sections. Vibratome sections from healthy Tg(WT-EGFP$^{+/0}$) mice (A, C, E) and ill, age-matched Tg(PG14-EGFP$^{+/+}$) mice (B, D, F) were prepared from the CA1 region of the hippocampus (A, B), the dentate gyrus (C, D), and the cerebellar cortex (E, F), and were imaged by fluorescence microscopy. The inset in panel A shows a brain section from a non-transgenic, *Prn-p$^{+/+}$* mouse, to illustrate the background level of fluorescence. PG14-EGFP forms numerous fluorescent aggregates, whereas WT-EGFP has a much more uniform distribution. (G-L) The number of PG14-EGFP aggregates is higher in mice with a homozygous transgene array. Sections from healthy Tg(PG14-EGFP$^{+/0}$) mice (G, I, K) and ill, age-matched Tg(PG14-EGFP$^{+/+}$) mice (H, J, L) were prepared from the neocortex (G, H), the striatum (I, J), and the CA3 region of the hippocampus (K, L). Aggregate concentration is increased in animals expressing twice the amount of the transgenic mutant protein. The arrowheads in D and J indicate linear aggregates of PG14-EGFP that probably lie within individual axons. The arrows in A, C and E indicate accumulations of WT-EGFP in the Golgi apparatus of neuronal cell bodies. The abbreviations are: OR, stratum oriens; PYR, pyramidal cell layer; RA, stratum radiatum; DGL, dentate granule cell layer; MF, mossy fibers; CGL, cerebellar granule cell layer; ML, molecular layer, PC, Purkinje cell layer. All scale bars represent 20 μm.

76

background of fluorescence that was similar in appearance to the pattern observed in

Tg(WT-EGFP) mice (Figure 4A-F). This latter signal was specific, since it was absent in

non-transgenic mice (inset, Figure 4A), and is likely attributable to non-aggregated forms

of PG14-EGFP (see Discussion).

Although fluorescent aggregates were observed in all Tg(PG14-EGFP) animals,

we found that aggregate concentration was directly correlated with the level of transgene

expression. Thus, Tg (PG14-EGFP) animals that were homozygous for the transgene

array accumulated more numerous fluorescent aggregates than animals that were

hemizygous for the transgene array (Figure 4G-L).

PG14-EGFP aggregates are present in axons but not dendrites. Aggregates of

PG14-EGFP were found at highest density in myelinated and unmyelinated axon bundles,

and could often be observed arrayed along the course of individual axons. In the

striatum, axonal fibers cut in cross-section were intensely fluorescent, and fibers cut

longitudinally displayed bright fluorescent puncta along their length (Figure s. 4J, 5F).

Aggregates were also visible in the alveus (Figure 5G) and corpus callosum (Figure 5H)

which contain myelinated axons, as well as along unmyelinated mossy fibers in the

hippocampus (Figure 4D). Aggregates were prominent in peripheral as well as central

axons, for example, along fibers of the sciatic nerve (Figure 5J). PG14-EGFP deposition

did not occur along all axonal tracts, however. For example, aggregates were sparse

along white matter tracts of the cerebellum (Figure 5I). In contrast to PG14-EGFP, WT-

EGFP displayed a relatively homogeneous, non-aggregated distribution in each of these

areas (Figure 5A-E). While WT-EGFP appeared to uniformly coat the surface of axonal

77

fibers, PG14-EGFP fluorescence was restricted to punctate deposits that seemed to be intra-axonal. This conclusion was borne out by analysis of neurons in culture (see below).

To determine whether PG14-EGFP aggregates were present in dendrites as well as axons, we stained brain sections with an antibody to MAP2, a somatodendritic marker protein. We found that fluorescent deposits of PG14-EGFP did not co-localize with MAP2, for example in the apical dendrites of pyramidal neurons in the stratum lucidum of the CA3 region of the hippocampus (Figure 5K-M). We conclude that PG14-EGFP, like WT-EGFP (Barmada et al., 2004), is present primarily in axons, and is largely absent from dendrites.

PG14-EGFP aggregates do not co-localize with markers for the ER, Golgi, or lysosomes. We reported previously that mutant PrP molecules, including those harboring the PG14 mutation, are partially retained in the ER of non-neuronal cells (Ivanova et al., 2001). In addition, PrP^{Sc} has been localized to the Golgi apparatus (Barmada and Harris, 2005) as well as to lysosomes (Laszlo et al., 1992) in brain tissue. To determine if PG14-EGFP is found in these intracellular organelles in neurons, we analyzed the distribution of the fluorescent protein in brain sections that were stained for markers representing the ER, Golgi, and lysosomes. We found that most PG14-EGFP aggregates did not co-localize in neuronal cell bodies with markers for the ER (TRAP), Golgi (giantin), or lysosomes (LAMP1) (Figure 6). As is the case for WT-EGFP (Barmada et al., 2004), a few PG14-EGFP puncta in the perinuclear region of large neurons appeared to co-

78
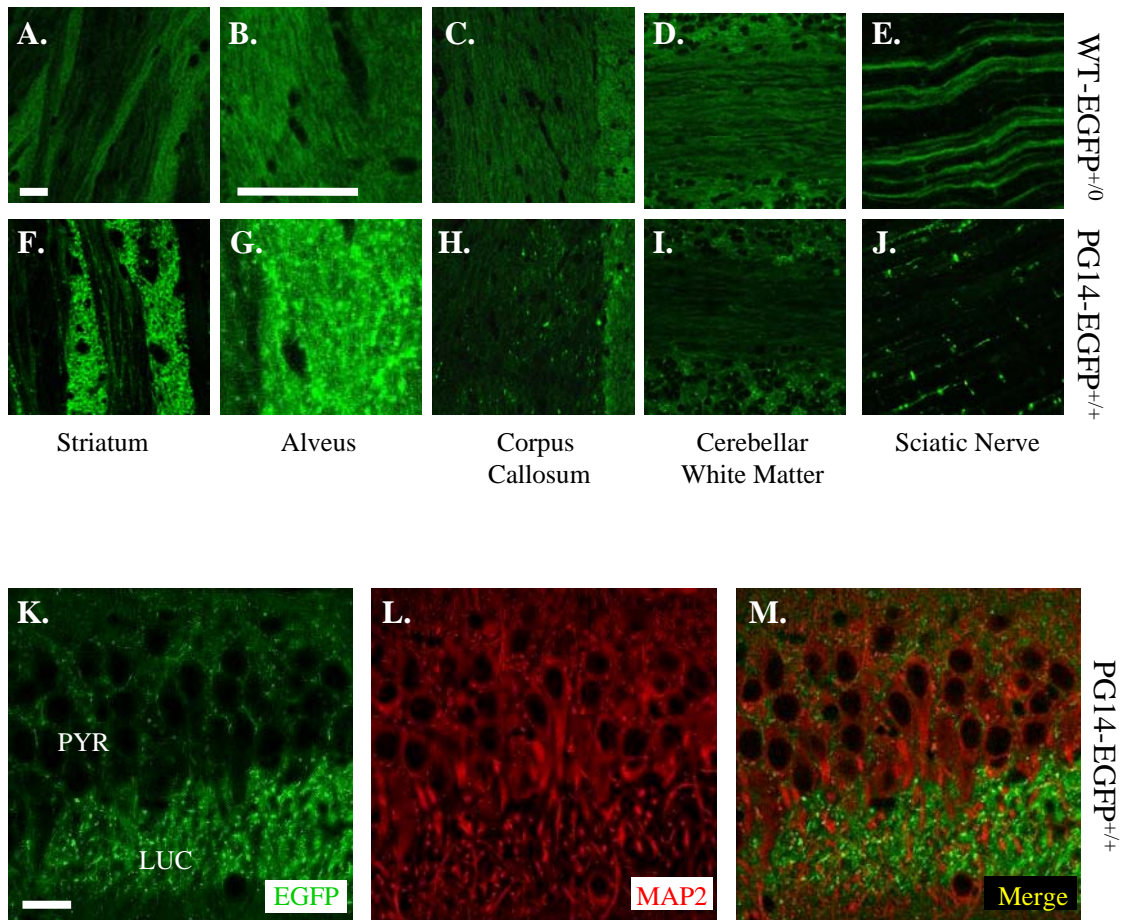
FIGURE 5. PG14-EGFP aggregates are present in axons but not dendrites. (A-J) Comparison of the distributions of WT-EGFP and PG14-EGFP in several axon-rich regions of the brain, and in peripheral nerve. Vibratome sections from healthy Tg(WT-EGFP$^{+/0}$) mice (A-E) and ill, age-matched Tg(PG14-EGFP$^{+/+}$) mice (F-J) were prepared from the striatum (A, F), the alveus (B, G), the corpus callosum (C, H), and the cerebellar white matter (D, I). Sciatic nerves were examined as whole mounts (E, J). (K-M) PG14-EGFP does not co-localize with a somatodendritic marker. A section from the CA3 area of the hippocampus from an ill Tg(PG14-EGFP$^{+/+}$) mouse was immunostained for MAP2. The section was then viewed for EGFP fluorescence (K), MAP2 staining (L), and as a merged image of the two signals (M). The abbreviations are: PYR, pyramidal cell layer; LUC, stratum lucidum. The scale bars in A (applicable to A, C-F, H-J), B (applicable to B, G), and K (applicable to K-M) represent 20 μm.
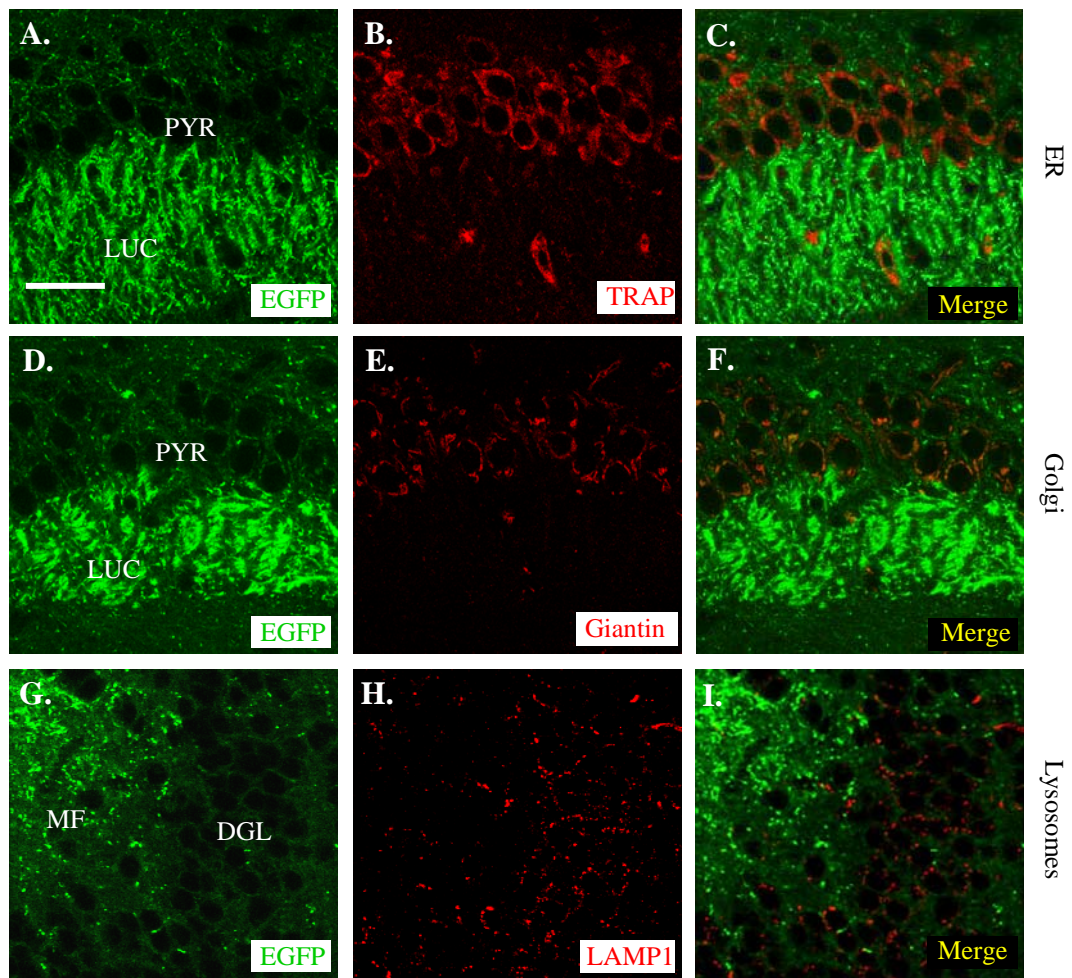
FIGURE 6. PG14-EGFP aggregates do not co-localize with markers for the ER, Golgi, or lysosomes. Vibratome sections from the brains of ill Tg(PG14-EGFP+/+) mice were stained with antibodies to TRAP (an ER marker) (A-C), giantin (a Golgi marker) (D-F), or LAMP1 (a lysosomal marker) (G-I). Sections were derived from the CA3 area of the hippocampus (A-F) or the dentate gyrus (G-I). Sections were viewed for EGFP fluorescence (A, D, G), for marker protein staining (B, E, H), or as a merged image of the two signals (C, F, I). The abbreviations are: PYR, pyramidal cell layer; LUC, stratum lucidum; DGL, dentate granule cell layer; MF, mossy fibers. The scale bar is 20 μm (applicable to all panels).

localize with the Golgi marker, giantin, presumably representing protein in transit through the secretory pathway (not shown).

PG14-EGFP forms aggregates along neurites of cultured neurons and is decreased at the cell surface. To determine the subcellular localization of WT-EGFP and PG14-EGFP more precisely, we analyzed cultures of cerebellar granule neurons (CGNs) prepared from neonatal transgenic mice. WT-EGFP was distributed in a rim around neuronal cell bodies, as well as along neuritic processes (Figure 7A, B). The protein showed a relatively uniform distribution, with only a few, small, perinuclear puncta corresponding to the location of the Golgi apparatus (not shown). In contrast, PG14-EGFP was distributed in numerous, large, intensely fluorescent aggregates along neuritic processes (Figure 7C, D).

In order to visualize the fluorescence signal in individual neurons more clearly, we transiently transfected cultures of non-transgenic CGNs with EGFP expression constructs. Because of the low efficiency of transfection (~1%), isolated, fluorescent neurons could then be observed against a background of non-fluorescent neurons. For these experiments, we employed plasmids encoding C-terminal PrP-EGFP fusions analogous to those used to construct the Tg(WT-EGFP) and Tg(PG14-EGFP) mice (data not shown), as well as N-terminal fusions in which EGFP was fused at codon 33, ten amino acids beyond the signal peptide cleavage site (Figure 7E, F). N- and C-terminal fusion proteins displayed similar distributions, arguing that the location of the EGFP moiety has no effect on protein localization. We observed that EGFP-WT uniformly filled the entire neuritic tree out to the smallest, terminal branches, and also formed a rim

around the cell soma (Figure 7E). In contrast, EGFP-PG14 was distributed in numerous, fluorescent puncta along the length of individual neurites, and was also visible in the cell soma in the form of cytoplasmic aggregates that were located at a distance from the surface membrane (Figure 7F).

To determine whether the fluorescent proteins were localized on the plasma membrane, we stained cultures with FM 4-64, a red fluorescent dye that selectively integrates into the lipid bilayer at the cell surface (Betz et al., 1992). We found that while WT-EGFP almost completely co-localized with FM 4-64 (Figure 7G-I), aggregates of PG14-EGFP showed little co-localization (Figure 7J-L).

Taken together, our studies of cultured CGNs demonstrate that neuronal PG14-EGFP aggregates are primarily intracellular (not on the cell surface), and are concentrated in neuritic processes. Since the culture conditions we used do not induce axo-dendritic polarization of CGNs (Powell et al., 1997), it is not possible to specify whether the neuritic PG14-EGFP aggregates we observe are in axons or dendrites.

2.5 Discussion

In this study, we have characterized Tg(PG14-EGFP) mice that express the EGFP-tagged version of a mutant PrP molecule carrying a nine-octapeptide insertion. This PG14 mutant is associated with an inherited dementia in humans (Duchen et al., 1993; Krasemann et al., 1995; Owen et al., 1992), and we have reported previously that it causes a strong neurodegenerative phenotype when expressed as a non-EGFP-tagged molecule in Tg(PG14) transgenic mice (Chiesa et al., 2000; Chiesa et al., 2005; Chiesa et al., 1998). We show here that Tg(PG14-EGFP) mice recapitulate key clinical,
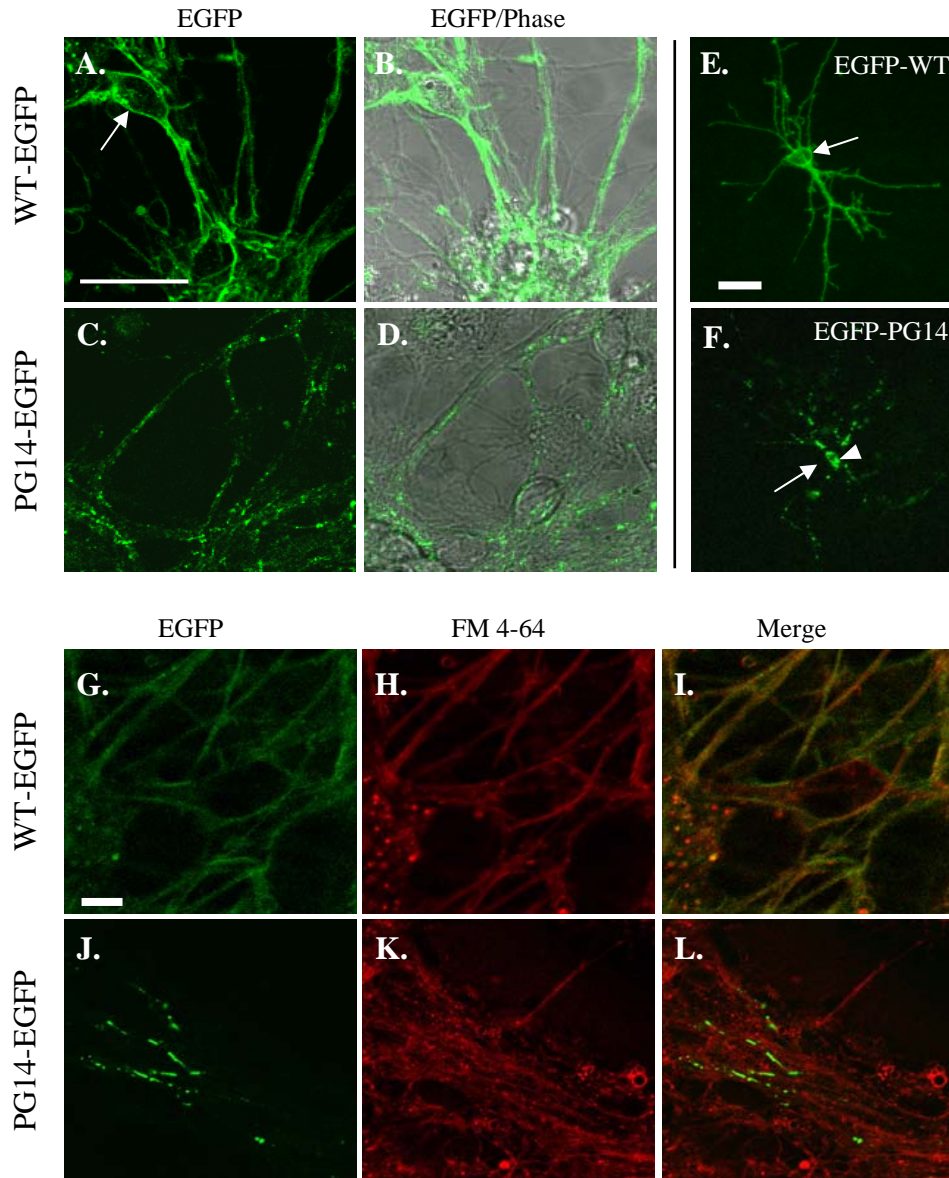
FIGURE 7. PG14-EGFP forms aggregates along neurites of cultured neurons and is decreased at the cell surface. (A-D) Comparison of the distribution of WT-EGFP and PG14-EGFP. Cerebellar granule neurons were cultured from neonatal Tg(WT-EGFP) mice (A, B) or Tg(PG14-EGFP) mice (C, D). After 4 days in culture, cells were viewed by fluorescence (A, C), or by fluorescence superimposed on phase contrast (B, D). The arrow in A points to a neuronal cell body, which is rimmed by fluorescence. (E, F) Distribution of N-terminal EGFP fusion proteins in individual neurons. Cerebellar granule neurons cultured from non-Tg mice were transfected with plasmids encoding EGFP-WT (E) or EGFP-PG14 (F), and were viewed 24 hrs later by fluorescence microscopy. The arrow in E points to a neuronal cell body, which is rimmed by fluorescence. The arrow in F points to the position of the surface membrane of the soma (visible in phase contrast; not shown), which is devoid of fluorescence. The arrowhead in F indicates intracellular accumulations of EGFP-PG14. (G-L) Localization of EGFP fusion proteins with respect to the plasma membrane. Cerebellar granule neurons cultured from Tg(WT-EGFP) mice (G-I) or Tg(PG14-EGFP) mice (J-L) were stained with FM 4-64 dye at 4°C, and then imaged to reveal EGFP fluorescence (G, J), FM 4-64 staining (H, K), or a merge of the two signals (I, L). WT-EGFP co-localizes extensively with FM 4-64, while PG14-EGFP shows little overlap. All scale bars represent 20 μm.

neuropathological and biochemical features of our original Tg(PG14) mice. However, the presence of the EGFP moiety has allowed us to visualize the anatomical and subcellular localization of the mutant protein without the need for antigen retrieval techniques typically required for immunohistochemical detection of aggregated, misfolded forms of PrP. Using Tg(PG14-EGFP) mice, we describe for the first time intracellular aggregates of mutant PrP in central and peripheral axons. Our results provide an entirely new picture of the localization of mutant PrP molecules in a familial prion disease, and they suggest a novel mechanism by which these proteins might induce neuropathology via interference with axonal transport.

Tg(PG14-EGFP) mice model a familial prion disease. Like Tg(PG14) mice, Tg(PG14-EGFP) animals spontaneously develop a progressive neurological disease characterized clinically by ataxia, kyphosis, and seizure. In addition, both kinds of mice exhibit astrogliosis and PrP deposition. Finally, PG14-EGFP displays abnormal biochemical properties like PG14 PrP. In contrast, Tg(WT-EGFP) mice do not develop neurological illness or neuropathology, and they do not accumulate biochemically abnormal PrP. Taken together, these results argue that the C-terminal addition of EGFP does not significantly alter the molecular properties or pathogenic effects of PG14 PrP. Thus, Tg(PG14-EGFP) mice, like the original Tg(PG14) animals, model key features of the corresponding human prion disease.

Tg(PG14-EGFP$^{+/+}$) mice (X4 line) develop disease at ~390 days of age, much later than Tg(PG14$^{+/+}$) or Tg(PG14$^{+/-}$) mice (65 or 240 days, respectively, for the A2 and A3 lines) (Chiesa et al., 1998). This difference is most likely attributable to the

significantly lower transgene expression level in the Tg(PG14-EGFP) X4 line compared to the Tg(PG14) lines (0.3X vs. 2X endogenous PrP levels when the transgene arrays are homozygous). We have previously observed a strong inverse correlation between protein expression level and age at disease onset in Tg(PG14) mice (Chiesa et al., 1998). Thus far, we have not recovered lines of Tg(PG14-EGFP) mice with higher transgene expression levels, but it is uncertain whether this reflects a particular toxicity of the PG14-EGFP molecule or other factors.

The relatively low transgene expression level in Tg(PG14-EGFP) mice is also likely to explain why these animals did not exhibit granule cell degeneration in the cerebellum, in contrast to Tg(PG14) mice which show dramatic granule cell apoptosis (Chiesa et al., 2000; Chiesa et al., 1998). In a previous study, we found that deletion of the Bax gene rescued granule cell death without altering clinical symptoms or synaptic degeneration in Tg(PG14) mice (Chiesa et al., 2005). We thus concluded that synaptic loss makes an important contribution to the Tg(PG14) phenotype that can account for the persistence of neurological symptoms in the absence of granule cell death. We hypothesize that in Tg(PG14-PrP) mice, which display a much more indolent clinical course compared to Tg(PG14) mice, the low expression level of the mutant protein produces synaptic degeneration before granule cell loss can ensue.

PG14-EGFP forms aggregates in axons. A major conclusion of our study is that PG14-EGFP forms prominent intra-axonal aggregates. These aggregates were visible in axon-rich areas of the brain such as the molecular layer of the cerebellum, striatum, corpus callosum, and mossy fibers of the hippocampus. They were also

85

prominent in peripheral axons, in particular those of the sciatic nerve. In cultured

cerebellar granule neurons, PG14-EGFP aggregates were evident within neurites, where

they did not colocalize with a marker for the plasma membrane, demonstrating that the

deposits are intracellular. The fluorescent aggregates visible microscopically presumably

correspond to those that are defined biochemically by detergent insolubility, protease and

PIPLC resistance, and 15B3 reactivity. In brain sections from Tg(PG14-EGFP) mice, we

observed, in addition to aggregates, a more uniform, but weaker fluorescence pattern

similar to the one seen in Tg(WT-EGFP) mice. This fluorescence signal presumably

corresponds to the proportion (50-75%) of PG14-EGFP that is soluble (see Figure 3B).

We have referred to the soluble form of PG14 PrP as PG14^{Sol}, and have shown that it

possesses all of the biochemical properties of PrP^C (Biasini et al., manuscript submitted).

It is likely that PG14-EGFP aggregates contribute to the disease phenotype,

although the precise relationship requires further investigation. We observed that the

number of PG14-EGFP aggregates is positively correlated with transgene expression

level: Tg(PG14-EGFP$^{+/+}$) mice, most of which become ill, displayed more aggregates

than Tg(PG14-EGFP$^{+/-}$) mice, most of which remain healthy. However, aggregation of

PG14 PrP occurs long before the onset of neuropathology or clinical disease, as indicated

by the existence of fluorescent aggregates in neonatal neurons (Figure 7) and by the

presence of detergent-insoluble protein in neonatal brain tissue (Chiesa et al., 1998).

These observations suggest that the pathological consequences of PrP aggregation may

take an extended time to evolve. Alternatively, aggregates may increase in size or

number over time until a critical threshold level is reached for induction of disease.

When we compared young and old animals, we did not observe dramatic differences in

the number, size, or distribution of aggregates (data not shown), although careful quantitation will be required to test the possibility that subtle alterations may occur slowly with aging.

Because PrP is a GPI-linked membrane protein, the intra-axonal deposits of PrP-EGFP we observe presumably reside in the lumen of intracellular transport vesicles. These deposits may represent aggregates of the mutant protein within individual vesicles, or possibly collections of multiple vesicles. The axonal localization of PG14-EGFP aggregates is consistent with evidence from immunolocalization studies demonstrating that endogenous PrP is present on axons and pre-synaptic nerve terminals (Moya et al., 2000; Salès et al., 1998), and that it is subject to both anterograde and retrograde fast axonal transport (Borchelt et al., 1994; Moya et al., 2004; Rodolfo et al., 1999).

New insights into mutant PrP localization and trafficking. The picture of PG14 PrP localization in brain provided here using the intrinsic fluorescence of an EGFP fusion protein differs markedly from the one suggested by previous studies of Tg(PG14) mice, all of which relied upon immunostaining following application of antigen retrieval techniques. These earlier studies revealed punctate deposits of the mutant protein in numerous brain regions, including the cerebellum, hippocampus and neocortex. The deposits, which were present primarily in neuropil regions and were largely absent from white matter, were characterized as "synaptic-like", since they had a distribution reminiscent of synaptic terminals (Chiesa et al., 2000; Chiesa et al., 1998). Recent electron microscopic studies indicate that these deposits are primarily extracellular (M. Jeffrey, A.Z. Medrano, S. Barmada, and D.A. Harris, unpublished data).

87

Although intracellular deposits of misfolded forms of PrP, including PrP^{Sc}, have been described in a few conventional immunohistochemical studies of brain (Kovacs et al., 2005; Laszlo et al., 1992), such deposits may be particularly susceptible to loss or redistribution induced by antigen retrieval methods, explaining why most studies have emphasized extracellular aggregates. Thus, we believe that PrP-EGFP fusion proteins provide a more accurate representation of the distribution of PrP aggregates, particularly those localized to intracellular compartments, than conventional immunocytochemistry. Recently, we have identified prominent intraneuronal deposits of PrP^{Sc} in scrapie-infected Tg(WT-EGFP) mice (Barmada and Harris, 2005). Some of these deposits were localized to the Golgi apparatus in neuronal cell bodies, and some were also present along axons. Thus, intra-axonal aggregation may be common to both PrP^{Sc} and mutant forms of PrP.

The findings reported here also significantly extend our previous studies of mutant PrP molecules in non-neuronal cell lines, which indicated altered localization and trafficking of these proteins. Consistent with the results presented here for neurons, immunostaining of transfected BHK and CHO cells revealed markedly reduced levels of PG14 and other mutant PrPs at the plasma membrane (Ivanova et al., 2001). This phenomenon is correlated with delayed maturation of mutant PrP molecules in biosynthetic labeling experiments (Drisaldi et al., 2003), and with evidence that mutant PrPs begin to aggregate very soon after synthesis in the ER (Daude et al., 1997). In contrast to our observations in neurons, however, the only abnormal intracellular accumulations of mutant PrP identified by immunostaining of CHO and BHK cells were localized to the ER (Ivanova et al., 2001). We think it likely that, since the

immunostaining experiments using transfected cells did not employ antigen retrieval techniques, they detected primarily soluble forms of mutant PrP in transit through the secretory pathway, and missed more highly aggregated deposits such as those visualized here using EGFP fusion proteins. The same limitation may apply to a previous immunolocalization study of PG14 PrP in cultured neurons (Fioriti et al., 2005).

Taken together, the available data suggest that, although PG14 PrP molecules may transit the secretory pathway more slowly than WT PrP, in neurons they are eventually delivered to axonal transport vesicles which are thought to bud from the trans-Golgi (Calakos and Scheller, 1996). Since PG14-EGFP aggregates can be observed arrayed along the length of axons *in vivo* and in culture, axonal transport of the mutant protein is not completely blocked. However, there is clearly a defect in delivery of PG14 PrP molecules to the surface membrane of axons and nerve terminals, perhaps due to retarded axonal transport or to failure of transport vesicles to fuse with axonal or synaptic target membranes.

A novel pathogenic mechanism. The results reported here suggest the novel hypothesis that PG14 and other aggregation-prone PrP molecules induce pathology by blocking or altering normal axonal transport processes. For example, vesicles laden with PG14 aggregates may fail to reach nerve terminals, or they may cause "traffic jams" of other axonally transported organelles, thereby preventing delivery of essential cargo molecules to synapses. As a consequence of these abnormalities, structural or functional abnormalities in axons or synapses may ensue. Our study of Bax-deficient Tg(PG14) mice, highlighting the importance of synaptic loss in the neurodegenerative process

(Chiesa et al., 2005), is consistent with this model, as are reports demonstrating a role for PrP in axon outgrowth and synaptic function (Herms et al., 1999; Kanaani et al., 2005; Moya et al., 2005; Salès et al., 2002). Interestingly, deficiencies in axonal transport have been associated with several other neurodegenerative diseases caused by protein aggregation, including Huntington's and Alzheimer's diseases (Goldstein, 2003; Gunawardena et al., 2003; Roy et al., 2005; Stokin et al., 2005). The availability of Tg(PG14-EGFP) mice will now make it possible to perform real-time, fluorescence imaging of the axonal transport of mutant PrP to determine whether abnormalities in cellular trafficking contribute to the disease phenotype.

2.6 Acknowledgments

2.7 References

Barmada, S., et al., 2004. GFP-tagged prion protein is correctly localized and functionally active in the brains of transgenic mice. Neurobiol. Dis. 16**,** 527-537.

Barmada, S. J., Harris, D. A., 2005. Visualization of prion infection in transgenic mice expressing green fluorescent protein-tagged prion protein. J. Neurosci. 25**,** 5824-5832.

Betz, W. J., et al., 1992. Activity-dependent fluorescent staining and destaining of living vertebrate motor nerve terminals. J. Neurosci. 12**,** 363-375.

Bolton, D. C., et al., 1991. Molecular location of a species-specific epitope on the hamster scrapie agent protein. J. Virol. 65**,** 3667-3675.

Borchelt, D. R., et al., 1996. A vector for expressing foreign genes in the brains and hearts of transgenic mice. Genet. Anal. Biomol. Eng. 13**,** 159-163.

Borchelt, D. R., et al., 1994. Rapid anterograde axonal transport of the cellular prion glycoprotein in the peripheral and central nervous systems. J. Biol. Chem. 269**,** 14711-14714.

Büeler, H., et al., 1992. Normal development and behavior of mice lacking the neuronal cell-surface PrP protein. Nature. 356**,** 577-582.

Calakos, N., Scheller, R. H., 1996. Synaptic vesicle biogenesis, docking, and fusion: a molecular description. Physiol. Rev. 76**,** 1-29.

Chiesa, R., et al., 2000. Accumulation of protease-resistant prion protein (PrP) and apoptosis of cerebellar granule cells in transgenic mice expressing a PrP insertional mutation. Proc. Natl. Acad. Sci. USA. 97**,** 5574-5579.

Chiesa, R., et al., 2005. *Bax* deletion prevents neuronal loss but not neurological symptoms in a transgenic model of inherited prion disease. Proc. Natl. Acad. Sci. USA. 102**,** 238-243.

Chiesa, R., et al., 1998. Neurological illness in transgenic mice expressing a prion protein with an insertional mutation. Neuron. 21**,** 1339-1351.

Chiesa, R., et al., 2003. Molecular distinction between pathogenic and infectious properties of the prion protein. J. Virol. 77**,** 7611-7622.

Daude, N., et al., 1997. Identification of intermediate steps in the conversion of a mutant prion protein to a scrapie-like form in cultured cells. J. Biol. Chem. 272**,** 11604-11612.

Drisaldi, B., et al., 2003. Mutant PrP is delayed in its exit from the endoplasmic reticulum, but neither wild-type nor mutant PrP undergoes retrotranslocation prior to proteasomal degradation. J. Biol. Chem. 278, 21732-21743.

Duchen, L. W., et al., 1993. Dementia associated with a 216 base pair insertion in the prion protein gene: clinical and neuropathological features. Brain. 116, 555-567.

Fioriti, L., et al., 2005. Cytosolic prion protein (PrP) is not toxic in N2a cells and primary neurons expressing pathogenic PrP mutations. J Biol Chem. 280, 11320-8.

Fischer, M., et al., 1996. Prion protein (PrP) with amino-proximal deletions restoring susceptibility of PrP knockout mice to scrapie. EMBO J. 15, 1255-1264.

Goldstein, L. S., 2003. Do disorders of movement cause movement disorders and dementia? Neuron. 40, 415-425.

Gunawardena, S., et al., 2003. Disruption of axonal transport by loss of huntingtin or expression of pathogenic polyQ proteins in *Drosophila*. Neuron. 40, 25-40.

Harris, D. A., 2003. Trafficking, turnover and membrane topology of PrP. Br. Med. Bull. 66, 71-85.

Herms, J., et al., 1999. Evidence of presynaptic location and function of the prion protein. J. Neurosci. 19, 8866-8875.

Ivanova, L., et al., 2001. Mutant prion proteins are partially retained in the endoplasmic reticulum. J. Biol. Chem. 276, 42409-42421.

Kanaani, J., et al., 2005. Recombinant prion protein induces rapid polarization and development of synapses in embryonic rat hippocampal neurons in vitro. J. Neurochem. 95, 1373-1386.

Kitamoto, T., et al., 1987. Formic acid pretreatment enhances immunostaining of cerebral and systemic amyloids. Lab. Invest. 57, 230-236.

Kitamoto, T., et al., 1992. Abnormal isoform of prion proteins accumulates in the synaptic structures of the central nervous system in patients with Creutzfeldt-Jakob disease. Am. J. Path. 140, 1285-1294.

Kong, Q., et al., Inherited prion diseases. In: S. B. Prusiner, (Ed.), Prion Biology and Diseases. Cold Spring Harbor Laboratory Press, Cold Spring Harbor, New York, 2004, pp. 673-775.

Korth, C., et al., 1997. Prion (PrP^{Sc})-specific epitope defined by a monoclonal antibody. Nature. 390, 74-77.

Kovacs, G. G., et al., 2005. Subcellular localization of disease-associated prion protein in the human brain. Am. J. Pathol. 166, 287-294.

Krasemann, S., et al., 1995. Prion disease associated with a novel nine octapeptide repeat insertion in the PRNP gene. Mol. Brain Res. 34**,** 173-176.

Laszlo, L., et al., 1992. Lysosomes as key organelles in the pathogenesis of prion encephalopathies. J. Pathol. 166**,** 333-341.

Lehmann, S., Harris, D. A., 1995. A mutant prion protein displays an aberrant membrane association when expressed in cultured cells. J. Biol. Chem. 270**,** 24589-24597.

Lund, C., et al., 2007. Characterization of the prion protein 3F4 epitope and its use as a molecular tag. J. Neurosci. Methods. 165**,** 183-190.

Miller, T. M., Johnson, E. M., Jr., 1996. Metabolic and genetic analyses of apoptosis in potassium/serum-deprived rat cerebellar granule cells. J. Neurosci. 16**,** 7487-7495.

Moya, K. L., et al., 2005. Axonal transport of the cellular prion protein is increased during axon regeneration. J. Neurochem. 92**,** 1044-1053.

Moya, K. L., et al., 2004. Enhanced detection and retrograde axonal transport of PrP^C in peripheral nerve. J. Neurochem. 88**,** 155-160.

Moya, K. L., et al., 2000. Immunolocalization of the cellular prion protein in normal brain. Microsc. Res. Tech. 50**,** 58-65.

Narwa, R., Harris, D. A., 1999. Prion proteins carrying pathogenic mutations are resistant to phospholipase cleavage of their glycolipid anchors. Biochemistry. 38**,** 8770-8777.

Owen, F., et al., 1992. A dementing illness associated with a novel insertion in the prion protein gene. Mol. Brain Res. 13**,** 155-157.

Pankiewicz, J., et al., 2006. Clearance and prevention of prion infection in cell culture by anti-PrP antibodies. Eur. J. Neurosci. 23**,** 2635-2647.

Powell, S. K., et al., 1997. Development of polarity in cerebellar granule neurons. J. Neurobiol. 32**,** 223-236.

Prusiner, S. B. (Ed.) 2004. Prion Biology and Diseases. Cold Spring Harbor Laboratory Press, Cold Spring Harbor, New York.

Rodolfo, K., et al., 1999. A novel cellular prion protein isoform present in rapid anterograde axonal transport. Neuroreport. 10**,** 3639-3644.

Roy, S., et al., 2005. Axonal transport defects: a common theme in neurodegenerative diseases. Acta Neuropathol. (Berl). 109**,** 5-13.

Salès, N., et al., 2002. Developmental expression of the cellular prion protein in elongating axons. Eur. J. Neurosci. 15**,** 1163-1177.

Salès, N., et al., 1998. Cellular prion protein localization in rodent and primate brain. Eur. J. Neurosci. 10**,** 2464-2471.

Shyng, S. L., et al., 1995. The N-terminal domain of a glycolipid-anchored prion protein is essential for its endocytosis via clathrin-coated pits. J. Biol. Chem. 270**,** 14793-14800.

Stokin, G. B., et al., 2005. Axonopathy and transport deficits early in the pathogenesis of Alzheimer's disease. Science. 307**,** 1282-1288.

Van Everbroeck, B., et al., 1999. Antigen retrieval in prion protein immunohistochemistry. J. Histochem. Cytochem. 47**,** 1465-1470.

Zanusso, G., et al., 1998. Prion protein expression in different species: analysis with a panel of new mAbs. Proc. Natl. Acad. Sci. USA. 95**,** 8812-8816.
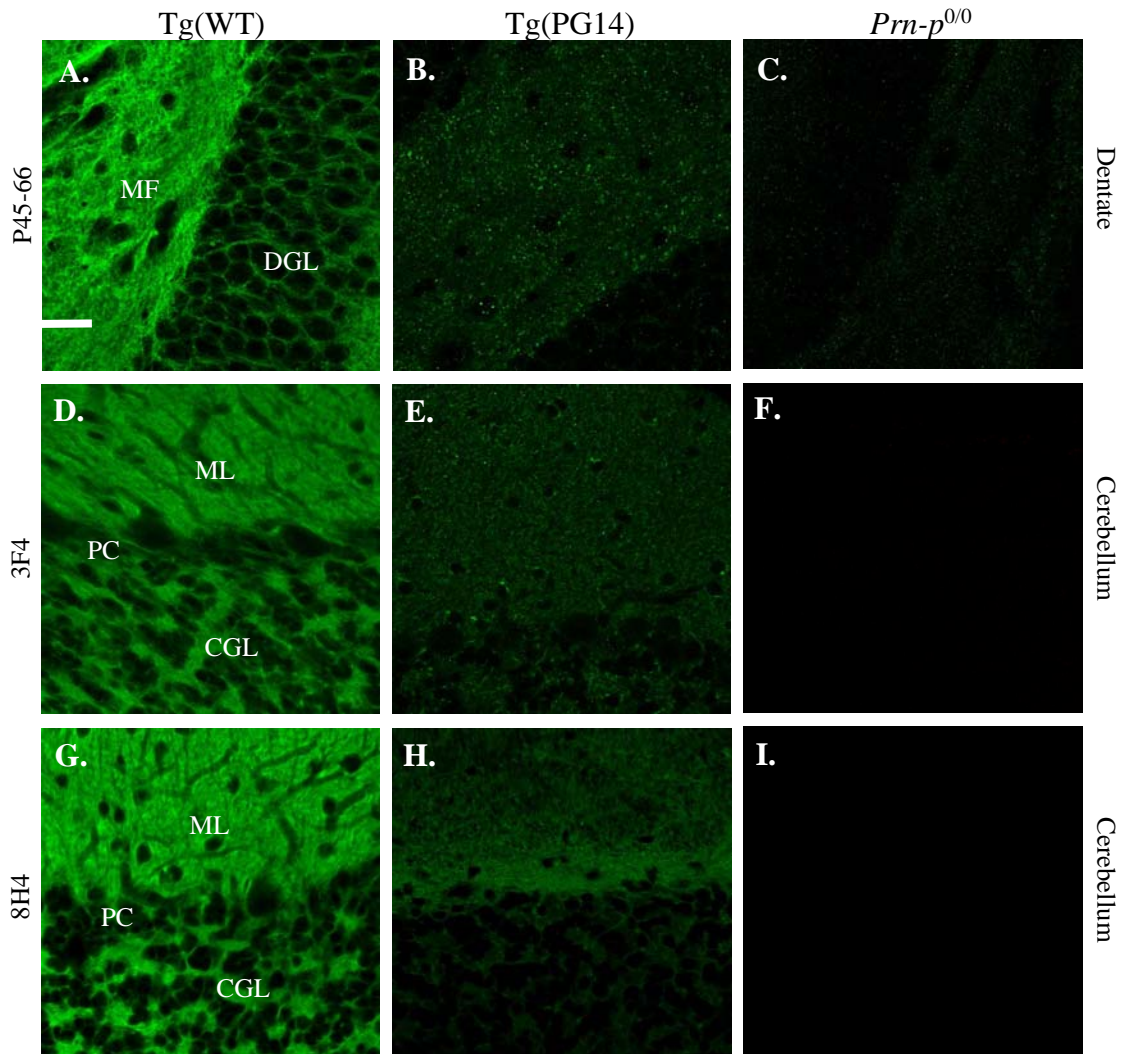
Supplemental Figure 1. PG14 PrP in brain sections stains weakly using conventional immunohistochemistry. Vibratome sections from the brains of Tg(WT) mice (A, D, G), Tg(PG14) mice (B, E, H), or *Prn-p0/0* mice (C, F, I) were immunostained using the following anti-PrP antibodies: P45-66 (which recognizes residues 45-66; (Lehmann and Harris, 1995)) (A-C); 3F4 (which recognizes residues 105-111; (Lund et al., 2007)) (D-F); or 8H4 (which recognizes residues 147-200; (Zanusso et al., 1998)) (G-I). The transgenically encoded PrP expressed by both Tg(WT) and Tg(PG14) mice carries an epitope tag for the 3F4 antibody (Chiesa et al., 1998). Sections were derived from the dentate gyrus (A-C), or the cerebellar cortex (D-I). Tg(WT) sections stain strongly with all three antibodies. Tg(PG14) sections stain weakly, but above background levels seen in *Prn-p0/0* mice. Abbreviations are: MF, mossy fibers; DGL, dentate granule cell layer; ML, molecular layer; PC, Purkinje cell layer; CGL, cerebellar granule cell layer. The scale bar in A (applicable to all panels) is 20 μm.
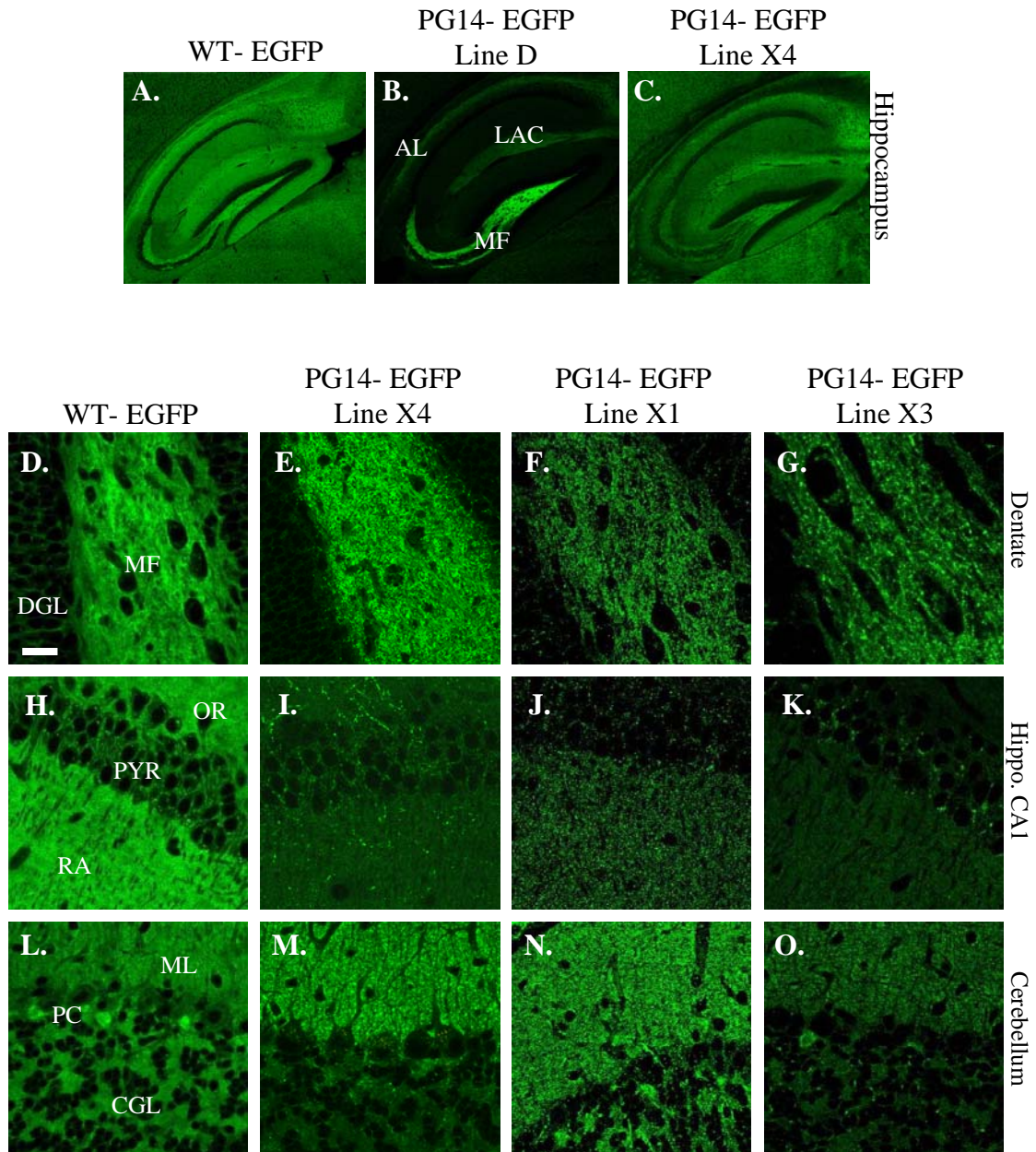
Supplemental Figure 2. Characterization of PG14-EGFP distribution in four lines of Tg(PG14-EGFP) mice. Vibratome sections were cut from the brains of Tg(WT-PrP) mice (A, D, H, L), as well as the following lines of Tg(PG14-EGFP) mice: line D (B); line X4 (C, E, I, M); line X1 (F, J, N); line X3 (G, K, O). The panels show the whole hippocampus (A-C), the dentate gyrus (D-G), the CA1 sub-field of the hippocampus (H-K), and the cerebellar cortex (L-O). Due to low transgene expression, it was necessary to stain sections from the X1 and X3 lines with anti-GFP antibody in order to detect PG14-EGFP. The abbreviations are: LAC, stratum lacunosum moleculare; AL, alveus; MF, mossy fibers; DGL, dentate granule cell layer; OR, stratum oriens; PYR, pyramidal cells; RA; stratum radiatum; PC, Purkinje cell layer; CGL, cerebellar granule cell layer; ML, molecular layer. The scale bar in A (applicable to A-C) is 200 μm and in D (applicable to D-O) is 20 μm.

CHAPTER 3

The role of the GPI anchor in the cellular behavior of a

disease-associated familial prion protein mutant

A Medrano & DA Harris.

3.1 Summary

Prion protein (PrP) is a GPI-anchored sialoglycoprotein involved in the pathogenesis of infectious and inherited forms of transmissible spongiform encephalopathies (TSEs). Wild-type PrP molecules lacking the GPI anchor (WTΔGPI) display aberrant glycosylation and are secreted into the extracellular space. When inoculated with scrapie, transgenic mice expressing WTΔGPI display dense intracerebral plaques that are larger and denser than those found in their wild-type counterparts, suggesting that GPI anchor deletion promotes aggregation in infectious prion disorders. Thus far, the role of the GPI anchor has not been determined for disease-associated familial mutants of PrP. PG14 is a disease-associated PrP mutant which contains a 217 base pair insertion resulting in a repeat expansion of endogenous octapeptide motifs. PG14 becomes glycosylated, forms spontaneous aggregates, and is partially retained within the ER and Golgi in cells. To determine whether the GPI anchor affects cellular behavior of the protein, we generated a PG14ΔGPI construct and investigated its glycosylation, localization, and spontaneous aggregation in transfected mammalian cells. We demonstrate that deletion of the GPI anchor impairs PG14 glycosylation, but has no effect the mutant's ability to aggregate, as assayed by detergent insolubility and sucrose gradient assays in cells. Furthermore, PG14ΔGPI shows similar intracellular retention and localization compared with full-length PG14. These studies show that the GPI anchor is crucial for proper glycosylation of PG14, but does not affect aggregation or localization of a genetic PrP mutant. Whether the GPI anchor affects clinical progression of familial prion disease remains to be determined. Our analysis provides foundational

information for the continued study of the role of the GPI anchor in familial prion disease pathogenesis.

3.2 Introduction

Prion diseases, such as bovine spongiform encephalopathy in cattle, Creutzfeldt-Jakob Disease, Fatal Familial Insomnia, and Gerstman-Straussler-Shenker syndrome in humans, are fatal neurodegenerative disorders that result in progressive dementia and motor dysfunction. These diseases can be acquired sporadically, through genetic mutation of the cellular prion protein (PrP^C), or by exposure to infectious scrapie molecules (PrP^{Sc}). The hallmarks of neuropathology include vacuolation and aggregation of the prion protein, presumably caused by the misfolding of the alpha-helical PrP^C into the more β-sheet rich PrP^{Sc} form (Prusiner et al. 1998). PrP^C, which is highly expressed in the central nervous system, is a cell surface sialoglycoprotein implicated in cell signal transduction (Westergard et al. 2007).

PrP^C is firmly attached to the plasma membrane via a glycophosphatidylinositol (GPI) anchor, a complex glycolipid structure linking the C-terminal end of the protein with the outer leaflet of the lipid bilayer. This anchor is responsible for tethering PrP^C to the membrane and localizing the protein to detergent-resistant membrane (DRM) microdomains (Taylor and Hooper 2006). GPI anchor loss caused by genetic deletion, chemical cleavage, or substitution with a foreign transmembrane domain, results in PrP^C detachment from the cell surface (Rogers et al. 1993; Kaneko et al. 1997; Campana et al. 2007). The GPI anchor also affects PrP glycosylation, as expression of anchorless forms

of PrP result in mainly unglycosylated protein products (Walmsley et al. 2001; Walmsley et al. 2003)

The exact location and mechanisms underlying the transition of PrP^C to PrP^{Sc} in infectious disease are ambiguous, but previous studies suggest that membrane attachment by GPI anchor plays a role in conversion and in disease. In cell-free experiments, the GPI anchor has a protective effect over PrP^C, embedding the protein in sphingolipid-cholesterol-rich raft-like liposomes (SCRLs) which prevent conversion to PrP^{Sc} (Baron and Caughey 2003). Conversely, investigations in cells demonstrate that proper localization at the cell surface is crucial for efficient PrP^{Sc} conversion (Caughey and Raymond 1991; Borchelt et al. 1992), and that loss of the GPI anchor impairs PrP^{Sc} formation and accumulation (Rogers et al. 1993; Kaneko et al. 1997). In transgenic mice that express a GPI anchorless form of PrP (PrPΔGPI), inoculation with scrapie results in the formation of PrP^{Sc} plaques that are larger and more dense than those of their wild-type counterparts. Interestingly, inoculated Tg(PrPΔGPI) animals remained healthy up to 500 days past their wild-type controls, which succumbed to sickness within 5 months. PrP^{Sc} in Tg(PrPΔGPI) animals is less infectious when tested in sequential passaging, despite its robust accumulation in brain (Chesebro et al. 2005; Trifilo et al. 2008), demonstrating that GPI anchor loss also affects PrP^{Sc} transmissibility.

Collectively, these data demonstrate that modifications in the GPI anchor affect glycosylation and localization of prion protein molecules, and have the ability to influence aggregation and infectivity in prion disease. Thus far, the relevance of GPI anchor-mediated membrane attachment for non-infectious *mutant* PrPs in glycosylation, localization, and aggregation has not been elucidated. In this work, we attempt to better

understand the role of the GPI anchor in the cellular behavior of mutant prion protein PG14 in cells.

PG14 is an insertion of 217 bp within the prion protein, and is associated with a variant of Creutzfeldt-Jakob disease in humans (Lehmann and Harris 1996; Lehmann and Harris 1996; Chiesa et al. 1998; Biasini et al. 2008). The mutation results in the expansion of five endogenous octapeptide repeat (OR) motifs, rich in proline and glycine, from five to fourteen. It is thought that the mutation alters the conformation of PrP such that it is more prone to misfolding and subsequent adoption of a more PrPSc-like pattern. PrP molecules containing the PG14 mutation are partially PK-resistant and detergent insoluble in cell lines and in transgenic mice (Lehmann and Harris 1996). Although biochemically similar to PrP[Sc] in this regard, PG14 differs from scrapie in that it is non-infectious and forms aggregates spontaneously inside cells (Bolton et al. 1991). Aggregates are retained intracellularly, with only a small fraction of molecules reaching the surface in cells and neurons (Lehmann and Harris 1995; Lehmann and Harris 1996; Lehmann and Harris 1996; Lehmann et al. 1997). Aggregated PG14 also accumulates over time and in transgenic mice to form small intracerebellar plaques displaying a synaptic-like distribution (Rogers et al. 1993; Walmsley et al. 2001; Walmsley et al. 2003; McNally et al. 2009). Although the localization and biochemical properties of PrP are altered in both infectious and familial forms of TSEs, it is unknown whether the mechanisms of aggregation or disease are similar.

To investigate the role of GPI anchor attachment in the cellular behavior of a disease-associated mutant PrP model, we constructed a PG14ΔGPI molecule and observed protein processing and trafficking in transfected CHO cells. PNGase and Endo

H assays demonstrate that PG14ΔGPI is predominantly unglycosylated. Analyses of cell and media fractions, as well as immunocytochemical studies, show that PG14ΔGPI is largely retained intracellularly. PG14ΔGPI is partially detergent insoluble and colocalizes with the dense fractions of sucrose gradients, demonstrating that the GPI anchor does not affect intracellular aggregation. Collectively, these data show that deletion of the GPI anchor affects PG14 protein glycosylation, but does not interfere with its intracellular localization or aggregation formation. These studies provide the foundation for future studies investigating the role of the GPI anchor in familial prion disease transmission.

3.3 Methods

PrP Constructs. Figure 1 shows the structure of all murine PrP constructs used in this study. All constructs were cloned into the pCDNA3.1(+) Hygromycin plasmid vector (Invitrogen), which drives high levels of protein expression through a CMV promoter. WT and PG14 sequences were excised from pCDNA3 vector (Ivanova et al. 2001), and inserted directly into pCDNA3.1(+)Hygromycin using restriction sites BamHI and HindIII, which flank the PrP sequences. WTΔGPI was constructed by amplifying DNA sequences encoding WT PrP codons 1-230, using primers encoding BamHI and HindIII at the 5' and 3' ends, respectively. PG14ΔGPI was generated by a XmaI/KpnI excision of the octarepeat region from the PG14 template, with subsequent insertion into the same restriction sites within the WTΔGPI plasmid. Both anchorless constructs were made within the pCDNA3.1(+) Hygromycin plasmid.

Cell Lines and Reagents. For biochemical and immunofluorescence experiments, PrP constructs were transiently transfected into Chinese Hamster Ovary (CHO) or African green monkey kidney (COS7) cells using Lipofectamine 2000 (Invitrogen). CHO cells were maintained in MEM-Alpha media containing 10% fetal bovine serum and antibiotics; COS7 cells in DMEM media containing 10% fetal bovine serum a antibiotics. Protein concentrations from each transfection was measured using a BCA Assay (Pierce, Rockford, IL). PrP was detected using antibodies 3F4 (Stewart et al. 2001) or 6H4 (Prionics, Zurich, Switzerland).

Deglycosylation of PrP. Cell lysates were first denatured, then treated with PNGase F and Endo Hf (New England Biolabs, Ipswich, MA) according to the manufacturer's directions. Reactions were terminated by addition of 2X SDS sample buffer, then analyzed by SDS-PAGE and Western blot.

Detergent Insolubility assay. 200μg total protein from cell lysates were diluted in detergent buffer (DB: 0.5% sodium deoxycholate, 0.5% NP-40, 150mM NaCl, 10mM Tris-HCl, pH 7.4) with complete Mini EDTA-free protease inhibitors (Roche) to obtain a final protein concentration of 0.4 μg/μL. Samples were rotated at 4C for 20 minutes, then centrifuged at 1500 x g for 10 min. Supernatants were recovered and centrifuged for 1 hr at 89,000 x g at 4C to separate soluble and insoluble fractions. Supernatants (S) from this centrifugation were methanol precipitated, then analyzed along with the pellet (P) fractions by SDS-PAGE and Western Blot.

Sucrose Gradient Sedimentation. Lysates of transiently transfected CHO cells were cleared by centrifugation at 16,000 rcf for 2 min. 150ug protein was then loaded on a 5 mL step gradient of 10-60% sucrose in DB buffer supplemented with protease

inhibitors. After centrifugation at 163,000 x g for 1 hr at 4C, 400μL fractions were methanol-precipitated then analyzed by Western Blot.

Florescence Microscopy. COS7 were seeded on flame-sterilized glass coverslips and transfected. For surface staining, cells were washed with PBS, incubated with monoclonal antibody 3F4 diluted in 5% goat serum in Opti-MEM (Invitrogen) for 1 hr at 4C, rinsed with PBS, then fixed in 4% paraformaldehyde solution for 10 min. Cells were again rinsed with PBS, blocked with 5% goat serum in PBS for 15 min, then incubated with 1:500 Alexa 488-conjugated goat anti-mouse IgG (Molecular Probes, Inc.) and DAPI in block solution. Coverslips were washed with PBS and mounted onto Superfrost glass microscope slides (Fisher Scientific) using Gel/Mount (Biomeda, Foster City, CA).

For intracellular colocalization studies, cells were grown on coverslips, washed with PBS, then fixed with 4% paraformaldehyde for 10 min. Cells were exposed to 0.1% TX-100 in PBS for 10 min for permeabilization, washed with PBS, blocked in 5% goat serum in PBS, then incubated with primary and secondary antibodies as described above, with the exception of the endosomes colocalization experiments, where polyclonal PrP antibody P45-66 (Rogers et al. 1993; Walmsley et al. 2001; Chesebro et al. 2005) was used in place of 3F4. Additional antibodies directed against calreticulin (polyclonal, Affinity Bioreagents), giantin (polyclonal, Covance, Berkeley, CA), or EEA1 (monoclonal, BD Biosciences) were used to detect the ER, Golgi, and endosomes, respectively. Alexa 594-conjugated anti-rat or anti-rabbit IgG (Molecular Probes, Inc) was used to detect these primary antibodies.

3.4 Results

PG14ΔGPI is mostly unglycosylated when expressed in cells. To investigate the effects of GPI deletion on a familial prion mutant, we constructed anchorless forms of WT PrP and PG14 PrP by abolishing amino acids 231-254, which encode the signal for GPI anchor attachment (Figure 1A). These constructs, along with their full-length counterparts, were transfected into Chinese Hamster Ovary (CHO) cells, which lack detectable levels of endogenous PrP and which have previously been used to biochemically characterize several inherited disease-associated PrP mutants, including PG14 (Campana et al. 2007).

In cells, full-length WT and PG14 molecules display typical patterns of unglycosylated and glycosylated forms of PrP, whereas only one predominant band is evident for both WTΔGPI and PG14ΔGPI cell lysates (Figure 1B). WTΔGPI has been shown previously to be expressed mainly in its unglycosylated form in cells and in mice (Rogers et al. 1993; Chesebro et al. 2005; McNally et al. 2009). However, because full-length PG14 is known to be partially retained within the ER (Walmsley et al. 2001), it was possible that the predominant band from PG14ΔGPI represented an incompletely glycosylated form of molecule, containing the only high-mannose type sugars normally attached in the ER. Indeed, another familial PrP mutant, T182A, is expressed primarily as a single glycoform that is Endo H-, but not neuraminidase-, sensitive (Lehmann and Harris 1995; Drisaldi et al. 2003). To rule out the possibility of incomplete glycosylation, we treated PrP-expressing cells with Endo H, an enzyme which cleaves only high-mannose type glycans (Figure 2). Full-length WT and PG14 molecules that have successfully processed through the Golgi are Endo H-resistant (see asterisks in
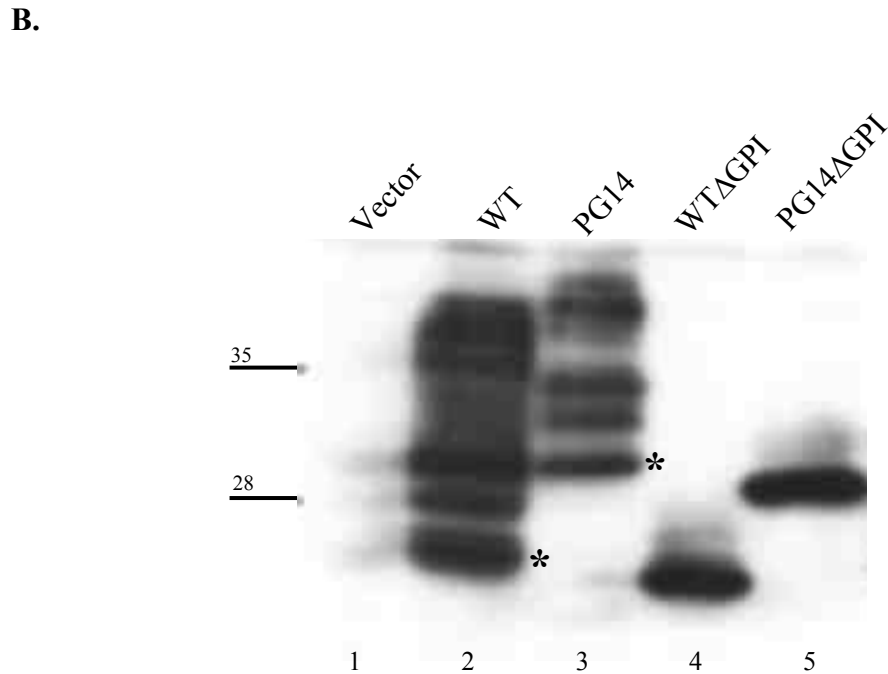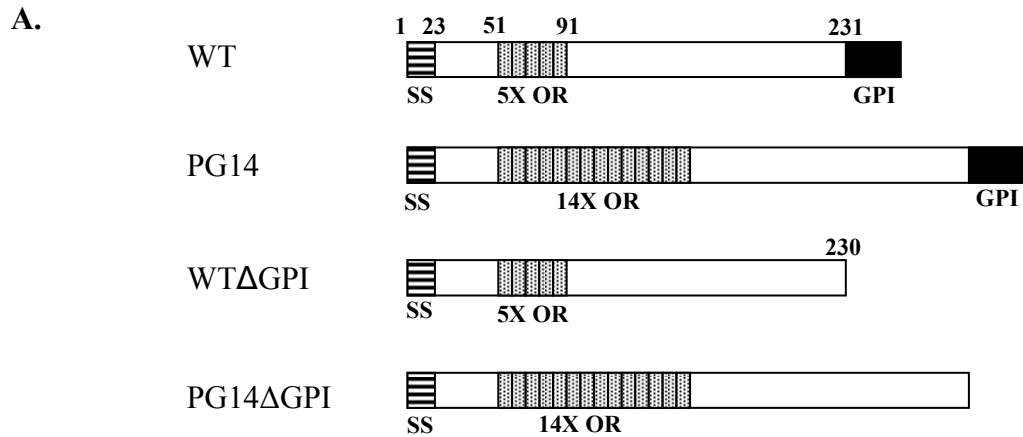
Figure 1. Structure and expression of WTΔGPI and PG14ΔGPI in CHO cells. (A) Schematic of structures of full-length WT PrP, full-length PG14, and anchorless constructs WTΔGPI and PG14ΔGPI. WT PrP protein contains an N-terminal signal sequence (SS), five octapeptide repeats (5X OR). PG14 contains an insertion encoding nine additional octapeptide repeats (14X OR), resulting in a totoal of 14 repeats. Anchorless versions of both WT and PG14 lack the C-terminal signal sequence for the GPI anchor (black box), and are truncated at amino acid 230. (B) Expression of PrP constructs in CHO cells. Cell lysates from transiently transfected CHO cells were analyzed by Western blot using anti-PrP antibody 3F4. Asterisks indicate unglycosylated PrP forms. Molecular size markers are given in kilodaltons.

Figure 2A, lanes 3,4 and 5,6). As a positive control, we used lysates of cells expressing L9R PrP, a PrP mutant known to be immaturely glycosylated due to complete ER retention (Medrano et al. 2008). There was no evident shift in the PG14ΔGPI band after deglycosylation treatment, indicating that the band did not represent immaturely glycosylated mutant PrPs.

When treated with PNGase, an enzyme which completely removes both high mannose and complex N-linked oligosaccharides from parent glycoproteins, all full-length WT and PG14 glycoforms were reduced to the non-glycosylated state (Figure 2B, lanes 3-6). However, the single bands evident from WTΔGPI or PG14ΔGPI cell lysates were not reduced after deglycosylation digestion, indicating that the anchorless forms of both are predominantly unglycosylated and do not represent altered glycoforms (Figure 2B, lanes 7-10).

Monoglycosylated forms of both WTΔGPI and PG14ΔGPI proteins was observed in overexposed blots (data not shown), but these fractions comprise >10% of the molecule populations. These results support previous evidence that the GPI anchor is crucial for proper N-linked glycosylation in both cells and animals (Ivanova et al. 2001).

PG14ΔGPI is retained intracellularly and is localized similarly to full-length PG14. The GPI anchor is crucial for proper WT PrP localization at the plasma membrane. PrP molecules lacking the signal sequence for the anchor are only loosely associated with lipid rafts during the processing pathway (Ivanova et al. 2001; Medrano et al. 2008), and are secreted into extracellular space upon reaching the surface (Campana et al. 2007). Full-length PG14 is retained intracellularly, with little to no

A.

B.
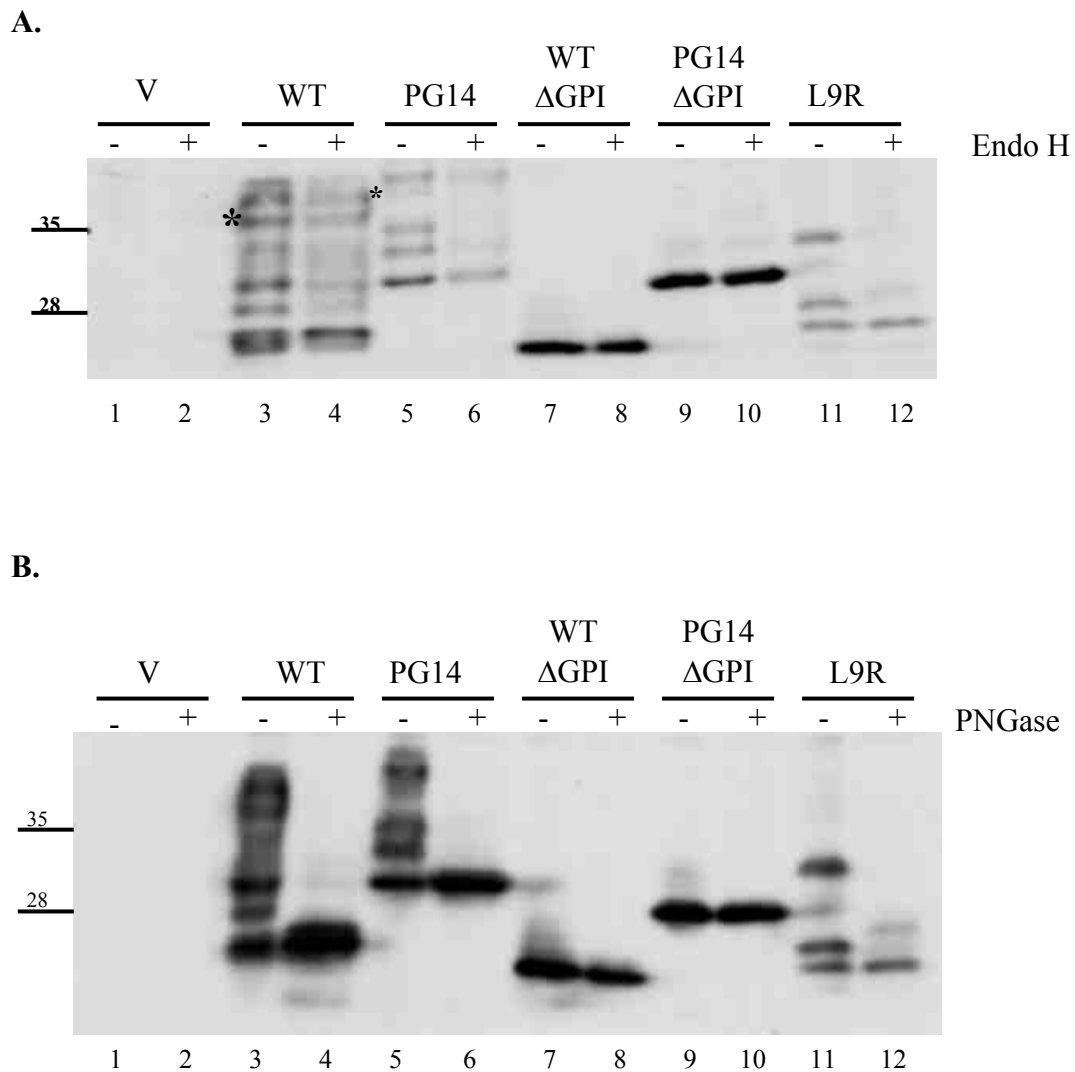
Figure 2. PG14ΔGPI is mainly unglycosylated. (A) Endo H deglycosylation. Cell lysates from cells expressing vector (lanes 1,2), WT PrP (lanes 3,4), PG14 (lanes 5,6), WTΔGPI (lanes 7,8), PG14ΔGPI (lanes 9,10), and L9R (lanes 11,12) were treated with deglycosylation enzyme Endo H, and then analyzed by Western blotting with 3F4 antibody. Immature glycoforms of WT, PG14, and L9R bands shifted, but ΔGPI molecules remained the same size. (B) PNGase F deglycosylation. Similar to (A), but cell lysates were treated with PNGase F and analyzed in the same manner. WT, PG14, & L9R glycoforms shift, but ΔGPI bands do not. Molecular size markers are given in kilodaltons.

protein reaching the cell surface (Lehmann and Harris 1997). In order to investigate cellular retention vs. secretion of PrPs lacking a GPI anchor, we collected cell and media fractions of transiently transfected CHO cells and compared expression levels of full-length and anchorless proteins by western blot (Figure 3). Our results confirm previous studies that show that large amounts of WTΔGPI molecules are secreted into the media (Yin et al. 2006), while full-length WT and PG14 remain associated with cells, either on the surface or intracellularly. PG14ΔGPI, unlike WTΔGPI, is not secreted in appreciable amounts, and the majority of protein remains in or on cells. However, the amount of PG14ΔGPI that is secreted is noticeably more than full-length PG14, indicating that the small fraction of PG14ΔGPI protein that does reach the surface is shed more easily than membrane-bound PG14.

To determine PG14ΔGPI localization in cells, we conducted several co-localization experiments using immunofluorescent cytochemistry. The first was to determine whether PG14ΔGPI was present at the cell surface. CHO cells were transiently transfected with WT, PG14, WTΔGPI, and PG14ΔGPI. All cells were co-transfected with a dsRed marker to serve as positive identification of transfected cells. After 24 hours, cells were incubated with α-PrP antibody 6H4, fixed, incubated with a green fluorescent secondary antibody, then analyzed by fluorescence microscopy (Figure 4). Surface staining in these non-permeabilized cells show that WT was present in appreciable amounts at the plasma membrane, but not PG14, WTΔGPI, nor PG14ΔGPI. Along with Figure 3, these data demonstrate that ΔGPI proteins are loosely associated with the membrane, if at all, and are secreted into the media upon exposure to the extracellular space.
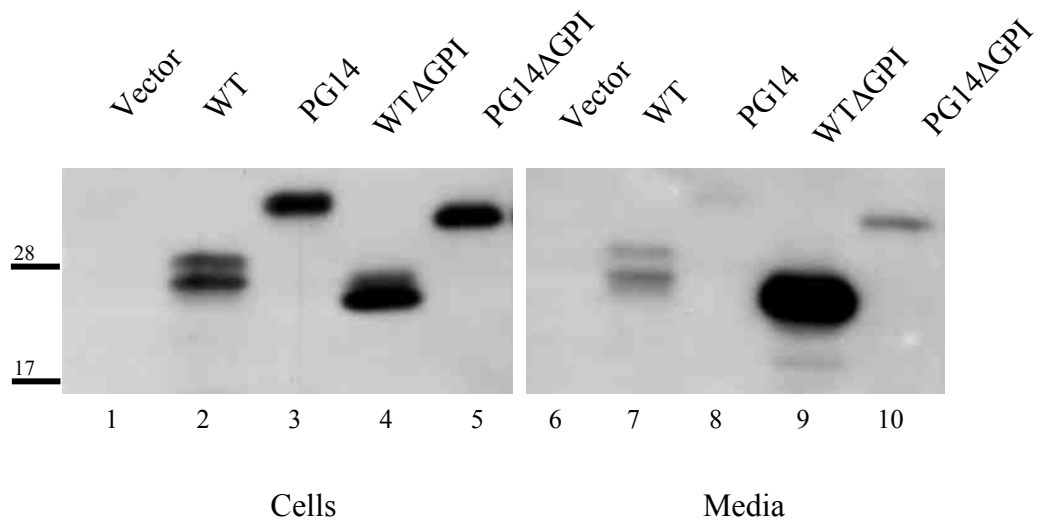
Figure 3. PG14ΔGPI is mainly intracellular. Equal amounts of protein from cell lysates (1-5) and equal volumes of media (lanes 6-10) from cells expressing vector (lanes 1,6), WT PrP (lanes 2,7), PG14 (lanes 3,8), WTΔGPI (lanes 4,9), and PG14ΔGPI (lanes 5,10) were treated with PNGase F, then analyzed by Western blotting with 3F4 antibody. Large amounts of WTΔGPI are secreted into the media, whereas PG14ΔGPI remains mostly intracellular. Molecular size markers are given in kilodaltons.
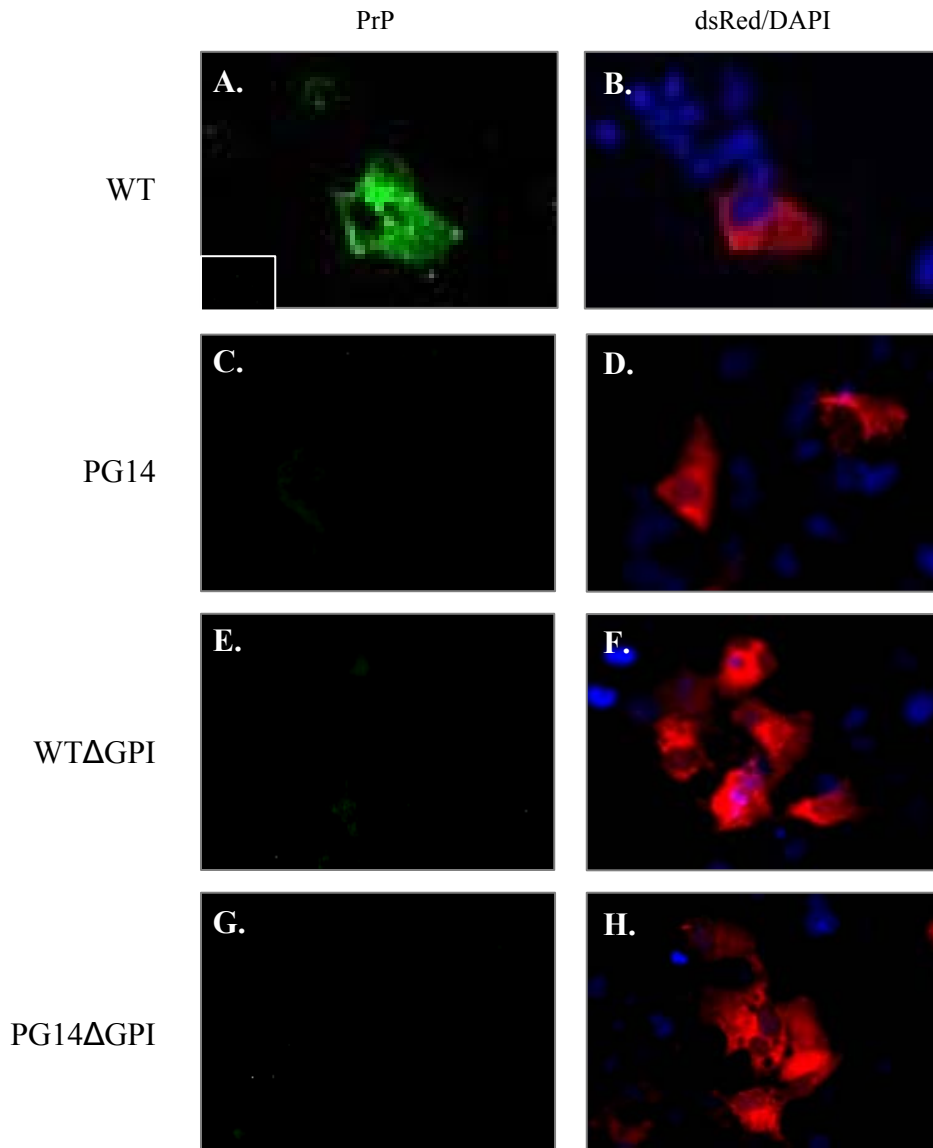
Figure 4. PG14ΔGPI is not detectable at the cell surface. CHO cells were co-transfected with PrP construct and dsRed-ER to detect transfected cells. Cells expressing vector (insert), WT (a,b), PG14 (c,d), WTΔGPI (e,f), and PG14ΔGPI (g,h) were stained with PrP primary antibody 6H4, fixed, then incubated with fluorescent green Alexa 488 secondary antibody and DAPI. Analysis by fluorescence microscopy allows observation of PrP (a, d, g, j) and dsRed marker with DAPI (b, d, f, h), revealing that only WT PrP is detectable at the cell surface.

The majority of PG14ΔGPI is associated with cells, but is not present at the cell surface. To determine where PG14ΔGPI was retained intracellularly, we performed colocalization studies in transfected cells. Cells transfected with full-length or anchorless PrP constructs were probed with α-PrP antibody 6H4 and α-calreticulin, a marker for endoplasmic reticulum (Figure 5). The large stores of intracellular WT and WTΔGPI do not colocalize with ER. However, both PG14 and PG14ΔGPI partially colocalize with calreticulin, indicating that these proteins are partially retained within the ER. There are pools of PG14 and PG14ΔGPI that do not correlate with ER, suggesting that the proteins are located elsewhere as well.

To determine whether PG14ΔGPI transits through the Golgi, we performed a similar colocalization experiment using an antibody directed against giantin (Figure 6). Staining in permeabilized cells demonstrates some full-length WT PrP in the Golgi, which likely corresponds to a pool of WT PrP molecules traveling within the secretory pathway. PG14 and PG14ΔGPI molecules also partially colocalize with Golgi, indicating that these proteins are able to escape the ER.

PG14ΔGPI forms aggregates. To ascertain whether PG14ΔGPI molecules aggregate in cells, we performed a detergent insolubility assay. Cell lysates and media from transfected cells were diluted in detergent buffer containing 0.5% NP-40 and 0.5% sodium deoxycholate, then subjected to high speed ultracentrifugation to separate insoluble from soluble material. Pellets (P) and supernatant (S) fractions were analyzed by Western Blot (Figure 7). Whereas full length WT and WTΔGPI proteins were entirely soluble (Figure 7A, lanes 3,4,7,8), both PG14 and PG14ΔGPI proteins were partially
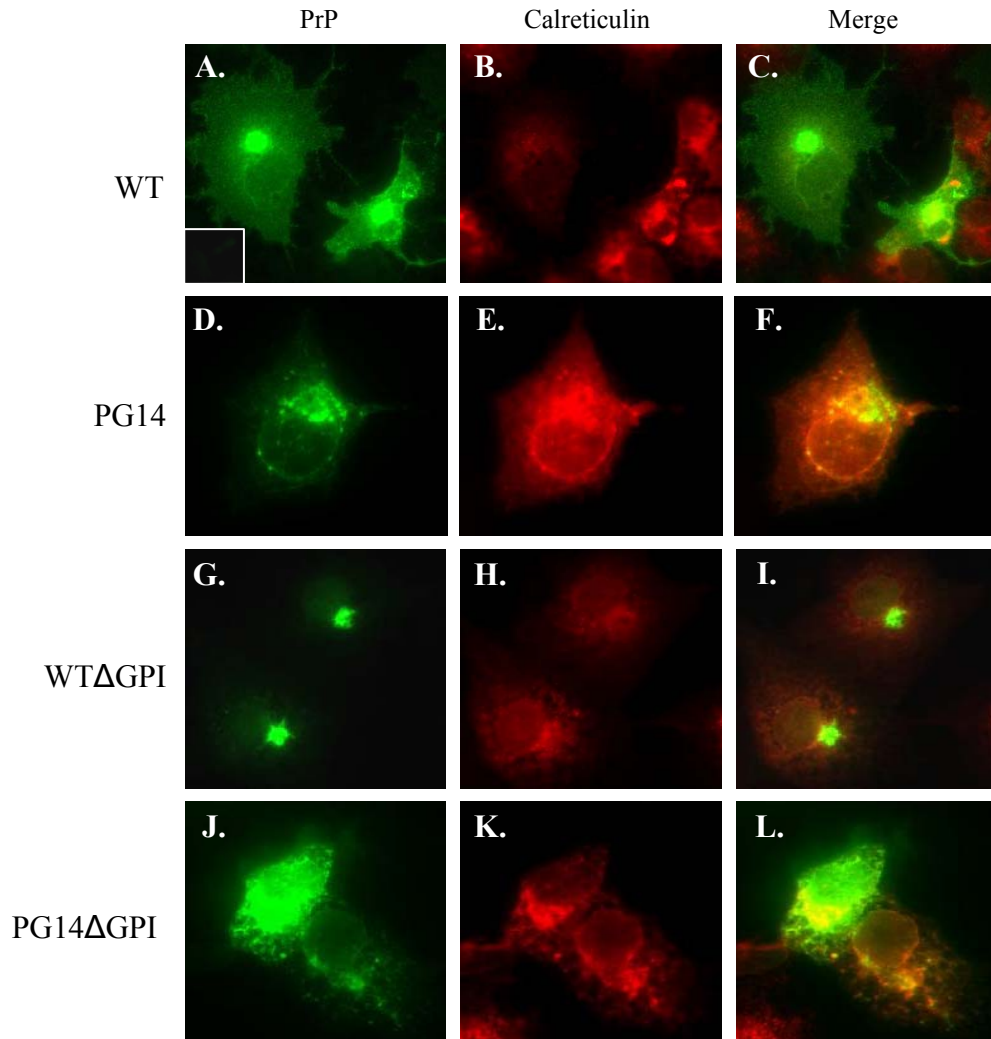
Figure 5. PG14ΔGPI partially colocalizes with ER. Cells expressing vector (inset), WT PrP (a-c), PG14 (d-f), WTΔGPI (g-i), and PG14ΔGPI (j-l) were fixed, permeabilized, then stained with PrP primary antibody 6H4 and α-calreticulin (b, e, h, k). Analysis by fluorescence microscopy allows observation of PrP (a, d, g, j), ER (b, e, h, k), and merged pictures (c, f, i, l). Both full-length PG14 and PG14ΔGPI partially colocalize with ER, WT and WTΔGPI do not.
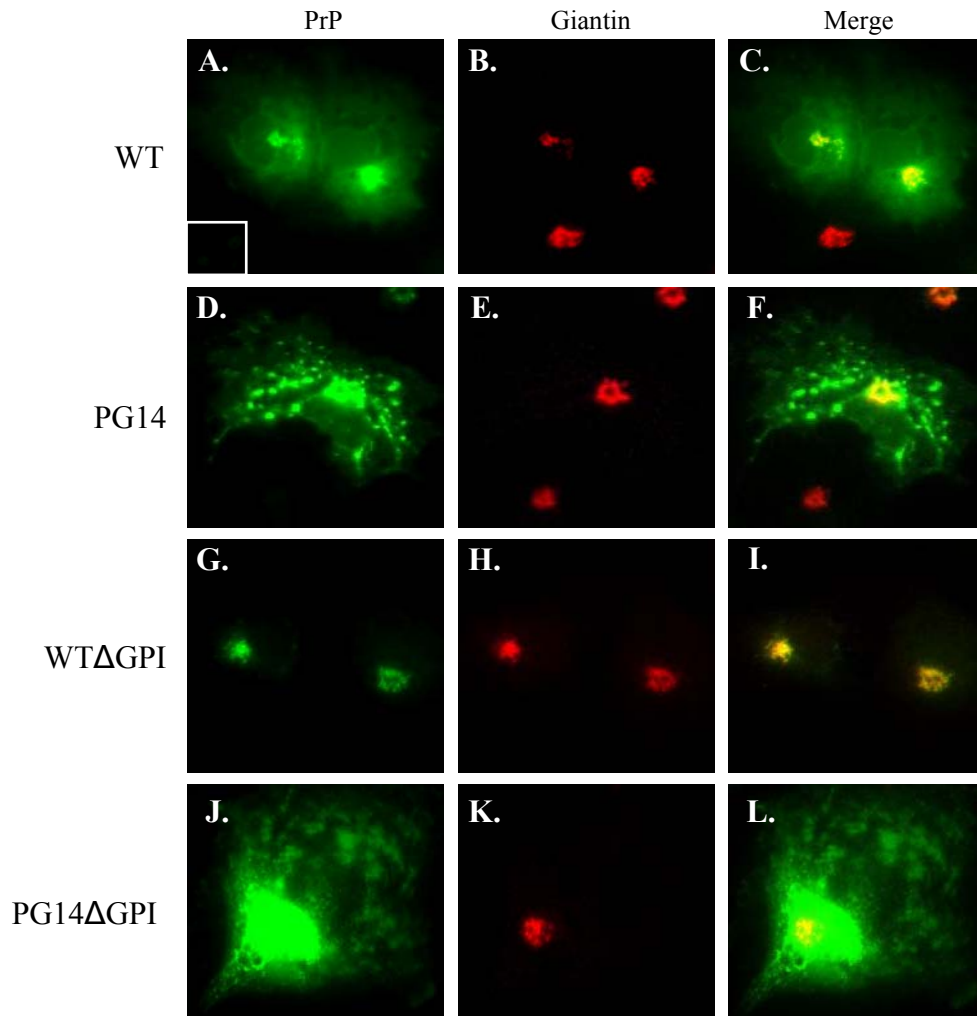
Figure 6. PG14ΔGPI partially colocalizes with the Golgi apparatus. Cells expressing vector (inset), WT PrP (a-c), PG14 (d-f), WTΔGPI (g-i), and PG14ΔGPI (j-l) were fixed, permeabilized, then stained with PrP primary antibody 6H4 and α-giantin (b, e, h, k). Analysis by fluorescence microscopy allows observation of PrP (a, d, g, j), Golgi (b, e, h, k), and merged pictures (c, f, i, l). All constructs show colocalization with the Golgi apparatus. PG14 and PG14ΔGPI can be found in Golgi and elsewhere.

insoluble in cell lysates (Figure 7A, lanes 5,6,9,10). These results demonstrate that loss

of the GPI anchor does not interfere with the ability of PG14 to aggregate within cells. In

media, WT and WTΔGPI were also entirely soluble (Figure 7B, lanes 3,4,7,8). Full-

length PG14 is rarely detected in the media (Figure 7B, lanes 5,6), however on occasion

we noticed a faint band that correlated with the soluble fraction (data not shown).

Interestingly, the small amount of PG14ΔGPI that escaped into the media was also found

to be entirely soluble (Figure 7B, lanes 11,12), suggesting that PG14 aggregates remain

retained, and only soluble molecules are able to reach the cell surface.

In transgenic mice inoculated with scrapie, WTΔGPI molecules formed larger

aggregates than mice expressing endogenous WT PrP, suggesting that the GPI anchor

affects aggregate size *in vivo*. To investigate whether the size of PG14ΔGPI aggregates

in cells were larger compared with full length PG14, cell lysates were centrifuged at high

speeds in sucrose step-gradients that ranged from 10% to 60% (Figure 8). WT and

WTΔGPI molecules are found at the lowest sucrose density fractions, indicating that they

are likely monomeric and do not form large aggregates. PG14, however, is found at low-

and mid-density fractions, as well as in the pellet, demonstrating that a range of aggregate

sizes are found in cells. The density profile for PG14ΔGPI was similar to that of full

length PG14, signifying that loss of the GPI anchor did not drastically affect aggregate

sizes in cells as determined by this assay. Differences in sizes of aggregates within the

pellet could not be distinguished by this assay.

A.
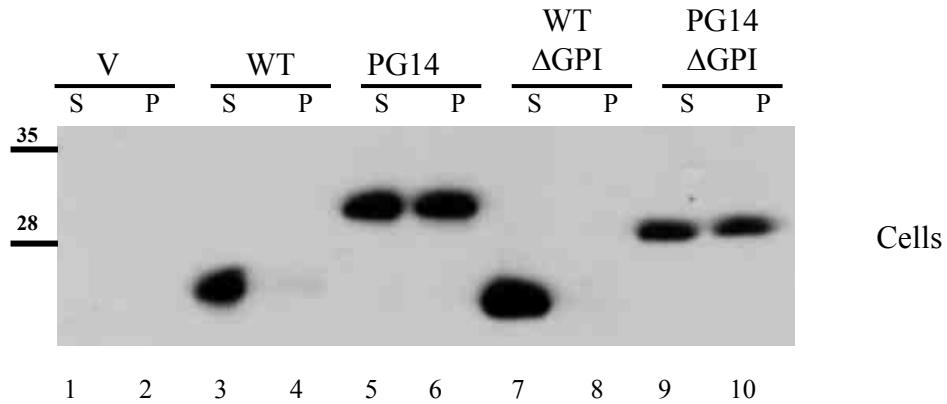
B.
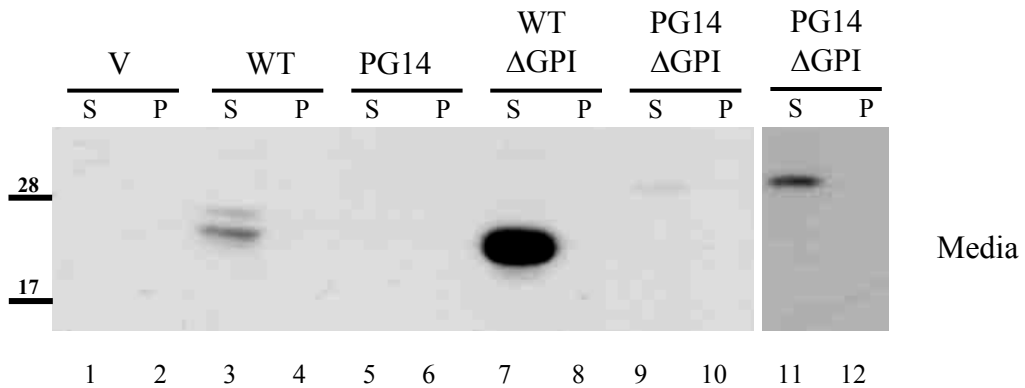
Figure 7. Intracellular PG14ΔGPI is partially insoluble. Cell lysates (A) and media (B) from cells expressing vector (lanes 1,2), WT PrP (lanes 3,4), PG14 (lanes 5,6), WTΔGPI (lanes 7,8), and PG14ΔGPI (lanes 9,10) were spun at high speeds in detergent buffer to separate soluble (S) from pelleted insoluble (P) fractions, then analyzed by Western blotting with 3F4 antibody. In cell lysates, WT and WTΔGPI molecules are entirely soluble, while PG14 and PG14ΔGPI are partially insoluble. In media, WT and WTΔGPI molecules are also soluble; the little PG14ΔGPI that escapes is also soluble. Lanes 11 & 12 show PG14ΔGPI at a darker exposure. Molecular size markers are given in kilodaltons.
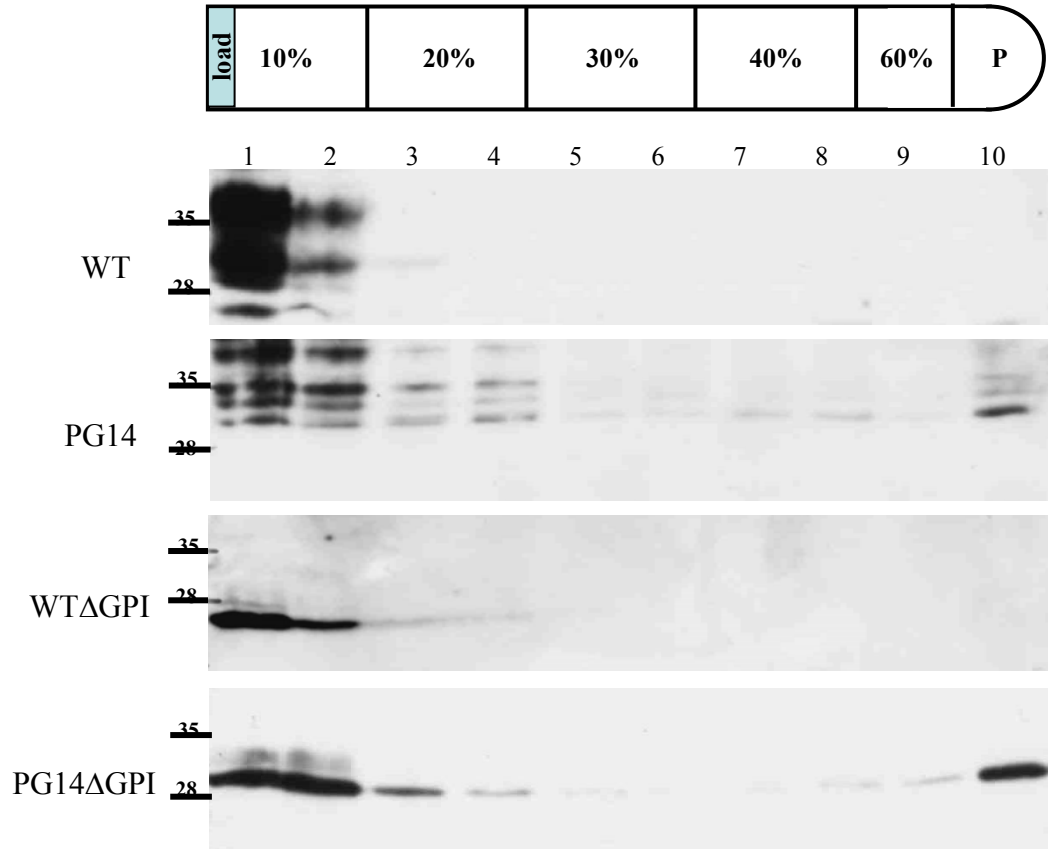
Figure 8. PG14ΔGPI forms large aggregates. Cell lysates from cells expressing WT PrP (lanes 3,4), PG14, WTΔGPI, and PG14ΔGPI were placed atop a sucrose step gradient (densities indicated by percentage), then centrifuged at high speeds separate aggregated molecules from monomers. Fractions from each step in the gradient were methanol-precipitated, then analyzed by Western blotting with 3F4 antibody. WT and WTΔGPI molecules monomers colocalize with low-density fractions, while PG14 and PG14ΔGPI can be found in higher density fractions and within the pellet (P), indicating the formation of large aggregates. There is no difference in the aggregate size profile between PG14 and PG14ΔGPI. Molecular size markers are given in kilodaltons.

3.5 Discussion

We have demonstrated that PG14ΔGPI expressed in mammalian cells is primarily

unglycosylated and retained intracellularly. Furthermore, deletion of the GPI anchor in

mutant PG14 does not affect intracellular localization, or ability to aggregate.

Collectively, these results reveal that the GPI anchor does not play a major role in

determining the aberrant biochemical and cellular trafficking characteristics that are

particular to the PG14 familial mutant prion protein. These data provide initial insights

of PG14ΔGPI molecular behavior, paving the way for future studies investigating the role

of the GPI anchor in PG14 toxicity in transgenic mice.

Loss of GPI anchor affects mutant PrP glycosylation. It is well documented

that GPI anchorage and membrane attachment are crucial for proper N-linked

glycosylation of PrP (Walmsley et al. 2001; Walmsley et al. 2003). In its absence,

WTΔGPI is expressed mainly as unglycosylated both in cells and *in vivo* (Rogers et al.

1993; Chesebro et al. 2005; McNally et al. 2009). It is speculated that the loss of

membrane attachment may localize PrP away from its protein interactors or

oligosaccharyltransferases within the ER lumen, thus leading to impaired glycosylation.

It is also possible that the lack of a GPI anchor causes PrP to adopt a differential

conformation that renders the glycosylation sites inaccessible (Walmsley et al. 2001).

We demonstrate here for the first time that deletion of a GPI anchor also impairs

glycosylation of a disease-associated familial mutant PrP in the same manner, wherein

the vast majority of PG14ΔGPI molecules are not glycosylated (Figure 2). The

deglycosylation effect observed is due solely to the lack of the GPI anchor and not the

PG14 mutation itself, because full-length PG14 is present in several different glycoforms when expressed in cells (Figure 1). Interestingly, even though a subset of PG14ΔGPI molecules are retained within the ER, where molecules have prolonged exposure to the site of oligosaccharyltransferase activity, glycosylation enzymes are still unable to recognize and/or transfer carbohydrate attachments to the PrP molecule.

Loss of GPI Anchor Does Not Affect PG14 Intracellular Localization. Like WT PrP, PG14 is synthesized and translocated into the ER, where it is glycosylated and fitted with a GPI anchor. It is further modified in the Golgi apparatus and presumably packed into secretory vesicles bound for the plasma membrane (Lehmann and Harris 1995; Drisaldi et al. 2003) . In neurons, PG14 can traverse within neurites, but remain intracellular, suggesting a defect in PG14-carrying secretory vesicles to fuse with the plasma membrane (Medrano et al. 2008). Although some PG14 reaches the surface, the majority remain retained intracellularly, partially within the ER and Golgi apparatus (Ivanova et al. 2001).

Though cell surface localization in PG14 and PG14ΔGPI is limited, the fraction of PG14ΔGPI molecules released into the media is noticeably higher than full-length PG14 (Figure 3), demonstrating that PG14ΔGPI that reaches the cell surface is more easily dissociated from the plasma membrane.

However, the vast majority of PG14 and PG14ΔGPI molecules are retained intracellularly and within the same organelles, emphasizing that PG14 and PG14ΔGPI have the same deficiency in the release of molecules to the plasma membrane. The main conclusion derived from these results is that the mechanism responsible for mutant

retention does not rely on membrane attachment by a GPI anchor. It is possible that

PG14ΔGPI also associates with the membrane intracellularly, as does WTΔGPI

(Campana et al. 2007). Our studies thus far have not been able to distinguish whether the

protein floats within the lumen of organelles and vesicles, or joins with the lipid bilayer

by a GPI anchor-independent mechanism. Although the mechanism for retention is

ambiguous, it is possible that mutant protein retention does not rely on GPI anchorage,

but on the state of aggregation. In support of this hypothesis, only a small pool of soluble

PG14 and PG14ΔGPI molecules reach the cell surface and are secreted (Figure 8).

Additionally, aggregation and retention may be exacerbated by the lack of glycosylation,

which can intensify PrP^C misfolding and accumulation within the Golgi (Lehmann and

Harris 1997).

Loss of a GPI Anchor Does Not Affect PG14 Misfolding and Aggregation. In

cells, both anchorless PG14ΔGPI molecules and PG14 proteins spontaneously aggregate

when expressed in transfected mammalian cells (Figures 8, 9), demonstrating that

aggregation is not dependent on either membrane attachment or glycosylation state for

inherited prion mutants. This conclusion is supported by previous evidence showing that

even recombinant PG14 molecules assemble into proteinase K-resistant structures

(Gauczynski et al. 2002). This evidence supports the notion that the repeat expansion

itself is sufficient to augment prion conversion, independent of a GPI anchor.

Although lack of the GPI anchor does not interfere with PG14 aggregation, it is

possible that the aggregate structures are modified. Tg(WTΔGPI) mice inoculated with

RML-PrP^{Sc} form dense thioflavin-S positive plaques within the central nervous system

(Chesebro et al. 2005). These amorphous aggregates are a stark contrast from the highly structured fibrils that are usually detected in RML-inoculated wild-type mice. Conformational differences in molecules, the lack of attached carbohydrates, or both, may contribute to the disparity between WT and WTΔGPI aggregate formations *in vivo*. Similarly, PG14ΔGPI aggregates may form and expand in different structural conformations as well when compared with PG14. Although our assays show no difference between the PG14 and PG14ΔGPI aggregate biochemical properties in detergent insolubility and sucrose gradient assays (Figures 7,8)—and thus no drastic differences in aggregate formation—further investigations will be necessary to determine whether the loss of the GPI anchor affects the structural properties of the inherited PrP mutant.

Does the GPI anchor play a role in the pathogenesis of PG14 familial prion disease? We have demonstrated that the loss of the GPI anchor of the PG14 mutant does not affect PG14 localization or ability to aggregate. However, it is difficult to ascertain whether GPI anchor deletion would affect disease onset and progression *in vivo*. The prion field lacks a model that can mimic PG14 toxicity in cell culture, thus the role of the GPI anchor in PG14 disease can only be fully appreciated *in vivo* in transgenic mice expressing PG14ΔGPI. We are currently generating these mice, confident that further investigation into the role of the GPI anchor in the context of a familial prion disorder would clarify mechanisms of cellular and physiological.

3.6 References

Baron, G. S. and B. Caughey (2003). "Effect of glycosylphosphatidylinositol anchor-dependent and -independent prion protein association with model raft membranes on conversion to the protease-resistant isoform." <u>J Biol Chem</u> **278**(17): 14883-92.

Biasini, E., A. Z. Medrano, et al. (2008). "Multiple biochemical similarities between infectious and non-infectious aggregates of a prion protein carrying an octapeptide insertion." <u>J Neurochem</u> **104**(5): 1293-308.

Bolton, D. C., S. J. Seligman, et al. (1991). "Molecular location of a species-specific epitope on the hamster scrapie agent protein." <u>J Virol</u> **65**(7): 3667-75.

Borchelt, D. R., A. Taraboulos, et al. (1992). "Evidence for synthesis of scrapie prion proteins in the endocytic pathway." <u>J Biol Chem</u> **267**(23): 16188-99.

Campana, V., A. Caputo, et al. (2007). "Characterization of the properties and trafficking of an anchorless form of the prion protein." <u>J Biol Chem</u> **282**(31): 22747-56.

Caughey, B. and G. J. Raymond (1991). "The scrapie-associated form of PrP is made from a cell surface precursor that is both protease- and phospholipase-sensitive." <u>J Biol Chem</u> **266**(27): 18217-23.

Chesebro, B., M. Trifilo, et al. (2005). "Anchorless prion protein results in infectious amyloid disease without clinical scrapie." <u>Science</u> **308**(5727): 1435-9.

Chiesa, R., P. Piccardo, et al. (1998). "Neurological illness in transgenic mice expressing a prion protein with an insertional mutation." <u>Neuron</u> **21**(6): 1339-51.

Drisaldi, B., R. S. Stewart, et al. (2003). "Mutant PrP is delayed in its exit from the endoplasmic reticulum, but neither wild-type nor mutant PrP undergoes retrotranslocation prior to proteasomal degradation." <u>J Biol Chem</u> **278**(24): 21732-43.

Gauczynski, S., S. Krasemann, et al. (2002). "Recombinant human prion protein mutants huPrP D178N/M129 (FFI) and huPrP+9OR (fCJD) reveal proteinase K resistance." <u>J Cell Sci</u> **115**(Pt 21): 4025-36.

Ivanova, L., S. Barmada, et al. (2001). "Mutant prion proteins are partially retained in the endoplasmic reticulum." <u>J Biol Chem</u> **276**(45): 42409-21.

Kaneko, K., M. Vey, et al. (1997). "COOH-terminal sequence of the cellular prion protein directs subcellular trafficking and controls conversion into the scrapie isoform." <u>Proc Natl Acad Sci U S A</u> **94**(6): 2333-8.

Lehmann, S., N. Daude, et al. (1997). "A wild-type prion protein does not acquire properties of the scrapie isoform when coexpressed with a mutant prion protein in cultured cells." Brain Res Mol Brain Res **52**(1): 139-45.

Lehmann, S. and D. A. Harris (1995). "A mutant prion protein displays an aberrant membrane association when expressed in cultured cells." J Biol Chem **270**(41): 24589-97.

Lehmann, S. and D. A. Harris (1996). "Mutant and infectious prion proteins display common biochemical properties in cultured cells." J Biol Chem **271**(3): 1633-7.

Lehmann, S. and D. A. Harris (1996). "Two mutant prion proteins expressed in cultured cells acquire biochemical properties reminiscent of the scrapie isoform." Proc Natl Acad Sci U S A **93**(11): 5610-4.

Lehmann, S. and D. A. Harris (1997). "Blockade of glycosylation promotes acquisition of scrapie-like properties by the prion protein in cultured cells." J Biol Chem **272**(34): 21479-87.

McNally, K. L., A. E. Ward, et al. (2009). "Cells Expressing Anchorless Prion Protein are Resistant to Scrapie infection." J Virol.

Medrano, A. Z., S. J. Barmada, et al. (2008). "GFP-tagged mutant prion protein forms intra-axonal aggregates in transgenic mice." Neurobiol Dis **31**(1): 20-32.

Prusiner, S. B., M. R. Scott, et al. (1998). "Prion protein biology." Cell **93**(3): 337-48.

Rogers, M., F. Yehiely, et al. (1993). "Conversion of truncated and elongated prion proteins into the scrapie isoform in cultured cells." Proc Natl Acad Sci U S A **90**(8): 3182-6.

Stewart, R. S., B. Drisaldi, et al. (2001). "A transmembrane form of the prion protein contains an uncleaved signal peptide and is retained in the endoplasmic Reticulum." Mol Biol Cell **12**(4): 881-9.

Taylor, D. R. and N. M. Hooper (2006). "The prion protein and lipid rafts." Mol Membr Biol **23**(1): 89-99.

Trifilo, M. J., M. Sanchez-Alavez, et al. (2008). "Scrapie-induced defects in learning and memory of transgenic mice expressing anchorless prion protein are associated with alterations in the gamma aminobutyric acid-ergic pathway." J Virol **82**(20): 9890-9.

Walmsley, A. R., F. Zeng, et al. (2001). "Membrane topology influences N-glycosylation of the prion protein." Embo J **20**(4): 703-12.

Walmsley, A. R., F. Zeng, et al. (2003). "The N-terminal region of the prion protein ectodomain contains a lipid raft targeting determinant." J Biol Chem **278**(39): 37241-8.

Westergard, L., H. M. Christensen, et al. (2007). "The cellular prion protein (PrP(C)): its physiological function and role in disease." Biochim Biophys Acta **1772**(6): 629-44.

Yin, S., S. Yu, et al. (2006). "Prion proteins with insertion mutations have altered N-terminal conformation and increased ligand binding activity and are more susceptible to oxidative attack." J Biol Chem **281**(16): 10698-705.

CHAPTER 4

Discussion

4.1 Summary

Post-translational or genetic aberrations in prion protein (PrP) are associated with a set of progressive neurodegenerative diseases termed prion disorders, marked clinically by cognitive decline and pathologically by PrP deposition, glial proliferation, and neuronal loss. The molecular, cellular, and physiological processes underlying sporadic or infectious, and inherited prion diseases remain ambiguous, although accumulation of PrP^{Sc}, or a toxic byproduct of conversion, is generally assumed to trigger pathology in sporadic and infectious cases.

In familial cases of prion disease, over 50 mutations have been identified as pathological forms of PrP^{M}. One such mutant, PG14, is a 217 base pair insertion that results in the extension of the five endogenous *p*roline- and *g*lycine-rich octapeptide motifs found in PrP, from five repeats to fourteen. In transgenic mice, PG14 causes spontaneous neurological disease marked by cerebellar granule degeneration and astrogliosis. Localization of the mutant prion protein is necessary to elucidate the mechanisms responsible for disease pathology. However, due to the PrP^{Sc}-like aggregate nature of PG14, visualization of PG14 requires potentially damaging antigen retrieval (AR) techniques. To circumvent the need for AR protocols and visualize PG14 directly, we generated transgenic mice expressing a PG14-EGFP fusion protein that can be detected readily using fluorescence microscopy.

In Chapter 2, I find that Tg(PG14-EGFP) mice, but not Tg(WT-EGFP) mice, also develop spontaneous neurological illness similar to their Tg(PG14) counterparts, thus demonstrating their value as a model system in which to study familial prion disease. Furthermore, I find that PG14-EGFP derived from brain homogenates retains the same

biochemical characteristics as PG14, including detergent insolubility, PK resistance, and reactivity with PrP aggregate-specific antibody 15B3. In cerebellar granule neurons and brain sections of Tg(WT-EGFP) animals, PrP distribution is uniformly even throughout the cell soma and neurites, indicating normal localization *in vivo* (Barmada et al. 2004). In contrast, brain sections of Tg(PG14-EGFP) mice display ubiquitous fluorescent puncta ubiquitous within the neuropil of the cerebrum and cerebellum, which correspond to accumulated PG14-EGFP protein. These presumed aggregates were found at the highest densities in axon-rich regions of both the central and peripheral nervous systems, including the dentate gyrus of the hippocampus, the molecular layer of the cerebellum, the striatum, and the sciatic nerve. Additionally, in primary neurons derived from transgenic pups, PG14-EGFP, but not WT-EGFP, demonstrated intracellular accumulation, with little or no mutant protein reaching the cell surface. These studies highlight the aberrant trafficking patterns of aggregated PG14 *in vivo* without the use of AR, and demonstrate that intracellular PG14 aggregation within axons may contribute to inherited prion disease pathology.

In a further attempt to understand what cell biological properties mediate mutant PG14 mislocalization, aggregation, and toxicity, I explore the role of the GPI anchor in PG14 cell behavior in transfected cells. In cells and in transgenic mice, the GPI anchor has demonstrated a regulatory role in proper WT PrP cell surface localization, and in PrP[Sc] aggregate formation and disease toxicity (Walmsley *et al.* 2003; Chesebro *et al.* 2005; Sim and Caughey 2008). However, what processes the GPI anchor might mediate in a mutant PrP have not yet been investigated. To this end, I generated a PG14 construct lacking the C-terminal end genetic signal sequence encoding the attachment of a GPI

anchor, then expressed the protein in mammalian cells under a strong CMV promoter. I

found that in contrast to its effect on WT PrP, deletion of the GPI anchor did not alter

normal PG14 localization. PG14ΔGPI, like PG14, was retained intracellularly within the

ER and Golgi, and failed to localize at the cell surface or in endosomes. PG14ΔGPI also

displayed detergent insolubility and fractionated with dense sucrose fractions,

demonstrating that, like PG14, the molecule aggregates spontaneously. This work

establishes that GPI-mediated membrane attachment does not affect mutant PrP

localization or aggregation in cells, thus initiating further investigation on its effect on

PG14 toxicity.

<p style="text-align:center">*　　*　　*</p>

These studies tackle two very relevant and related issues in the field of prion

biology, including the possible mechanisms of familial prion disease pathogenesis, and

whether the same molecular and cellular pathways underlie inherited and infectious prion

diseases. The contributions of my research are discussed within the context of these

issues below.

4.2 What Causes Familial Prion Disease?

A. The Role of Aggregation

Cell and mouse studies highlighting the aberrant cellular trafficking and abnormal

accumulation of untagged PG14 suggests that aggregation is involved with the PG14

cellular pathogenesis. Indeed, many protein aggregates are associated with a wide variety

of neurodegenerative diseases, including Alzheimer's, Parkinson's, and Huntington's

Disease (Dimakopoulos 2005). The length of OR expansion correlates directly with rate

of aggregation (Moore *et al.* 2006; Yin *et al.* 2006; Yu *et al.* 2007) and inversely with age

of onset and disease duration in familial CJD patients (Mead 2006; Mead et al. 2006), suggesting that increased numbers of ORs leads to greater aggregation, which in turn results in increased mutant toxicity. In support of this idea, sick Tg(PG14) mice display higher levels of insoluble material within their brain homogenates compared with mice that are subclinical, indicating a correlation between aggregation and familial prion disease in transgenic animals. Additionally, Tg(PG14) lines expressing low amounts of the mutant protein demonstrate mostly soluble PG14 protein molecules and remain healthy. In Chapter 2, I find that aggregation correlates with disease in Tg(PG14-EGFP) mice, supporting the notion that degree of insolubility is associated with clinical illness. Sick animals qualitatively displayed higher densities of punctate deposits within neuropil and axons, especially those within the mossy fibers of the dentate gyrus and the molecular layer of the cerebellum, compared with healthy transgenic littermates, which presented with the same depositions, but to a lesser extent.

However, the presence of insoluble material in healthy animals demonstrates that protein aggregation in and of itself is insufficient to cause toxicity in familial prion disease. Tg(PG14) animals exhibit insoluble material within brain homogenates as young as five days old. Because Tg(PG14) mice do not develop neurological illness for ~270 days, they develop into adulthood without any major physical constraints, and remain healthy for ~9 months before onset of symptoms even with aggregates present. Insoluble material is present during early stages of development, then accrues over the duration of a lifetime, indicating that a possible threshold of accumulation needs to be breached before the onset of symptoms—large amounts of aggregation may be necessary in order to cause sufficient cellular and physiological pathology to cause onset of clinical symptoms.

Consistent with this data, I detect fluorescent punctate deposits within the soma and neurites in cerebellar granule neurons derived from healthy Tg(PG14-EGFP) four day-old pups (Chapter 2). Tg(PG14-EGFP) heterozygotes display conspicuous amounts of aggregation, but remain healthy for over two years. Additionally, brain sections of ill mice display increased amounts of fluorescent deposits in axon-dense regions compared with healthy controls.

Accumulating evidence suggests a role for PrP in synaptic development and/or function (see Introduction). Wild-type PrP travels both anterogradely and retrogradely within axons and is enriched along axons and pre-synaptic regions, indicating that its localization at these points may be crucial for its function. We find that mutant PG14-EGFP is also prominently located in axons, especially within the dentate gyrus of the hippocampus, the alveus oriens, and the molecular layer of the cerebellum, regions where PrP is expressed very strongly (Medrano *et al.* 2008). However, unlike soluble WT PrP and WT-EGFP, PG14-EGFP aggregates intracellularly within the soma and neurites of neurons, both in brain section and in cell culture. Steady accumulation of mutant PrP within axons may lead to disruption of intracellular transport machinery (microtubules, kinesins, dyneins), thus preventing PrP, or other synaptic proteins, from reaching the presynaptic site (Figure 1). Indeed, a decrease in synaptophysin-positive terminals was observed in Tg(PG14) animals, supporting this theory (Chiesa *et al.* 2005). Axonal blockage has also been observed in flies overexpressing APP-like protein and several poly-Q mutants, associated with Alzheimer's Disease and Huntington's disease, respectively (Gunawardena and Goldstein 2001; Gunawardena *et al.* 2003; Gunawardena and Goldstein 2005). It is speculated that blockage prompts or aids in neuronal
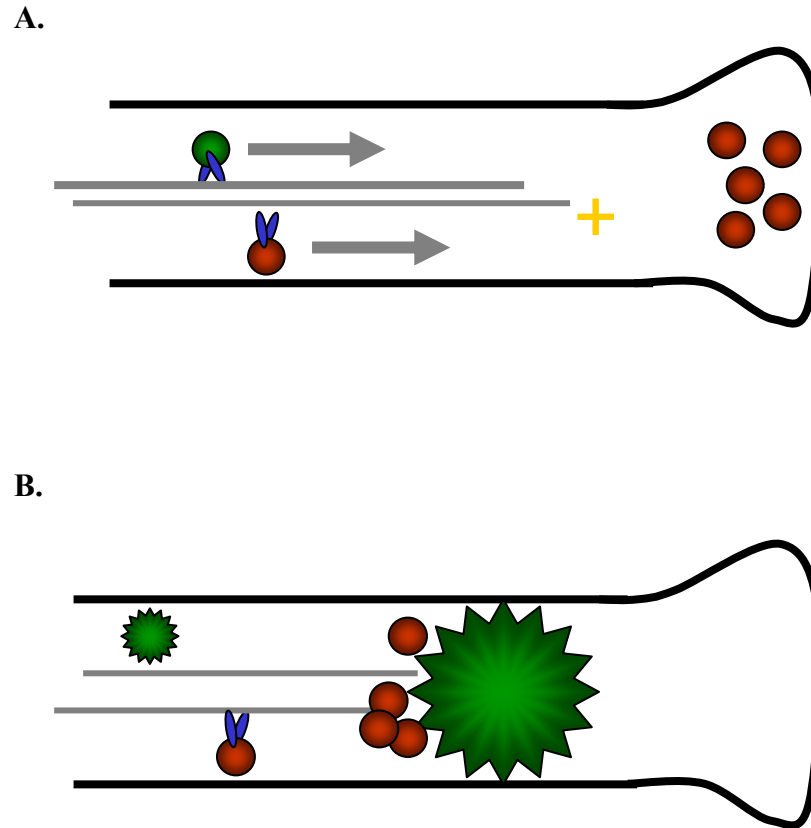
Figure 1. Axonal Blockage Model (A) WT PrP (blue) and synaptic proteins in vesicles (red) travel along microtubule tracks (gray) toward the axon terminal. (B) PG14 (green star) accumulation in the axon blocks axonal transport, preventing synaptic proteins from reaching the presynaptic site.

dysfunction and subsequent neuronal cell death. It would be informative to compare axonal rates of transport in WT PrP and mutant PrPs to determine whether abnormal trafficking patterns of mutants also disrupts delivery of other synaptic proteins and leads to neurotoxicity. For example, one may be able to co-transfect polarized primary neurons with green fluorescently tagged WT or PG14 PrPs along with red fluorescently tagged proteins that use fast axonal transport mechanisms, such as synaptophysin or kinesin-I, then use kymograph analysis to measure the speed and/or number of particles that travels through axons. If PG14 does cause blockages in axonal transport, we would expect that PG14 itself would show slower rates of travel compared with WT PrP. A decrease in speed or efficiency of transport of other axonal proteins co-transfected with PG14 would suggest that the mutant PrP is able to affect trafficking of other proteins as well. Work attempting such experiments is described in Appendix 3, and further investigations, similar to the experiments listed above, will be necessary to solidly support or refute the axonal blockage model.

Although aggregation seems well-correlated with transgenic PG14 models of disease, this is not the case with many other disease-associated PrP^M mutants. P101L, D197N, and V209I exhibit detergent solubility and some PK-sensitivity, much like endogenous PrP^C. They also exhibit normal rates of synthesis and degradation, as well as proper cell-surface localization when expressed in transfected mammalian cell lines, indicating that formation of large aggregates is not necessary in order to produce toxicity. It is possible that the PG14 mode of toxicity is entirely different from other soluble PrP^M counterparts, and that aggregation alone induces clinical symptoms. This viewpoint, however, is too simplistic and unlikely, given the number of soluble and insoluble

132

mutations that result in the same clinical symptoms. It is more likely that every one of the 50+ PrP mutant utilizes a common mechanism of disease, and interferes with the same as-of-yet unidentified pathways in all familial prion disorders. If this platform is taken as an assumption, then protein aggregation can be considered a factor that may contribute to disease, but is neither necessary nor sufficient to induce PrP^M toxicity.

B. PrP^M Toxicity

What then, could be the cause of PrP^M toxicity? One clue may be found in the size of toxic PrP^{Sc} particles. Beta-oligomers synthesized from recombinant PrP or from thermal refolding were both able to induce neurotoxicity when introduced into cell cultures and to primary neurons (Novitskaya *et al.* 2006; Simoneau *et al.* 2007), demonstrating that both small and large PrP aggregates had the ability to confer toxicity. Indeed, oligomeric forms of disease-associated proteins have demonstrated increased neurotoxicity compared with larger fibrillar or amorphous aggregates in several neurodegenerative disease, including amyloid β protein in Alzheimer's disease, α-synuclein in Lewy Body disease, and huntingtin protein in Huntington's Disease (Dimakopoulos 2005; Haass and Selkoe 2007). It is feasible then, that PG14 and other PrP mutants confer toxicity by forming PK-soluble or slightly PK-insoluble oligomers which interfere with normal cellular processes. The work accomplished in Chapter two does not exclude this possibility.

Alternatively, aberrations in signal transduction may also play a role in prion toxicity. The GPI anchor, attached at the C-terminal end of PrP, tethers the protein to the outer leaflet of the lipid bilayer of the plasma membrane. Because of the high affinity of

GPI anchors for saturated lipid species, PrP^C is concentrated in lipid raft domains along with several cell-signaling proteins, including Fyn and Src (Taylor and Hooper 2006), and several studies have implicated PrP as a neuroprotective cell signaling molecule (see Introduction). In one model of PrP^{Sc} disease, once PrP^C transforms into PrP^{Sc}, the normal signal is subverted into one that is toxic (Figure 2A). In support of this hypothesis, transgenic mice expressing anchorless PrP demonstrate robust PrP^{Sc} propagation, but no appearance of clinical illness. These combined results led to the hypothesis that the lack of GPI-mediated PrP attachment to the plasma membrane interferes with the delivery of neurotoxic signals induced by PrP^{Sc} formation (Figure 2B) (Brandner *et al.* 1996; Solforosi *et al.* 2004).

Whether GPI anchorage is necessary to transduce toxic signals induced by PrP^M remains ambiguous. Chapter three describes work that lays the foundation for answering this question. PG14ΔGPI retains the same cellular localization, aggregate patterns, and biochemical characteristics as PG14 in cells, with the main structural difference being the absence of a membrane-bound anchor. Thus, we can use PG14ΔGPI to test the specific effects of GPI anchor loss on toxicity *in vivo* without affecting any of the abnormal properties associated with the PG14 mutant. These experiments are presently under way.

The prion field lacks a model that can mimic PG14 toxicity in cell culture, thus the role of the GPI anchor in PG14 disease can only be fully appreciated in transgenic mice expressing PG14ΔGPI. We are currently generating these animals, confident that further investigation into the role of the GPI anchor in the context of a familial prion disorder would clarify mechanisms of cellular and physiological pathology. If the GPI anchor does indeed mediate toxicity, either by transducing signals itself or by properly

A. PrP^{Sc} + PrP^C
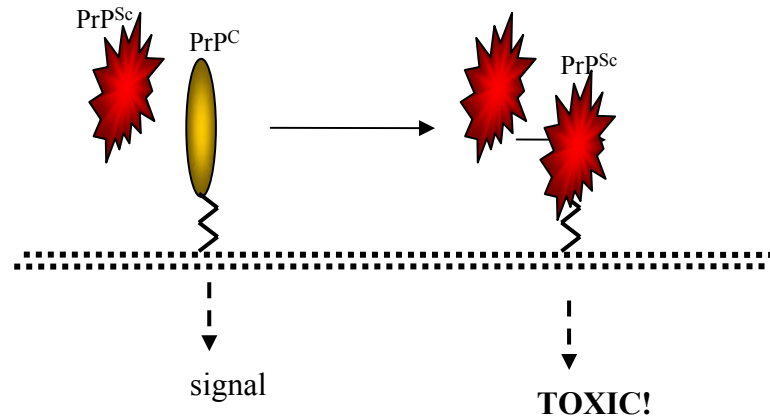
B. PrP^{Sc} + PrPΔGPI
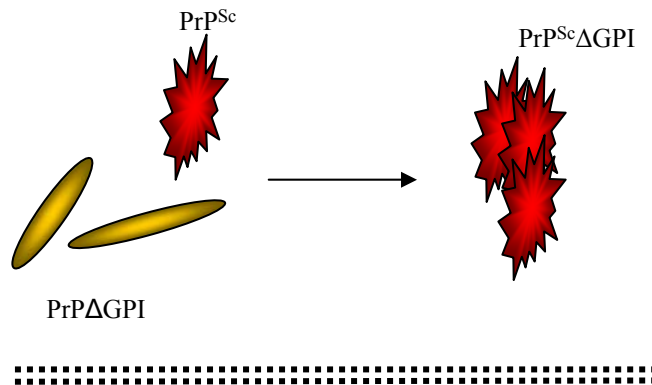
Figure 2. The GPI Anchor Mediates Toxic Signal Transduction in Prion Disease. (A) In WT mice, PrP^C is capable of transducing a signal to the cell. Upon exposure to PrP^{Sc}, anchored PrP^C is converted to PrP^{Sc}, thus stimulating toxic signals into the cell. (B) In Tg(PrPΔGPI) mice, untethered PrP^C is secreted into extracellular space and does not stimulate any signal transduction. Upon exposure to PrP^{Sc}, PrPΔGPI is converted to PrP^{Sc}, and because of a lack of membrane attachment, does not produce any toxic signal.

localizing PrPs for interaction with other signaling molecules, PG14ΔGPI will propagate

aggregated PrP but will be unable to confer the toxic signals that result in a physiological

display of clinical symptoms. Conversely, if transgenic PG14ΔGPI mice develop illness,

we can conclude that GPI-mediated membrane attachment is unnecessary for toxic signal

transduction.

4.3 Are PrP^{Sc} and PrP^{M} Pathways of Disease the Same?

PrP^{M} is commonly assumed to mimic an PrP^{Sc} intermediate molecule. Support

for this theory comes in the form of shared clinical symptoms between patients suffering

from inherited and infectious prion disease and from biochemical similarities between

some PrP genetic mutants and PrP^{Sc}. Patients from both PrP^{M} and PrP^{Sc} groups display

many overlapping subsets of clinical symptoms. For example, sporadic and infectious

CJD patients often present with rapidly progressive dementia, involuntary muscle

contractions, and abnormal EEG readings. These same features are also found in patients

carrying familial mutations of CJD. Additionally, the biochemical characteristics of

some PrP mutants resemble those which define PrP^{Sc}. For example, PrP^{Sc} is resistant to

up to 50 μg/mL protease K, while PrP mutants PG14, D177N, and E199K are partially

resistant to protease K, albeit to a lesser degree, maintaining protein structure in up to two

μg/mL PK. These same mutants also have the tendency to aggregate and are insoluble in

detergents, like PrP^{Sc}. Additionally, aggregated familial mutants react with PrP^{Sc}-specific

antibodies 15B3 and G19 (Biasini *et al.* 2008), suggesting that PrP^{M} and PrP^{Sc}

conformations are similar enough that some shared epitopes are exposed. These data

suggest that both infectious PrP^{Sc} and some inherited PrP mutants are similar in

biochemical characteristics and induced pathologies, and thus may interfere within the same pathways to induce prion disease toxicity.

However, PrP^{Sc} inoculation of mice expressing disease-associated prion mutants does not hasten progression of PrP^{Sc} disease, strongly arguing that PrP^{M} is not solely an intermediate destined for PrP^{Sc} replication (Chiesa *et al.* 2003). Additionally, there are many other cell biological and biochemical differences between some PrP mutants and PrP^{Sc}, suggesting that there are variable factors and pathways that mediate infectious versus inherited prion pathology. One of the most obvious discrepancies is the non-infectivity of inherited prion mutants. PrP^{Sc} by definition must be infectious. In contrast, in cells and in transgenic mice, P101L and PG14 are unable to bind and convert wild-type PrPs into a mutant conformation bearing the same biochemical properties or toxic effects (Telling *et al.* 1996; Lehmann *et al.* 1997; Chiesa *et al.* 2003) (see Appendix 1). At least one prion mutant demonstrates infectivity when brain homogenates from human patients carrying the mutation and disease are inoculated into transgenic mice (Piccardo *et al.* 2007). However, many PrP mutants differ from PrP^{Sc} in that they are not infectious.

Differences in subcellular localization also argue against similar origins of toxicity. PrP^{Sc} aggregate formation requires PrP^{C} exposure at the extracellular interface or within the endosomal pathway (Caughey and Raymond 1991; Borchelt *et al.* 1992; Marijanovic *et al.* 2009). PrP^{Sc} has been detected mainly in endosomes and the Golgi apparatus in scrapie-infected neuroblastoma cells and brains, and aggregated in extracellular spaces within neuropil *in vivo*. However, PG14 is synthesized within the ER, aggregates spontaneously, and is retained intracellularly, with little to no PG14 molecules at the surface and no co-localization within endosomes either in cells or *in vivo*

(Daude *et al.* 1997; Ivanova *et al.* 2001). Studies in Tg(PG14-EGFP) mice confirm these findings and further report that that majority of aggregates are found in axon-dense regions.

Ultimately, whether PrP^M and PrP^{Sc} share the same pathways of toxicity is unclear. There are many arguments that suggest that the pathological mechanisms between the two may be variable, such as differential localization, dissimilar biochemical properties, and inability of PrP^M to affect PrP^{Sc} disease progression in inoculated PrP^M-expressing animals. However, because the routes of pathogenicity for both PrP^M and PrP^{Sc} are undefined, comparisons between modes of inherited versus infectious prion toxicity remain conceptual. Clearly, additional investigation is necessary to elucidate the cellular and physiological pathways involved with prion pathogenesis.

4.4 References

Barmada, S., P. Piccardo, et al. (2004). "GFP-tagged prion protein is correctly localized and functionally active in the brains of transgenic mice." Neurobiol Dis **16**(3): 527-37.

Biasini, E., M. E. Seegulam, et al. (2008). "Non-infectious aggregates of the prion protein react with several PrP(Sc)-directed antibodies." J Neurochem.

Borchelt, D. R., A. Taraboulos, et al. (1992). "Evidence for synthesis of scrapie prion proteins in the endocytic pathway." J Biol Chem **267**(23): 16188-99.

Brandner, S., S. Isenmann, et al. (1996). "Normal host prion protein necessary for scrapie-induced neurotoxicity." Nature **379**(6563): 339-43.

Caughey, B. and G. J. Raymond (1991). "The scrapie-associated form of PrP is made from a cell surface precursor that is both protease- and phospholipase-sensitive." J Biol Chem **266**(27): 18217-23.

Chesebro, B., M. Trifilo, et al. (2005). "Anchorless prion protein results in infectious amyloid disease without clinical scrapie." Science **308**(5727): 1435-9.

Chiesa, R., P. Piccardo, et al. (2005). "Bax deletion prevents neuronal loss but not neurological symptoms in a transgenic model of inherited prion disease." Proc Natl Acad Sci U S A **102**(1): 238-43.

Chiesa, R., P. Piccardo, et al. (2003). "Molecular distinction between pathogenic and infectious properties of the prion protein." J Virol **77**(13): 7611-22.

Daude, N., S. Lehmann, et al. (1997). "Identification of intermediate steps in the conversion of a mutant prion protein to a scrapie-like form in cultured cells." J Biol Chem **272**(17): 11604-12.

Dimakopoulos, A. C. (2005). "Protein aggregation in Alzheimer's disease and other neoropathological disorders." Curr Alzheimer Res **2**(1): 19-28.

Gunawardena, S. and L. S. Goldstein (2001). "Disruption of axonal transport and neuronal viability by amyloid precursor protein mutations in Drosophila." Neuron **32**(3): 389-401.

Gunawardena, S. and L. S. Goldstein (2005). "Polyglutamine diseases and transport problems: deadly traffic jams on neuronal highways." Arch Neurol **62**(1): 46-51.

Gunawardena, S., L. S. Her, et al. (2003). "Disruption of axonal transport by loss of huntingtin or expression of pathogenic polyQ proteins in Drosophila." Neuron **40**(1): 25-40.

Haass, C. and D. J. Selkoe (2007). "Soluble protein oligomers in neurodegeneration: lessons from the Alzheimer's amyloid beta-peptide." Nat Rev Mol Cell Biol **8**(2): 101-12.

Ivanova, L., S. Barmada, et al. (2001). "Mutant prion proteins are partially retained in the endoplasmic reticulum." J Biol Chem **276**(45): 42409-21.

Lehmann, S., N. Daude, et al. (1997). "A wild-type prion protein does not acquire properties of the scrapie isoform when coexpressed with a mutant prion protein in cultured cells." Brain Res Mol Brain Res **52**(1): 139-45.

Marijanovic, Z., A. Caputo, et al. (2009). "Identification of an intracellular site of prion conversion." PLoS Pathog **5**(5): e1000426.

Mead, S. (2006). "Prion disease genetics." Eur J Hum Genet **14**(3): 273-81.

Mead, S., M. Poulter, et al. (2006). "Inherited prion disease with six octapeptide repeat insertional mutation--molecular analysis of phenotypic heterogeneity." Brain **129**(Pt 9): 2297-317.

Medrano, A. Z., S. J. Barmada, et al. (2008). "GFP-tagged mutant prion protein forms intra-axonal aggregates in transgenic mice." Neurobiol Dis **31**(1): 20-32.

Moore, R. A., C. Herzog, et al. (2006). "Octapeptide repeat insertions increase the rate of protease-resistant prion protein formation." Protein Sci **15**(3): 609-19.

Novitskaya, V., O. V. Bocharova, et al. (2006). "Amyloid fibrils of mammalian prion protein are highly toxic to cultured cells and primary neurons." J Biol Chem **281**(19): 13828-36.

Piccardo, P., J. C. Manson, et al. (2007). "Accumulation of prion protein in the brain that is not associated with transmissible disease." Proc Natl Acad Sci U S A **104**(11): 4712-7.

Sim, V. L. and B. Caughey (2008). "Ultrastructures and strain comparison of under-glycosylated scrapie prion fibrils." Neurobiol Aging.

Simoneau, S., H. Rezaei, et al. (2007). "In vitro and in vivo neurotoxicity of prion protein oligomers." PLoS Pathog **3**(8): e125.

Solforosi, L., J. R. Criado, et al. (2004). "Cross-linking cellular prion protein triggers neuronal apoptosis in vivo." Science **303**(5663): 1514-6.

Taylor, D. R. and N. M. Hooper (2006). "The prion protein and lipid rafts." Mol Membr Biol **23**(1): 89-99.

Telling, G. C., T. Haga, et al. (1996). "Interactions between wild-type and mutant prion proteins modulate neurodegeneration in transgenic mice." Genes Dev **10**(14): 1736-50.

Walmsley, A. R., F. Zeng, et al. (2003). "The N-terminal region of the prion protein ectodomain contains a lipid raft targeting determinant." J Biol Chem **278**(39): 37241-8.

Yin, S., S. Yu, et al. (2006). "Prion proteins with insertion mutations have altered N-terminal conformation and increased ligand binding activity and are more susceptible to oxidative attack." J Biol Chem **281**(16): 10698-705.

Yu, S., S. Yin, et al. (2007). "Aggregation of prion protein with insertion mutations is proportional to the number of inserts." Biochem J **403**(2): 343-51.

APPENDIX 1

WT PrP-EGFP does not bind PG14 aggregates

A1.1 Summary

Aggregated forms of infectious scrapie prions (PrP^{Sc}) and familial mutant PG14 PrP, which contains a 217 base pair insertion, are difficult to detect by standard immunohistochemical techniques due to epitope burial, a phenomenon whereby antigens are concealed by protein misfolding and accumulation. EGFP-tagged wild-type prion protein (WT-EGFP) was able to bind untagged infectious scrapie prion (PrP^{Sc}) aggregates *in vivo*, although WT-EGFP molecules themselves remained unconverted. PrP^{Sc} aggregate detection by this method revealed intracellular PrP^{Sc} accumulation in the Golgi apparatus of cells, via fluorescence microscopy of brain sections of RML-inoculated Tg(WT-EGFP) mice (Barmada and Harris 2005). This pool of molecules had not previously been identified by traditional scrapie detection protocols such as electron microscopy or antigen retrieval techniques, suggesting that detection of aggregates by fluorescently-tagged WT-EGFP allowed for greater sensitivity.

To determine whether WT-EGFP could detect aggregates of familial mutant PG14 PrP, we crossed Tg(WT-EGFP) with Tg(PG14) animals and analyzed bi-transgenic offspring both clinically and neuropathologically. We find that WT-EGFP does not interfere with PG14 disease onset or progression. In contrast with findings for PrP^{Sc} aggregates, WT-EGFP is unable to bind to and tag aggregated PG14, as assayed by fluorescence microscopy of cerebellar granule neurons and of brain sections from bigenic mice expressing both WT-EGFP and PG14. The difference in WT-EGFP molecules' capability to bind PrP^{Sc} but not PG14 aggregates suggests that PrP^{Sc} infectivity may be facilitated by the ability to directly interact with WT PrP whereas PG14 non-infectivity may be explained by the lack of this interaction.

A1.2 Introduction

Prion diseases are a group of neurological disorders characterized by dementia, ataxia, and intracerebral prion protein (PrP) deposition. In humans, illness can be acquired sporadically, inherited by genetic mutation of the PrP gene, or obtained by exposure to infectious scrapie prions (PrP^{Sc}) (Prusiner 1998). Normal cellular PrP (PrP^C) is a GPI-anchored sialoglycoprotein of ambiguous function that may be involved with cell signaling and/or neuroprotectivity (Westergard et al. 2007).

PG14 is a 217 base pair insertional mutation of the prion protein (PrP) that results in a repeat expansion of endogenous octapeptide motifs that are known to bind copper (Brown et al. 1997). These repeats are rich in *p*roline and *g*lycine, and are extended from 5 to 14 in the PG14 mutation. This dominantly inherited mutation is associated with a familial form of Creutzfeldt-Jakob Disease (CJD), a progressive neurological disorder characterized clinically by dementia and ataxia, and pathologically by mutant PrP aggregation in the form of cerebellar plaques (Owen et al. 1992; Duchen et al. 1993; Krasemann et al. 1995). Transgenic mice that express PG14 develop a similar illness, displaying ataxia, kyphosis, and marked PrP deposition within the cerebellum and other regions of the brain (Chiesa et al. 1998; Chiesa et al. 2000; Chiesa et al. 2001). The molecular pathogenesis of disease remains poorly understood.

To gain a better understanding of the cellular, and consequently physiological, mechanisms of pathology underlying familial prion disorders, it is crucial to identify the subcellular and anatomical localization of the insoluble PG14 PrP protein, which accumulates over the course of the time (Chiesa et al. 1998). However, visual identification of the mutant protein within the brain proves to be challenging, due in part

144

to the burial of normally accessible epitopes within aggregated molecules or irregularly folded protein structures. Several techniques have been adopted to overcome this difficulty. Antigen retrieval procedures, such as treatment with guanidine thiocyanate or hydrolytic autoclaving, denature proteins to help expose hidden epitopes. Brain sections of both scrapie-inoculated and Tg(PG14) mice that undergo antigen retrieval treatments before immunohistochemistry reveal plaque formations within the brain. However, the abrasive nature of these techniques easily damages the integrity of the tissue, and may introduce a number of potential artifacts.

Further attempts to localize PG14 *in vivo* included the generation of transgenic mice expressing a PG14 construct carrying an enhanced green fluorescent protein (EGFP) tag inserted at the C-terminal end of the protein (Medrano et al. 2008). These mice developed clinical illness similar to untagged Tg(PG14) mice. When analyzing brain sections, PG14-EGFP displayed irregular and punctate patterns of localization, similar to the synaptic-like deposition detected in the cerebellum of untagged Tg(PG14) animals (Chiesa et al. 1998; Chiesa et al. 2005). Additionally, we found that PG14-EGFP aggregates were discovered at the highest densities in axon-rich regions of the brain, a previously unidentified feature of pathology indicating axonopathy as a possible mode of pathology. Studies in cerebellar granule neurons cultured from Tg(PG14-EGFP) mice offered more detailed localization reports at the subcellular level, displaying for the first time intracellular mutant PrP localization and accumulation within cell soma and neurites. However, PG14-EGFP in this work was expressed at 0.15 X that of endogenous PG14 and it remains unclear how protein expression level affects protein distribution (Medrano et al. 2008). To determine localization of PG14 in mice that express

physiological levels of the mutant protein, we sought yet another method to visually detect PG14 aggregates.

Previous work from our lab has demonstrated that fluorescently-tagged wild type prion protein (WT-EGFP) has the ability to recognize and bind infectious PrP^{Sc} aggregates *in vivo* without itself being converted (Barmada and Harris 2005). Tg(WT-EGFP) animals inoculated with scrapie display delayed onset of scrapie disease compared with wild type animals, indicating a significant interaction between the WT-EGFP molecule and scrapie particles. In brain sections of diseased animals, we observed intracellular accumulation of PrP^{Sc} in the Golgi apparatus of cells, highlighting a pool of molecules that had not previously been identified by traditional scrapie detection protocols such as electron microscopy or immunohistochemistry with antigen retrieval techniques. This finding suggests that detection of aggregates by fluorescently-tagged WT-EGFP allowed for greater sensitivity when compared with standard immunohistochemistry.

To expand our repertoire of tools for mutant PrP aggregate detection *in vivo*, we crossed Tg(WT-EGFP) mice with Tg(PG14) animals and analyzed bigenic offspring that expressed both proteins. In contrast to PrP^{Sc}-induced illness, the presence of WT-EGFP did not affect PG14 disease age of onset. In brain sections of bigenic mice, WT-EGFP failed to co-aggregate with PG14 cerebellar deposits, instead maintaining the smooth and uniform distribution of WT PrP throughout the neuropil and molecular layers of the cerebellum. WT-EGFP was also unable to recognize and bind PG14 accumulations in primary neuronal cultures derived from bigenic mice. Whereas PG14 accumulated intracellularly in the cell soma and along neurites, WT-EGFP again adopted the

146

localization pattern of WT PrP, normally located on the surface of the cell soma and neuritic extensions. The ability of WT-EGFP to bind and tag PrP^{Sc}, but not PG14, aggregates suggests that there may be a structural or conformational difference between the two molecules, which influences their ability to interact with other PrP molecules. This distinction may help explain why PrP^{Sc}, but not PG14, is infectious.

A1.3 Materials & Methods

Transgenic Mice. Construction of Tg(WT-EGFP), Tg(PG14-EGFP), and Tg(PG14) mice have been described previously (Chiesa et al. 1998; Barmada et al. 2004; Medrano et al. 2008). Tg(WT-EGFP$^{+/o}$) mice, A line, were maintained on a mixed CBA/C57BL6 PrP$^{+/+}$ background. These were crossed with Tg(PG14$^{+/o}$) animals, A2 line, kept on a recombinant inbred CBA/C57BL6 PrP$^{o/o}$ background. F1 progeny were genotyped and classified into the following groups: (1) PG14$^{+/o}$ WT-EGFP$^{+/o}$, (2) PG14$^{+/o}$ WT-EGFP$^{o/o}$, (3) PG14$^{o/o}$ WT-EGFP$^{+/o}$, or (4) PG14$^{o/o}$ WT-EGFP$^{o/o}$. All F1 progeny had a PrP$^{+/o}$ background. At least 13 animals from each genotype group were collected. Tg(PG14-EGFP$^{+/o}$) mice on a PrP$^{+/+}$ background were used as positive controls for fluorescent aggregates in brain sections and cerebellar granule neurons.

Clinical Evaluation. Mice were checked biweekly for symptoms of neurological dysfunction. Kyphosis, foot clasp, and hyperexcitability were determined by visual observation, while ataxia was tested by placing mice in the center of a horizontally oriented grill (45 x 45 cm) consisting of 3 mm diameter steel rods spaced 7 mm apart. Mice unable to maneuver around the grid were scored as ataxic. Animals that exhibited at least two symptoms were scored as ill.

Brain Sections. Animals were fixed by intracardiac perfusion as described previously (Medrano et al. 2008). Brains were then removed and then post-fixed in the same solution for 2 hrs before transfer to 0.1M sodium phosphate buffer (pH 7.2) containing 0.02% sodium azide for storage at 4°C. A Vibratome (The Vibratome Company, St. Louis, MO) was used to cut the tissue into 60 μm thick sagittal sections. Sections were mounted on glass slides using Gel/Mount (Biomeda, Foster City, CA). Intrinsic EGFP fluorescence was imaged using a Zeiss LSM 510 inverted confocal microscope with an Axiovert 200 laser scanning system.

Primary Neurons. Cerebellar granule neurons (CGNs) were isolated from 4 day old mouse pups according to methods detailed previously (Medrano et al. 2008). CGNs were imaged live using a Zeiss LSM 510 inverted confocal microscope with an Axiovert 200 laser scanning system.

A1.4 Results

Construction of Tg(WT-EGFP$^{+/o}$ PG14$^{+/o}$) mice. To study whether WT-EGFP molecules are able to tag PG14 aggregates *in vivo*, we crossed existing lines of Tg(WT-EGFP) and Tg(PG14) mice to obtain bigenic mice expressing both proteins. Tg(WT-EGFP$^{+/o}$) mice kept on a PrP$^{+/+}$ background (Barmada et al. 2004) were crossed with Tg(PG14$^{+/o}$) mice maintained on a PrP null background (Chiesa et al. 1998). F1 progeny were grouped according to genotype: (1) WT-EGFP$^{+/o}$ PG14$^{+/o}$, (2) WT-EGFP$^{+/o}$, (3) PG14$^{+/o}$, and (4) WT-EGFP$^{o/o}$ PG14$^{o/o}$. F1 progeny from the expressing one or both transgenes were used for experimentation in these studies (Groups 1-3). Mice negative for both transgenes were discarded (Group 4). Previous investigations demonstrate that

both Tg(WT-EGFP) and Tg(PG14) mice express transgenic protein at 1X endogenous PrP level, and are presumably expressed at equal levels in bigenic mice.

WT-EGFP does not interfere with PG14 disease onset. All transgenic and bigenic mice were checked for the following neurological symptoms biweekly: kyphosis, foot clasp, hyperexcitability, and ataxia. Mice testing positive for at least two of these symptoms were scored at ill. Tg(PG14) mice that were heterozygous for the transgene developed spontaneous neurological illness at 317±21 days (Table 1). This statistic is much later than the age of onset previously recorded (235±10 days; (Chiesa et al. 2000)), and is likely due to two factors: 1) genetic changes over the course of a decade of inbreeding, and 2) slight variability in methods for determining disease. These differences do not affect results from these experiments since mice used in these studies are littermates and are assessed for illness in a consistent manner.

Mice expressing both PG14 and WT-EGFP developed disease at 321±28 days, similar to mice expressing only PG14 (Table 1). This result reveals that WT-EGFP does not hinder disease onset of this familial PrP mutant. As expected, 100% of all Tg(WT-EGFP$^{+/o}$) mice remained healthy for the duration of the experiments, confirming previous results (Barmada et al. 2004). These animals ranged in age from 448 to 623 days.

WT-EGFP does not tag aggregated familial PrP mutant PG14. PG14 molecules form insoluble aggregates within 1 hour of synthesis in mammalian cells (Daude et al. 1997) and Tg(PG14) transgenic pups as young as 4 days old exhibit protease-resistant, detergent insoluble PG14 aggregates (Chiesa et al. 1998). These

Table 1. Disease onset in Tg(WT-EGFP$^{+/o}$ PG14$^{+/o}$) animals

Genotype	Age of Onset
WT-EGFP$^{+/o}$	>448 (0/15)
PG14$^{+/o}$	317±21 (19/19)
PG14$^{+/o}$ WT-EGFP$^{+/o}$	321±28 (13/13)

Age of onset is recorded in days. Numbers in parentheses indicate the number of ill mice over the total number of animals observed.

aggregates can be visualized in cerebellar granule neurons derived from transgenic mice, of the same age, expressing EGFP-tagged PG14 (Figure 1B and (Medrano et al. 2008)) Aggregates are displayed in primary neuronal culture as small, bright puncta that accumulate within the cell soma and in neurites. This aberrant distribution is easily distinguished from WT-EGFP, which is uniformly distributed along the surface of neurons (Figure 1A and (Medrano et al. 2008)) To investigate whether WT-EGFP molecules are able to recognize and bind to PG14 aggregates, we analyzed cerebellar granule cells derived from pups co-expressing both WT-EGFP and PG14 (Figure 1C). These cultures show a uniform pattern of expression identical to cultures expressing only WT-EGFP, indicating that the fluorescent WT protein does not bind with PG14 aggregates in primary neuronal culture.

Insoluble PG14 aggregates accumulate over the course of time *in vivo* in transgenic mice and are distributed throughout the cerebellum in a synaptic-like pattern (Chiesa et al. 1998; Chiesa et al. 2000). This aberrant localization is visible in brain sections of mice as young as 71 days of age by standard immunohistochemistry after treatment with antigen retrieval techniques (Figure 2A). In brain sections from mice that express inherently fluorescent PG14-EGFP, punctate spots that correlate with accumulated PG14-EGFP are detectable as young as 100 days using confocal fluorescence microscopy (unpublished data). Earlier ages had not been checked, although punctate distribution of PG14-EGFP is likely at all ages, given that PG14-EGFP aggregates are detected in cerebellar granule neurons of pups as young as four days old (Medrano et al. 2008).

Tg(WT-EGFP$^{+/o}$)   Tg(PG14-EGFP$^{+/o}$)   Tg(PG14$^{+/o}$ WT-EGFP$^{+/o}$)
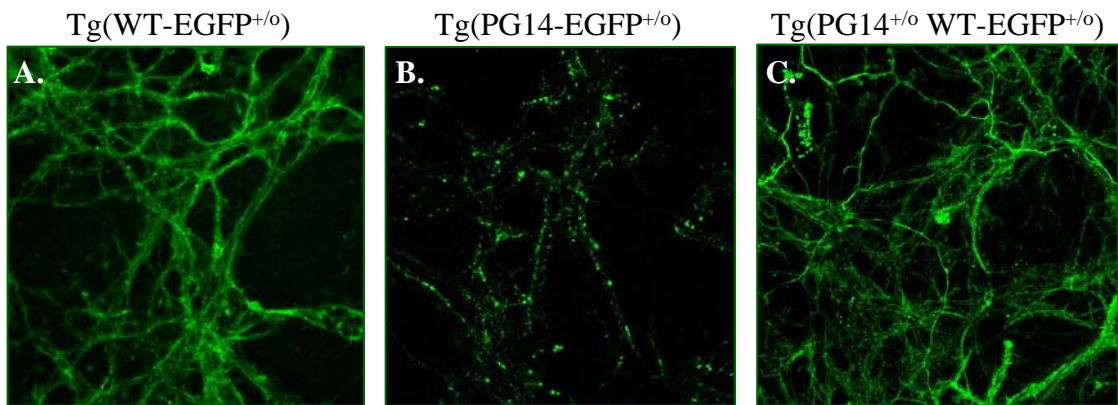
Figure 1. WT-EGFP does not tag PG14 aggregates in cerebellar granule neurons. Live cerebellar granule neurons from mice expressing WT-EGFP (A), PG14-EGFP (B), or both untagged PG14 and WT-EGFP (C) were observed via fluorescence microscopy. WT-EGFP uniformly coats the surface of cell soma and neurites (A), wherease PG14-EGFP displays punctate distribution along neurites (B). Cells expressing both PG14 and WT-EGFP display the same localization as (C), demonstrating that the two proteins do not co-aggregate. This work was published in Biasini *et al.*, 2008.
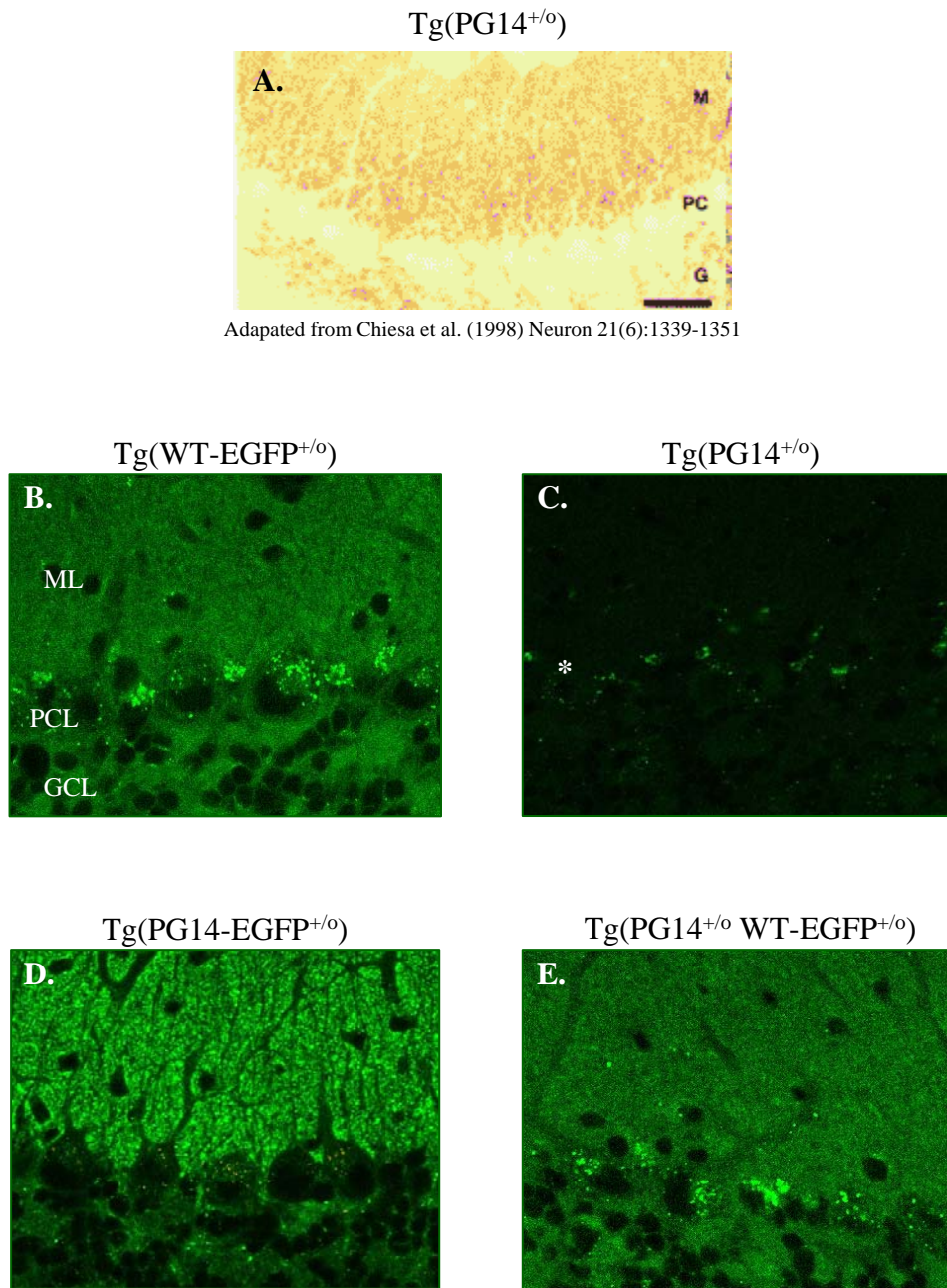
Figure 2. WT-EGFP does not tag PG14 aggregates in cerebellar brain sections. A paraffin brain section derived from a 71 day old Tg(PG14) cerebellum was treated with 3M guanidine thiocyanate and hydrolytic autoclaving before staining with monoclonal PrP antibody 3F4, showing synaptic-like PG14 distribution in the molecular and cerebellar granule layers (A, from Chiesa 1998). Vibratome sections (b-e) from mice expressing WT-EGFP (B), untagged PG14 (C), PG14-EGFP (D), or both PG14 and WT-EGFP (E) were analyzed by fluorescence microscopy. WT-EGFP distribution in the bigenic mouse (E) is uniform, similar to that of WT-EGFP expressed alone (B), but not aggregated like PG14-EGFP (C), revealing that WT-EGFP does not colocalize with PG14 aggregates. ML = molecular layer; PCL = Purkinje cell layer; GCL = granule cell layer. Asterisk indicates autofluorescent dots. This work was published in Biasini *et al.*, 2008.

Knowing that PG14 aggregates are readily detectable by 100 days by both these methods, we investigated whether we could detect the aggregates by WT-EGFP binding to them in brain sections of mice expressing both PG14 and WT-EGFP (Figure 2). Vibratome sections from a Tg(WT-EGFP mouse) at 175 days reveals a smooth, uniform pattern of expression throughout the molecular layer (ML) and granule cell layer (GCL) of the cerebellum. Autofluorescent dots in the Purkinje cell layer (PCL) are evident in all sections, including that of a transgenic mouse expressing untagged non-fluorescent PG14 (Figure 2C, asterisk). The distribution pattern of WT-EGFP remains the same in an age-matched Tg(PG14$^{+/o}$ WT-EGFP$^{+/o}$) mouse (Figure 2E), in contrast to Tg(PG14-EGFP) sections that show the synaptic-like distribution pattern in the molecular and cerebellar granule layers, similar to that of Tg(PG14) (Figure 2A,D). These results demonstrate that WT-EGFP is unable to recognize and bind PG14 aggregates *in vivo*.

A1.5 Discussion

Bigenic mice expressing WT-EGFP and PG14 were created in order to attempt PG14 aggregate visualization by WT-EGFP recognition and binding. Here we demonstrate that co-expression of WT-EGFP and PG14 does not hinder PG14 disease onset. Furthermore, WT-EGFP molecules do not bind PG14 aggregates either in primary neuronal cell culture or in brain sections of bigenic animals as assayed by fluorescence microscopy. These results demonstrate that PG14 aggregates are unable to interact with the WT-EGFP marker, in contrast with PrP^{Sc} aggregates, which are capable of binding with and sequestering WT-EGFP molecules (Barmada). Together, these data emphasize

154

the difference that PrP^{Sc}, but not PG14, has the ability to interact with another PrP molecule, which give clues as to why PrP^{Sc}, but not PG14, is infectious *in vivo*.

PG14 does not interact with other PrP molecules. In our experiments, WT-EGFP does not bind PG14 mutant prion protein aggregates *in vivo*, suggesting that both pools of PrP do not directly interact. Previous work has demonstrated that untagged PG14 and WT PrP maintain their separate biochemical identities when co-expressed in cells (Lehmann et al. 1997); that PG14 disease age of onset and progression are unaffected by endogenous PrP level (Chiesa et al. 2000); that PG14 aggregates are unable to seed the misfolding of WT PrP^C in an *in vitro* protein misfolding cyclic amplification (PMCA) reaction (Biasini et al. 2008); and that PG14 brain homogenates are unable to transmit disease when inoculated into mice expressing WT PrP (Chiesa et al. 2003). Collectively, these data indicate that there is minimal, if any, significant physical interaction or signaling between the PG14 mutant and wild type prion protein, which may help explain why PG14 is not infectious.

Infectivity is a distinguishing feature between PrP^{Sc} and PG14. In scrapie-inoculated Tg(WT-EGFP) animals on a PrP$^{+/+}$ background, WT-EGFP acts as a dominant negative inhibitor of PrP^C to PrP^{Sc} conversion. WT-EGFP recognizes and binds to scrapie aggregates, thus slowing PrP^{Sc} accumulation and delaying disease in WT-EGFP$^{+/o}$ PrP$^{+/+}$ animals (Barmada and Harris 2005). This delay in disease onset was not observed when WT-EGFP was co-expressed with a similar amount of PG14 protein (Table 1),

155

indicating that PrP^{Sc} and PG14 aggregates differ in their ability to interact with other PrP molecules.

It is possible that distinctions in aggregate structure may explain the disparity between PG14's and PrP^{Sc}'s ability to interact with WT and WT-EGFP PrP. However, previous studies using brain homogenates demonstrate that both spontaneously aggregated PG14 and infectious PrP^{Sc} from RML-inoculated wild type mice share many similar biochemical properties, including detergent insolubility, protease K resistance, and PIPLC-resistance (Lehmann and Harris 1996; Lehmann and Harris 1996; Lehmann et al. 1997). Like PrP^{Sc}, PG14 can also be precipitated by sodium phosphotungstic acid, recognized by PrP^{Sc} –specific antibodies, and replicate protease-resistant PrP *in vitro* from a PrP^{C} template using the protein misfolding cyclic amplification (PMCA) technique (Biasini et al. 2008; Biasini et al. 2008). All these properties are distinct from normal healthy cellular PrP^{C} and argue that indeed, PG14 shares enough structural homology with PrP^{Sc} to mimic its biochemical profile. However, in order to completely rule out significant structural variation between the two, accurate molecular reconfigurations obtained from crystallographic studies, such as x-ray crystallography, will be necessary.

Though non-infectivity is a trait shared by several familial PrP mutants, some mutations, such as E200K and V210I, have been shown to transmit disease when brain homogenates from diseased patients are inoculated into transgenic mice susceptible to human prions (Telling et al. 1994; Mastrianni et al. 2001). Further investigations will be necessary in order to define the variable that modulates infectivity in these familial mutants and PrP^{Sc} but not in PG14.

A1.6 References

Barmada, S., P. Piccardo, et al. (2004). "GFP-tagged prion protein is correctly localized and functionally active in the brains of transgenic mice." <u>Neurobiol Dis</u> **16**(3): 527-37.

Barmada, S. J. and D. A. Harris (2005). "Visualization of prion infection in transgenic mice expressing green fluorescent protein-tagged prion protein." <u>J Neurosci</u> **25**(24): 5824-32.

Biasini, E., A. Z. Medrano, et al. (2008). "Multiple biochemical similarities between infectious and non-infectious aggregates of a prion protein carrying an octapeptide insertion." <u>J Neurochem</u> **104**(5): 1293-308.

Biasini, E., M. E. Seegulam, et al. (2008). "Non-infectious aggregates of the prion protein react with several PrP(Sc)-directed antibodies." <u>J Neurochem</u>.

Brown, D. R., K. Qin, et al. (1997). "The cellular prion protein binds copper in vivo." <u>Nature</u> **390**(6661): 684-7.

Chiesa, R., B. Drisaldi, et al. (2000). "Accumulation of protease-resistant prion protein (PrP) and apoptosis of cerebellar granule cells in transgenic mice expressing a PrP insertional mutation." <u>Proc Natl Acad Sci U S A</u> **97**(10): 5574-9.

Chiesa, R., A. Pestronk, et al. (2001). "Primary myopathy and accumulation of PrPSc-like molecules in peripheral tissues of transgenic mice expressing a prion protein insertional mutation." <u>Neurobiol Dis</u> **8**(2): 279-88.

Chiesa, R., P. Piccardo, et al. (2005). "Bax deletion prevents neuronal loss but not neurological symptoms in a transgenic model of inherited prion disease." <u>Proc Natl Acad Sci U S A</u> **102**(1): 238-43.

Chiesa, R., P. Piccardo, et al. (1998). "Neurological illness in transgenic mice expressing a prion protein with an insertional mutation." <u>Neuron</u> **21**(6): 1339-51.

Chiesa, R., P. Piccardo, et al. (2003). "Molecular distinction between pathogenic and infectious properties of the prion protein." <u>J Virol</u> **77**(13): 7611-22.

Daude, N., S. Lehmann, et al. (1997). "Identification of intermediate steps in the conversion of a mutant prion protein to a scrapie-like form in cultured cells." <u>J Biol Chem</u> **272**(17): 11604-12.

Duchen, L. W., M. Poulter, et al. (1993). "Dementia associated with a 216 base pair insertion in the prion protein gene. Clinical and neuropathological features." <u>Brain</u> **116 (Pt 3)**: 555-67.

Krasemann, S., I. Zerr, et al. (1995). "Prion disease associated with a novel nine octapeptide repeat insertion in the PRNP gene." Brain Res Mol Brain Res **34**(1): 173-6.

Lehmann, S., N. Daude, et al. (1997). "A wild-type prion protein does not acquire properties of the scrapie isoform when coexpressed with a mutant prion protein in cultured cells." Brain Res Mol Brain Res **52**(1): 139-45.

Lehmann, S. and D. A. Harris (1996). "Mutant and infectious prion proteins display common biochemical properties in cultured cells." J Biol Chem **271**(3): 1633-7.

Lehmann, S. and D. A. Harris (1996). "Two mutant prion proteins expressed in cultured cells acquire biochemical properties reminiscent of the scrapie isoform." Proc Natl Acad Sci U S A **93**(11): 5610-4.

Mastrianni, J. A., S. Capellari, et al. (2001). "Inherited prion disease caused by the V210I mutation: transmission to transgenic mice." Neurology **57**(12): 2198-205.

Medrano, A. Z., S. J. Barmada, et al. (2008). "GFP-tagged mutant prion protein forms intra-axonal aggregates in transgenic mice." Neurobiol Dis **31**(1): 20-32.

Owen, F., M. Poulter, et al. (1992). "A dementing illness associated with a novel insertion in the prion protein gene." Brain Res Mol Brain Res **13**(1-2): 155-7.

Prusiner, S. B. (1998). "Prions." Proc Natl Acad Sci U S A **95**(23): 13363-83.

Telling, G. C., M. Scott, et al. (1994). "Transmission of Creutzfeldt-Jakob disease from humans to transgenic mice expressing chimeric human-mouse prion protein." Proc Natl Acad Sci U S A **91**(21): 9936-40.

Westergard, L., H. M. Christensen, et al. (2007). "The cellular prion protein (PrP(C)): its physiological function and role in disease." Biochim Biophys Acta **1772**(6): 629-44.

APPENDIX 2

WT PrP-EGFP is resistant to conversion to PrP^{Sc}

A2.1 Summary

Identifying the trafficking pattern of infectious scrapie prions (PrP^{Sc}) is essential for understanding the mechanism of transmission in prion disease. However, PrP^{Sc} detection usually requires specimen fixation, followed by treatment with hydrolytic autoclaving or other harsh antigen retrieval (AR) techniques that have the potential to damage tissue and redistribute proteins. In order to facilitate visual detection of PrP^{Sc} without AR, we attempted to convert an EGFP-tagged murine wild-type PrP (WFP) into the infectious conformation through inoculation of prion molecules into Tg(WFP) mice. In this chapter, I describe three separate experiments attempting to detect or generate WFP^{Sc}. Our efforts were unable to produce infectious, aggregated, PK-resistant EGFP-tagged PrP material. These collective results demonstrate that WFP is highly resistant to conversion.

A2.2 Introduction

Transmission of prion disease occurs most efficiently through intracranial injection of infected material into the host. However, disease also spreads naturally through ingestion, or experimentally via intraperitoneal infection, scarified skin, or nasal contraction (for review, see (Weissmann *et al.* 2002)). Regardless of type of exposure, the end result is neurodegeneration caused by PrP^{Sc}-associated toxicity in the central nervous system (CNS), indicating that PrP^{Sc} molecules are able to replicate and traverse peripheral biological systems before neuroinvasion. When introduced non-cerebrally in animal hosts, PrP^{Sc} replicates and accumulates on follicular dendritic cells (FDCs) in lymphoid tissues, and proceeds along the peripheral nervous system (PNS) to reach the brain, presumably by intracellular transfer (Mabbott and MacPherson 2006).

However, the mode of intracellular transfer and propagation of PrP^{Sc} is ambiguous. Recently, PrP^{Sc} transmission has been detected in the transfer from bone marrow-derived dendritic cells to primary neurons via tunneling nanotubes (TNTs) (Gousset *et al.* 2009). TNTs are a recently discovered cell communication device consisting of long protruding tunnel-like membrane extensions connecting two separate cells (reviewed in (Gurke *et al.* 2008)). However, there is other evidence showing that PrP^{Sc} can be transferred without direct cell contact. Scrapie-infected epithelial cells have been shown to secrete infectious PrP^{Sc} associated with exosomes (Fevrier *et al.* 2004), and media incubated with an infected neuronal cell line is capable of inducing PrP^{Sc} propagation when placed over healthy cells (Schatzl *et al.* 1997). Although several studies strongly suggest that the PrP^{C} conversion process takes place once PrP^{Sc} and PrP^{C} are colocalized within endocytic recycling compartments (Marijanovic *et al.* 2009), how

and where PrP^{Sc} travels when initially associated with a newly exposed cell is unclear. Imaging of PrP^{Sc} in living cells and in animals would provide a beneficial tool to study the behavior of intercellular PrP^{Sc} trafficking.

Our lab has generated a transgenic mouse line expressing fluorescently-tagged wild-type prion protein (WFP). Tg(WFP) animals synthesize and produce a fusion protein consisting of a murine PrP with an enhanced green fluorescent protein (EGFP) tag inserted near the C-terminal end, upstream of the GPI-anchor attachment signal. The resulting transgene is properly synthesized as a glycosylated, GPI-anchored molecule, and like endogenous PrP, localizes to the cell surface of neurons. Neuroanatomically, WFP is expressed in a spatio-temporal pattern comparable with endogenous PrP, displaying highest concentrations in axon-dense regions. WFP also proves to be functional *in vivo*, acting as a neuroprotective agent against a truncated form of PrP that induces neurological illness (Barmada *et al.* 2004).

In order to visualize PrP^{Sc} trafficking in real time, we attempted to generate fluorescently-tagged PrP^{Sc} *in vivo* by inoculating Tg(WFP) PrP$^{+/+}$ animals with scrapie prions through intracerebral injection. Although endogenous PrP rearranged into the PrP^{Sc} conformation, WFP itself was unable to adopt protease resistance and detergent insolubility after RML prion inoculation. Interestingly, WFP was able to recognize and bind to PrP^{Sc} derived from PrP^{C}, while maintaining its own structural integrity. RML-inoculated Tg(WFP) PrP$^{+/+}$ also developed prion disease, but much later than RML-inoculated PrP$^{+/+}$ animals, demonstrating that WFP binding to PrP^{Sc} had a negative effect on the conversion of endogenous PrP^{C}. Additionally, RML-inoculated Tg(WFP) animals on the PrP-null background failed to demonstrate any symptoms of prion disease,

162

arguing that WFP was resistant to PrP^{Sc} conversion and toxicity (Barmada and Harris 2005).

In this work, we describe our continued efforts to generate fluorescently-tagged PrP^{Sc} through conversion of WFP molecules to infectious, protease-resistant isoforms (WFP^{Sc}). We extend our previous study by attempting to detect WFP^{Sc} in RML-inoculated Tg(WFP) brain homogenate using a more sensitive bioassay. We had previously found no trace of PK-resistant WFP^{Sc} material in RML-inoculated Tg(WFP) PrP$^{o/o}$ brain homogenates (Barmada and Harris 2005), perhaps because the amount of WFP^{Sc} was too small to detect biochemically. We describe here a more sensitive assay that tests for any infectivity in RML-inoculated Tg(WFP) brain homogenates by inoculation intoTga20 mice, which express 10X the amount of endogenous PrP and provide a sensitized background for detection of prion transmissibility (Fischer *et al.* 1996).

We also endeavor to generate WFP^{Sc} by 1) inoculating Tg(WFP) mice with 22L, a different prion strain able to convert PrP^{C} in cell culture and neural stem cells (Nishida *et al.* 2000; Milhavet *et al.* 2006); and 2) sequentially passaging RML-inoculated Tg(WFP) brain homogenate into a second round of Tg(WFP) recipients, in an attempt to overcome a possible species barrier. In each experiment, we recorded clinical data to observe any WFP^{Sc} toxicity, and we assayed brain homogenates from experimental animals to biochemically detect GFP-tagged PrP^{Sc}. None of our efforts yielded successful conversion of WFP to infectious, aggregated, or protease-resistant WFP^{Sc}, indicating that WFP is highly resistant to prion conversion.

163

A2.3 Materials & Methods

Transgenic Mice. Construction of Tg(WFP), Tg(PG14-EGFP), Tga20, and PrP knockout mice have been described previously (Bueler et al. 1992; Fischer et al. 1996; Barmada et al. 2004; Medrano et al. 2008).

Injections & Clinical Evaluation. RML inoculum was prepared as previously described (Barmada and Harris 2005). 22L inoculum was derived from the brain of a terminally ill CD-1 mouse infected with 22L scrapie (a gift from the lab of Su Priola). Brains from three healthy Tg(WFP$^{+/+}$)/PrP$^{o/o}$ (age > 600 days) that had been infected with E1-passaged RML scrapie were isolated and pooled to produce E1-injected Tg(WFP$^{+/+}$)/PrP$^{o/o}$ inoculum. Brains from three healthy PrP knockout mice that had been injected with E1-passaged RML scrapie were pooled to produce RML-injected PrP$^{o/o}$ inoculum. Brains from two severely ill Tg(WFP$^{+/o}$)/PrP$^{+/+}$ mice injected with E1-passaged RML scrapie were pooled to produce RML-injected Tg(WFP$^{+/o}$)/PrP$^{+/+}$ inoculum.

For all inocula samples, ten percent (w/v) brain homogenates were prepared in cold sterile PBS using a Teflon-glass tissue homogenizer with pestle revolving at 3500 rpm, 10 strokes. (Wheaton Science Products, Millville, NJ). Homogenates were centrifuged at 1000 x g for 5 min to obtain a postnuclear supernatant. For inocula derived from multiple brains, post-nuclear supernatants were pooled in equal volumes before dilution with sterile PBS to a final concentration of 1% brain homogenate. 30µL of these solutions was injected intracerebrally into 4- to 6-week old mice using a 25 gauge needle.

Mice were checked biweekly for symptoms of neurological dysfunction. Kyphosis, foot clasp, and hyperexcitability were determined by visual observation, while ataxia was tested by placing mice in the center of a horizontally oriented grill (45 x 45 cm) consisting of 3 mm diameter steel rods spaced 7 mm apart. Mice unable to maneuver around the grid were scored as ataxic. Animals that exhibited at least two symptoms were scored as ill. Animals showing extreme pruritis were sacrificed when scratching became chronically severe.

Biochemistry. To assay protease resistance, frozen brain hemispheres were homogenized in detergent buffer (DB: 10 mM Tris-HCl, pH 7.4, 0.5% sodium deoxycholate, 0.5% NP-40, 150 mM NaCl), then assayed for protein concentration as described above. Protein concentration was determined using a BCA assay (Pierce, Rockford, IL). Two hundred μg of total protein were diluted in DB to a final concentration of 1 μg/μl. The solution was mixed for 10 min at 4°C, then centrifuged at 1,500 x g for 5 min at 4°C. 20 μg/ml of proteinase K was added to the supernatant and the mixture was incubated at 37°C for 30 min. Phenylmethylsulfonyl fluoride (PMSF; 10 mg/ml) was added to terminate digestion. Proteins were isolated using methanol precipitation, then analyzed by SDS-PAGE and Western blotting.

To immunoprecipitate aggregated PrP with antibody 15B3, we followed the procedure recommended by Prionics (Zurich, Switzerland), utilizing the buffers supplied by them. First, a 100 μl aliquot of mouse anti-IgM Dynabeads (Dynal, Carlsbad, CA) was coated with 20 μg of mAb 15B3. Ten μl of 15B3-coated Dynabeads were then added to 200 μg of total protein from brain homogenates. Samples were incubated on a rotating wheel for 2 hr at 25°C, after which beads were washed three times with 1 ml of

15B3 Wash Buffer (Prionics, Zurich, Switzerland). Washed beads were suspended in 40

µl of 2X 15B3 Loading Buffer (Prionics) and heated for 5 min at 96°C.

Immunoprecipitated proteins were resolved by SDS-PAGE followed by Western blotting

with 6D11 antibody (Pankiewicz *et al.* 2006) or α-GFP antibody (gift from M. Linder).

A2.4 Results

RML-injected Tg(WFP^{+/+}) PrP[o/o] brain homogenate does not contain

infectious, aggregated, PK-resistant WFP[Sc]. Transgenic animals expressing

fluorescently-labeled murine PrP (WFP) are denoted as Tg(WFP) mice. Tg(WFP) PrP[o/o]

mice inoculated with murine prion strain RML exhibit no symptoms of prion disease, and

do not produce detectable amounts of PK-resistant WFP[Sc] (Barmada and Harris 2005). In

order to test whether any infectious WFP[Sc] was produced, we injected RML-inoculated

Tg(WFP) PrP[o/o] brain homogenate into Tga20 animals. Tga20 mice express wild-type

PrP at 10X endogenous levels Because of the heightened levels of PrP expression, Tga20

animals produce PrP[Sc] more rapidly and succumb to prion disease twice as fast as wild-

type mice when inoculated with RML (Fischer *et al.* 1996). Thus, these mice provide a

sensitized background on which we can test for the presence of small amounts of

infectious material. Our inoculum was derived from RML-injected Tg(WFP) mice

homozygous for the transgene array to maximize detection of any WFP[Sc].

As a positive control, we injected Tga20 animals with the RML prions. One

hundred percent of RML-inoculated Tga20 animals developed rapid onset of illness at 79

± 9 days (Table 1), similar to ages of onset recorded previously (Fischer *et al.* 1996).

Infected mice were sacrificed when they reached the terminal stage of disease, defined by

severe kyphosis and paralysis. Disease progression was rapid, and mice became terminal within one week of symptom onset.

It is possible that residual RML from the original Tg(WFP) infection may trigger disease during the second passage of inoculation in Tga20s. To control for this phenomenon, we used inoculum from RML-injected PrP-null mice as a negative control. PrP null mice are resistant to prion disease, and do not propagate PrP^{Sc} (Bueler *et al.* 1993). Thus, the presence of any residual RML molecules in the primary inoculation would be detected upon passage into Tga20 mice.

Tga20 mice inoculated with RML-injected PrP$^{o/o}$ inoculum did not develop prion disease. However, these mice did display kyphosis and severe pruritis as they aged (Table 1). These symptoms were discovered to be an artifact of our Tga20 mouse line, which had been maintained on a PrP knockout background. We discovered, as a result of these experiments, that approximately 60% of animals in our Tga20s and our particular line of knockout mice develop the same symptoms beginning at around 5 months of age (data not shown). The illness is likely due to the effect of prolonged inbreeding and not the lack of PrP, as multiple lines of independently-generated PrP$^{o/o}$ mice maintain good health throughout the duration of their lives (Bueler *et al.* 1992; Manson *et al.* 1994). Unlike the positive controls, mice in our negative control group did not develop rapidly progressive ataxia, or exhibit symptoms definitive for prion-related illness. While infectious PrP^{Sc} usually displays complete penetrance, only 9 of 20 mice were affected by pruritis, and the others remained healthy. These data argue strongly against the presence of prion disease in Tga20 mice inoculated with brain homogenate from PrP-null mice.

Our experimental group, Tga20 mice injected with RML-injected Tg(WFP) PrP$^{o/o}$ inoculum, developed pruritis similar to negative controls at approximately the same age. However, mice did not display progressive ataxia or prion-related disease(Table 1), indicating that the inoculum did not contain any infectious WFP^{Sc}. This conclusion is supported by the following biochemical studies.

Brain homogenates from age-matched Tga20 mice in the positive control, negative control, and experimental groups were analyzed for presence of WFP^{Sc} by reactivity with PrP^{Sc}–specific antibody 15B3. 15B3 is a motif-grafted antibody that recognizes insoluble PrP^{Sc} and aggregated PrP familial mutants, but not soluble PrP^C (Moroncini *et al.* 2004; Biasini *et al.* 2008). Brain homogenates were incubated with Dynabeads coated with antibody 15B3 for 2 hours to immunoprecipitate any aggregated PrP^{Sc}. Beads and homogenates were then analyzed by Western Blot to detect the presence of any aggregated PrP (Figure 1A). As expected, 15B3 was able to pull down aggregated PrP^{Sc} from RML-inoculated Tga20 animals, but not animals injected with RML-inoculated PrP$^{o/o}$. Mice injected with RML-injected Tg(WFP) PrP$^{o/o}$ homogenate did not yield any PrP^{Sc} detectable by 15B3, arguing that there was little or no WFP^{Sc} in the inoculum capable of converting endogenous PrP^C in Tga20 mice.

We also tested brain homogenates for presence of PK-resistant PrP^{Sc} material (Figure 1B). Homogenates were subjected to treatment with 20 μg/mL protease K, then analyzed by Western Blot with PrP antibody 6D11. Only RML-injected Tga20 brains demonstrated PK-resistant PrP^C, but not the negative control or experimental group. This is further evidence confirming that RML-injected Tg(WFP) inoculum did not instigate PrP^{Sc} conversion in Tga20 animals. Collectively, results from our clinical data and

168

Table 1. RML-inoculated Tg(WFP$^{+/o}$) brain homogenates do not contain infectious scrapie.

Inoculum	Recipient Genotype	Age of Onset (dpi)
RML	Tga20$^{+/+}$ PrP$^{o/o}$	78 $\pm$ 9 (18/18)
RML-injected PrP$^{o/o}$ brain homogenate	Tga20$^{+/+}$ PrP$^{o/o}$	242 $\pm$ 43 (9/20) [a]
RML-injected Tg(WFP$^{+/+}$)/PrP$^{o/o}$ brain homogenate	Tga20$^{+/+}$ PrP$^{o/o}$	290 $\pm$ 46 (15/20) [a]

[a] Mice exhibited kyphosis and extreme pruritis. These symptoms were not due to prion-related illness because negative controls also exhibited the same defects.
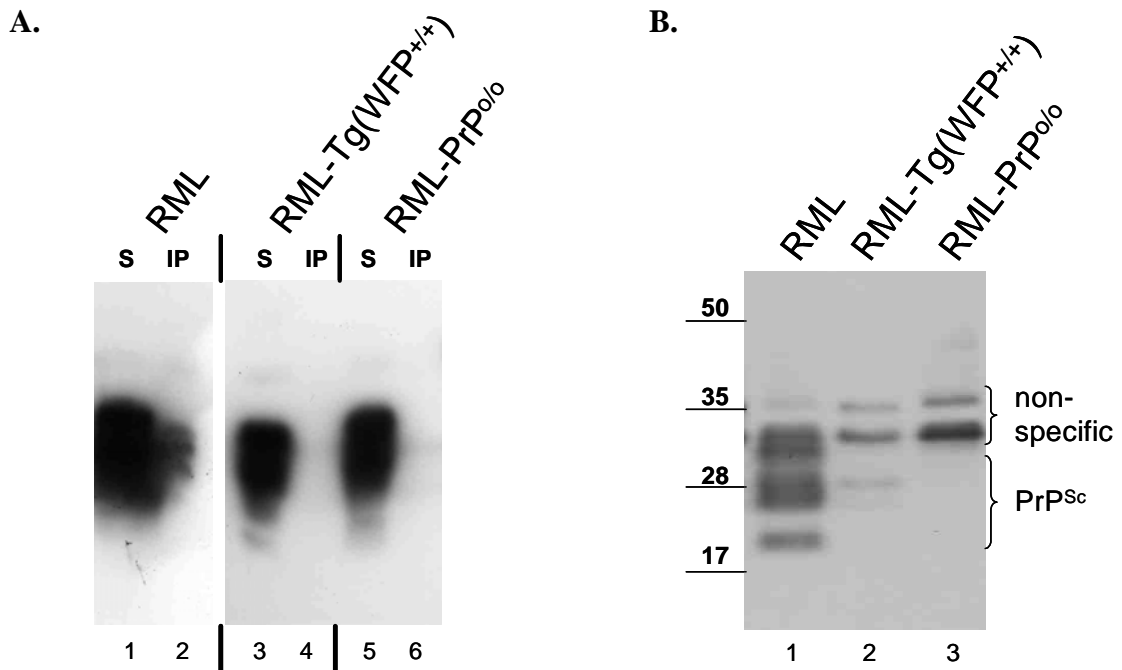
Figure 1. RML-inoculated Tg(WFP$^{+/o}$) brain homogenates do not contain PrP^{Sc}. Brain homogenate from Tga20 mice inoculated with RML (lanes1,2), RML passaged through Tg(WFP+/+) mice (lanes 3,4), and RML passaged through PrP knockouts (lanes 5,6) were subject to immunoprecipitation with aggregate PrP-specific antibody 15B3 (A). Immunoprecipitated material (IP) was analyzed along with a fraction of the input solution (S) by Western blot. Only homogenates from mice injected with RML demonstrated reactivity with 15B3. Brain homogenates from the same samples were treated with 20μg/mL protease K, and analyzed by Western Blot with α-PrP antibody 6D11 (B). Brackets indicate non-specific bands and PrPSc. Molecular weight is marked on the left in kilodaltons. Data in each of the panels are from the same gel, spliced for organizational purposes.

biochemical assays argue that RML-injected Tg(WFP) PrP$^{o/o}$ inoculum did not contain any aggregated WFP^{Sc} capable of transmitting prion disease.

Sequential passaging of RML-inoculated Tg(WFP) brain homogenate does not generate infectious, aggregated, PK-resistant WFP^{Sc}. PrP^{Sc} generated from wild-type PrP^{C} may not be able to efficiently convert WFP due to the "species barrier" effect, whereby conversion is delayed or inhibited by non-homologous amino acid sequences between PrP^{Sc} and template PrP^{C} molecules (Horiuchi *et al.* 2000). The species barrier can at times be overcome *in vivo* by sequential passaging. This phenomenon is attributed to PrP^{Sc} strain adaptation to the new host. To overcome a potentially obstructive species barrier between GFP-tagged PrP^{C} templates and untagged PrP^{Sc} inoculum, we sequentially passaged RML-inoculated Tg(WFP) brain homogenate into Tg(WFP$^{+/o}$) PrP$^{o/o}$ mice.

As controls, we injected RML into Tg(WFP$^{+/o}$) mice either on a PrP$^{+/+}$ or PrP-null background. Mice expressing endogenous PrP along with the transgene developed disease at 215 days, while mice on the null background remained healthy past 460 days (Table 2). These results are similar to previously published results (Barmada and Harris 2005). On the PrP$^{+/+}$ background, endogenous PrP^{C} is converted to infectious and toxic PrP^{Sc}, causing disease in Tg(WFP) PrP$^{+/+}$ animals. The WFP transgene is not converted at this initial inoculation and RML-inoculated Tg(WFP) PrP$^{o/o}$ mice remain disease-free. To ensure that injection of WFP molecules themselves would not cause disease, we inoculated Tg(WFP) PrP$^{o/o}$ mice with brain homogenate from non-injected Tg(WFP)

PrP$^{+/+}$ animals as negative controls. As expected, these mice did also not develop prion disease (Table 2).

To determine whether WFP^{Sc} could be generated after sequential passaging, we injected brain homogenates from RML-inoculated Tg(WFP$^{+/o}$) PrP$^{+/+}$ animals into Tg(WFP$^{+/o}$) recipients expressing only transgenic WFP and not endogenous PrP. We checked mice biweekly for ataxia, kyphosis, foot clasp, and hyperexcitability. Clinically, these mice did not develop any prion disease symptoms and remained healthy until death (Table 2), showing that sequential passaging did not produce clinical disease in mice.

Brain homogenates from these animals did not contain any aggregated PrP material, as demonstrated by a 15B3 immunoprecipitation assay (Figure 2A, lanes 3,4). WFP from the same samples seem to show mild resistance to protease K treatment (Figure 2B, lane 2), but these bands are not specific to WFP^{Sc}. This is demonstrated by lack of aggregated 15B3 material and by Western Blotting PK-treated brain homogenates with an α-GFP antibody (Figure 2C), which shows that although the ~30kDa GFP tag itself is PK-resistant when detached from PrP (Figure 2C, all lanes), no GFP-tagged PrP is detected at the 60-70kDa range. In contrast, RML-injected Tg(WFP) PrP$^{+/+}$ mice demonstrated aggregated PrP^{Sc} by both 15B3 immunoprecipitation (Figure 2A, lanes 7,8) , PK resistance (Figure 2B, lane 4), and exhibited infectivity *in vivo* (Table 2). The PrP^{Sc} here is derived solely from the non-tagged PrP^C, since WFP did not react with 15B3 (Figure 2A, lanes 7,8) was not detected by 15B3 reactivity nor PK-resistance (Figure 2B, lane 4).

These results reveal that WFP^{Sc} generation by a single round of sequential passaging was unsuccessful.

Table 2. Sequential passaging does not induce prion disease in Tg(WFP) animals.

Inoculum*	Recipient Genotype	Age of Onset (dpi)
RML	WFP$^{+/o}$ PrP$^{o/o}$	>460 (15/15)
RML-injected Tg(WFP$^{+/o}$)/PrP$^{+/+}$ brain homogenate	WFP$^{+/o}$ PrP$^{o/o}$	>451 (19/19)
Non-injected Tg(WFP$^{+/o}$)/PrP$^{+/+}$ brain homogenate	WFP$^{+/o}$ PrP$^{o/o}$	>399 (16/16)
RML	WFP$^{+/o}$ PrP$^{+/+}$	215±18 (13/13)
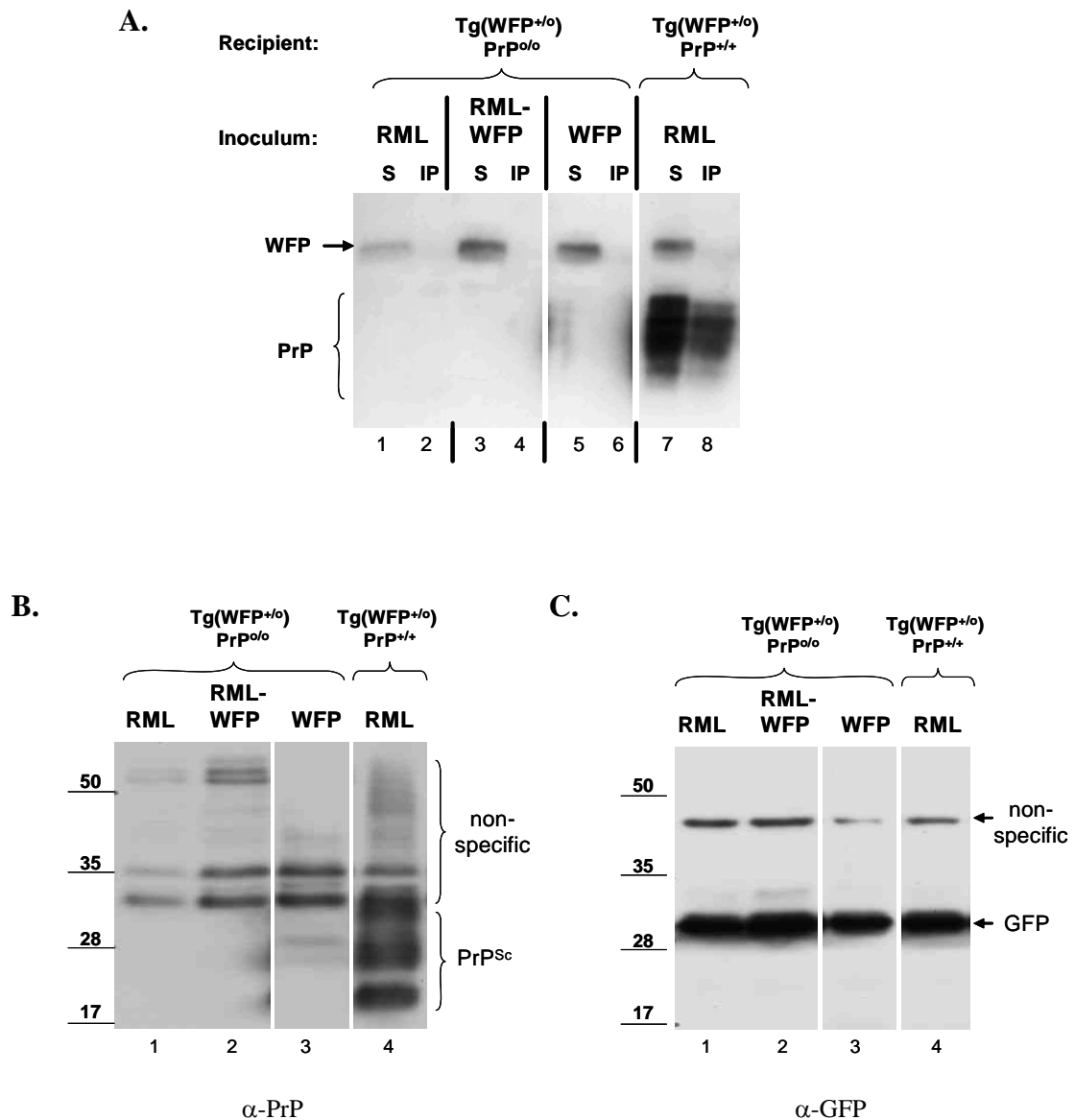
Figure 2. Sequential passaging of brain homogenates from inoculated Tg(WFP) mice does not produce WFP[Sc]. Brain homogenate from Tg(WFP+/o) PrPo/o mice inoculated with RML (lanes 1,2), RML passaged through Tg(WFP+/+) PrP+/+ mice (lanes 3,4), and untreated Tg(WFP+/+) PrP+/+ brain material (lanes 5,6) were subject to immunoprecipitation with aggregate PrP-specific antibody 15B3 (A). Brain homogenate from Tg(WFP+/o) PrP+/+ mice inoculated with RML were used as a positive control (lanes 7,8). Immunoprecipitated material (IP) was analyzed along with a fraction of the input solution (S) by Western blot. Only homogenates from mice injected with RML demonstrated reactivity with 15B3. Brain homogenates from the same samples were treated with 20μg/mL protease K, and analyzed by Western Blot with α-PrP antibody 6D11 (B) or α-GFP antibody (C). Brackets and arrows indicate non-specific bands, PrPSc, and the GFP tag when cleaved from PrP. Molecular weight is marked on the left in kilodaltons. Data in each of the panels are from the same gel, spliced for organizational purposes.

174

Injection of prion strain 22L into Tg(WFP) mice does not generate infectious, aggregated, PK-resistant WFP^{Sc}. Murine strains of scrapie differ in their incubation times, patterns of neuropathology, and rates of PrP^{Sc} accumulation. It was possible then, that another prion strain may be more successful for facilitating WFP conversion. The 22L strain was a prime candidate because of its ability to produce infection in a wide range of cell culture systems, including neuroblastoma and fibroblast cell lines (Nishida *et al.* 2000; Vorberg *et al.* 2004), as well as neuronal stem cells derived from embryonic mice (Milhavet *et al.* 2006). Additionally, 22L proved to be more robust in its ability to sustain persistent infection in fibroblast cell culture, whereas RML, ME7, and 87V strains could only prompt acute infection (Vorberg *et al.* 2004).

22L injection into wild-type PrP$^{+/+}$ mice, or non-transgenic littermates of Tg(WFP) mice, results in onset of scrapie symptoms at ~ 146 days (Table 1). 22L inoculation of mice expressing endogenous PrP^C as well as a single copy of the WFP transgene also succumbed to disease at a similar time, 124 ± 22 days. This time frame is not significantly different from non-transgenic PrP$^{+/+}$ animals inoculated with 22L, indicating that in this case, WFP did not act as an inhibitor of disease onset, as was the case in RML-injected animals (Barmada and Harris 2005). Like RML-induced disease, 22L prion illness progresses rapidly, with animals reaching terminal stages within seven days (data not shown). Tg(WFP) animals on the PrP null background were injected with 22L, but did not develop prion disease (Table 3).

Analysis of 22L-inoculated Tg(WFP$^{+/o}$) PrP$^{+/+}$ brain homogenates by 15B3-reactivity showed only the generation of PrP^{Sc}, but not WFP^{Sc} (Figure 3A, lanes 5,6). Additionally, WFP in brain homogenates from Tg(WFP$^{+/o}$) PrP$^{o/o}$ animals was not 15B3-

reactive (Figure 3A, lanes 7,8). 22L-injected PrP$^{+/+}$ positive controls showed the presence of aggregated PrP^{Sc} (Figure 3A, lanes 3,4), and injected PrP$^{o/o}$ negative controls did not express any PrP (Figure 3A, lanes 1,2).

PK-resistance assays also confirm that endogenous PrP^C can be converted to PrP^{Sc}, but WFP cannot (Figure 3b, lanes 2 vs 3, 4). The smear at the 50 kDa marker in lane 3 where WFP migrates is non-specific because it is also present in lane 2, which contains non-transgenic brain homogenate. No PK-resistant WFP^{Sc} was detected by α-PrP or α-GFP antibodies in brain homogenates of 22L-inoculated Tg(WFP)$^{+/o}$ PrP$^{o/o}$ mice (Fig 3B, lane 4 and Fig3C, lane 4). Some non-specific banding was seen in PrP knockout brain homogenate (Fig 3B, lane 1). These data demonstrate that Tg(WFP) inoculation with prion strain 22L does not induce conversion of the GFP-tagged protein.

A2.5 Discussion

We demonstrate here that fluorescently-tagged PrP fitted with an EGFP moiety at the C-terminal end is impervious to conversion to an infectious scrapie form *in vivo.* Our attempts to generate WFP^{Sc} by inoculation with prion strains RML and 22L, and by sequential passaging of RML-inoculated brain homogenate from Tg(WFP) mice, were unsuccessful. Difficulty in converting the WFP fusion protein is likely due to the addition of the EGFP tag, whose structural presence interferes with the conversion process.

Previous studies have demonstrated that sequence heterology between PrP^{Sc} and template PrP^C molecules can profoundly interfere with prion formation in cells and *in*

176

Table 3. 22L-inoculated Tg(WFP$^{+/o}$) mice do not acquire prion disease.

Inoculum	Recipient Genotype	Age of Onset
22L	PrP$^{+/+}$	146 ± 3 (11/11)
22L	PrP-EGFP$^{o/o}$ PrP$^{+/+}$ [a]	148 ± 17 (17/17)
22L	PrP-EGFP$^{+/o}$ PrP$^{+/+}$	124 ± 22 (5/5)
22L	PrP$^{o/o}$	> 379 (20/20)
22L	PrP-EGFP$^{+/o}$ PrP$^{o/o}$	> 264 (7/7)
22L	PrP-EGFP$^{+/+}$ PrP$^{o/o}$	> 469 (3/3)

[a] Non-transgenic littermates of Tg(PrP-EGFP$^{+/o}$)/PrP$^{+/+}$ animals.
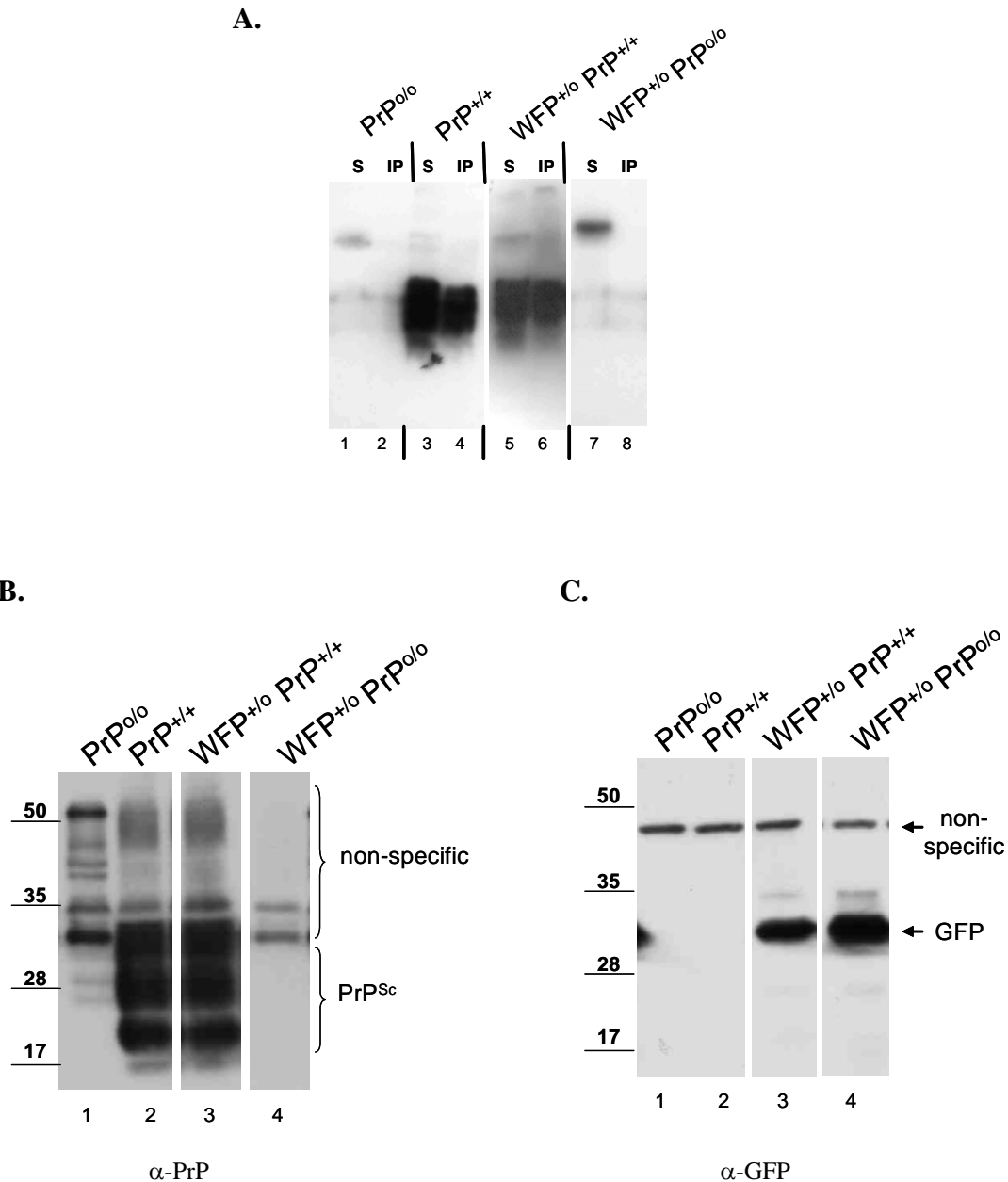
Figure 3. 22L-inoculated Tg(WFP) mice do not produce WFP^{Sc}. Brain homogenate from PrP knockout mice (lanes 1,2), wild-type mice (lanes 3,4), Tg(WFP+/o) PrP+/+ mice (lanes 5,6), and Tg(WFP+/o) PrPo/o mice, all inoculated with 22L prions, were subject to immunoprecipitation with aggregate PrP-specific antibody 15B3 (A). Immunoprecipitated material (IP) was analyzed along with a fraction of the input solution (S) by Western blot. Only homogenates from mice injected with RML demonstrated reactivity with 15B3. Brain homogenates from the same samples were treated with 20µg/mL protease K, and analyzed by Western Blot with α-PrP antibody 6D11 (B) or α-GFP antibody (C). Brackets and arrows indicate non-specific bands, PrPSc, and the GFP tag when cleaved from PrP. Molecular weight is marked on the left in kilodaltons. Data in each of the panels are from the same gel, spliced for organizational purposes.

vivo, sometimes even when the difference is a single amino acid (Priola et al. 1994; Horiuchi et al. 2000). This "species barrier" is thought to stem from a deficiency in either the initial binding step between heterologous PrP^{Sc} and PrP^{C} proteins, or the subsequent reaction whereby the PrP^{C} template undergoes the conformational rearrangement for transformation to PrP^{Sc}. WFP withstands structural reconformation to the WFP^{Sc} form even in the abundant presence of RML PrP^{Sc} (Figure 1 & Figure 2), but can physically interact and tag RML PrP^{Sc} (Barmada and Harris 2005). Thus, its conversion to WFP^{Sc} is likely impeded in a reaction that takes place after the initial binding step.

WFP binds to RML-PrP^{Sc} and acts as a dominant negative inhibitor of endogenous PrP^{C} conversion in mice expressing both WFP and PrP^{C}, as demonstrated by immunofluorescence studies in brain section showing accumulation of punctate fluorescent aggregates, and by the delayed onset of disease in RML-inoculated animals (Barmada and Harris 2005). The ability of WFP to bind with the 22L strain of PrP^{Sc} was not investigated by immunofluorescence. However, any significant interaction between the two molecules is unlikely, given that the presence of the WFP transgene did not interfere with 22L disease progression (Table 3). WFP is also unable to bind or inhibit PG14 familial prion disease (See Appendix 1). The ability for WFP to interfere with RML disease progression, but not 22L or PG14, is consistent with the idea that each PrP^{Sc} strain or aggregated PrP has a unique structure that leads to conformation-specific interactions with PrP^{C}. Possibly, RML PrP^{Sc} binds WFP with higher affinity than 22L PrP^{Sc}, resulting in the delay in endogenous PrP^{C} conversion. Although 22L was not able

to stimulate WFP conversion using this model system, we cannot rule out that other PrP^{Sc}

strains may be capable of inducing WFP re-conformation and aggregation.

Why is WFP resistant to conversion? There are several potential explanations.

EGFP folds into a stable barrel-like structure, composed of eleven β sheets and several α-

helices (Yang *et al.* 1996). The rigidity of the molecule may inhibit the range of

flexibility and fold of PrP^{C}, thus impeding structural reconformation of the protein. It is

also possible that inhibition is not related to the structure of the GFP protein, but its

placement at the C-terminal end of PrP^{C}. We chose to insert the tag at a location where

interference with proper PrP^{C} folding and localization would be minimal. The tag was

placed at codon 223 at the end of the third α-helix, to allow for GPI anchor attachment.

However, PrP^{C} conversion to PrP^{Sc} can be effectively blocked when PrP^{C} substrates are

incubated with an antibody directed toward PrP epitope 219-232 (Horiuchi and Caughey

1999), indicating that this area is crucial for proper PrP^{Sc}/PrP^{C} interaction and PrP^{C} re-

conformation. It is possible that WT PrP-EGFP conversion was restricted because the

GFP tag was placed directly within this epitope. Additionally, the GFP tag is flanked by

only 7 and 12 amino acids at the N- and C-terminal side, respectively. The linkers are

short, and are not designed specifically to give flexibility between PrP and the GFP motif.

Because of these factors, GFP may partially block PrP^{Sc} access to PrP^{C}, leading to

inefficient conversion. GFP may also deter intermolecular aggregation if oligomerization

is highly dependent on interlocking structures at PrP's C terminal end.

Alternate experiments with fusion proteins with variable GFP placement has been

attempted in cells and in yeast by our laboratory. GFP placement at the N-terminal end

of PrP^{C} reveals that a significant portion of proteins are cleaved, separating the tag and

PrP (Christensen, Westergard, & Harris, unpublished data). Because this separation may cause differential localization between GFP and GFP-tagged PrP, this construct is ill-suited to study PrP^{Sc} trafficking. We have constructed several other GFP-tagged PrP constructs, varying insertion site and linker lengths, to continue our endeavors to convert GFP-tagged PrP using a cell culture-based system, although none yet have demonstrated adoption of the scrapie conformation. Continued development of fluorescently tagged PrP^{Sc} technology will facilitate investigations into PrP^{Sc} routes of infection at both the physiologic and cellular levels, *in vivo* and in cell culture.

A2.6 References

Barmada, S., P. Piccardo, et al. (2004). "GFP-tagged prion protein is correctly localized and functionally active in the brains of transgenic mice." <u>Neurobiol Dis</u> **16**(3): 527-37.

Barmada, S. J. and D. A. Harris (2005). "Visualization of prion infection in transgenic mice expressing green fluorescent protein-tagged prion protein." <u>J Neurosci</u> **25**(24): 5824-32.

Biasini, E., M. E. Seegulam, et al. (2008). "Non-infectious aggregates of the prion protein react with several PrP(Sc)-directed antibodies." <u>J Neurochem</u>.

Bueler, H., A. Aguzzi, et al. (1993). "Mice devoid of PrP are resistant to scrapie." <u>Cell</u> **73**(7): 1339-47.

Bueler, H., M. Fischer, et al. (1992). "Normal development and behaviour of mice lacking the neuronal cell-surface PrP protein." <u>Nature</u> **356**(6370): 577-82.

Fevrier, B., D. Vilette, et al. (2004). "Cells release prions in association with exosomes." <u>Proc Natl Acad Sci U S A</u> **101**(26): 9683-8.

Fischer, M., T. Rulicke, et al. (1996). "Prion protein (PrP) with amino-proximal deletions restoring susceptibility of PrP knockout mice to scrapie." <u>Embo J</u> **15**(6): 1255-64.

Gousset, K., E. Schiff, et al. (2009). "Prions hijack tunnelling nanotubes for intercellular spread." <u>Nat Cell Biol</u> **11**(3): 328-36.

Gurke, S., J. F. Barroso, et al. (2008). "The art of cellular communication: tunneling nanotubes bridge the divide." <u>Histochem Cell Biol</u> **129**(5): 539-50.

Horiuchi, M. and B. Caughey (1999). "Specific binding of normal prion protein to the scrapie form via a localized domain initiates its conversion to the protease-resistant state." <u>Embo J</u> **18**(12): 3193-203.

Horiuchi, M., S. A. Priola, et al. (2000). "Interactions between heterologous forms of prion protein: binding, inhibition of conversion, and species barriers." <u>Proc Natl Acad Sci U S A</u> **97**(11): 5836-41.

Mabbott, N. A. and G. G. MacPherson (2006). "Prions and their lethal journey to the brain." <u>Nat Rev Microbiol</u> **4**(3): 201-11.

Manson, J. C., A. R. Clarke, et al. (1994). "129/Ola mice carrying a null mutation in PrP that abolishes mRNA production are developmentally normal." <u>Mol Neurobiol</u> **8**(2-3): 121-7.

Marijanovic, Z., A. Caputo, et al. (2009). "Identification of an intracellular site of prion conversion." <u>PLoS Pathog</u> **5**(5): e1000426.

Medrano, A. Z., S. J. Barmada, et al. (2008). "GFP-tagged mutant prion protein forms intra-axonal aggregates in transgenic mice." Neurobiol Dis **31**(1): 20-32.

Milhavet, O., D. Casanova, et al. (2006). "Neural stem cell model for prion propagation." Stem Cells **24**(10): 2284-91.

Moroncini, G., N. Kanu, et al. (2004). "Motif-grafted antibodies containing the replicative interface of cellular PrP are specific for PrPSc." Proc Natl Acad Sci U S A **101**(28): 10404-9.

Nishida, N., D. A. Harris, et al. (2000). "Successful transmission of three mouse-adapted scrapie strains to murine neuroblastoma cell lines overexpressing wild-type mouse prion protein." J Virol **74**(1): 320-5.

Pankiewicz, J., F. Prelli, et al. (2006). "Clearance and prevention of prion infection in cell culture by anti-PrP antibodies." Eur. J. Neurosci. **23**(10): 2635-2647.

Priola, S. A., B. Caughey, et al. (1994). "Heterologous PrP molecules interfere with accumulation of protease-resistant PrP in scrapie-infected murine neuroblastoma cells." J Virol **68**(8): 4873-8.

Schatzl, H. M., L. Laszlo, et al. (1997). "A hypothalamic neuronal cell line persistently infected with scrapie prions exhibits apoptosis." J Virol **71**(11): 8821-31.

Vorberg, I., A. Raines, et al. (2004). "Acute formation of protease-resistant prion protein does not always lead to persistent scrapie infection in vitro." J Biol Chem **279**(28): 29218-25.

Weissmann, C., M. Enari, et al. (2002). "Transmission of prions." J Infect Dis **186 Suppl 2**: S157-65.

Yang, F., L. G. Moss, et al. (1996). "The molecular structure of green fluorescent protein." Nat Biotechnol **14**(10): 1246-51.

APPENDIX 3

PrP-EGFP Axonal Transport Studies

A3.1 Introduction

Prion protein (PrP), a cell surface glycoprotein of unknown function, is located along the plasma membrane of cell soma and axons of neurons, and at the presynaptic terminal. Expression of mutant PrP containing an expansion of the octapeptide repeat region, designated PG14, causes spontaneous neurological illness in both mice and humans. Evidence demonstrating PG14 aggregation along axons suggest that PG14 aggregates may be forming axonal blockages, which hinder normal transport of proteins to and from the synapse. I hypothesized that PG14 aggregation within neurons causes blockages that disrupt normal axonal transport of synaptic proteins, which then contributes to inherited prion disease.

In order to test this theory in primary neurons, I attempted to measure anterograde and retrograde rates of EGFP-tagged WT PrP and EGFP-tagged PG14 PrP transport via live imaging microscopy of cultured neurons. There are two main branches to this project: the first is setting up the cultures for imaging, and the second is imaging and analysis. Below I describe in mainly chronological order the progress achieved for each branch, and the factors that ultimately limited further advancement of the project.

A3.2 Materials & Methods

Cerebellar granule neuron (CGN) cultures. CGNs were isolated from 4 day old mouse pups according to methods described previously (Miller and Johnson 1996). Neurons were plated in CGN medium (basal medium Eagle's with Earle's salts, 10% fetal calf serum, 2 mM glutamine, 25 mM KCl, 0.1 mg/ml gentamycin). Cells were

plated at a density of 375,000-450,000/cm^2 onto 35 mm glass-bottom dishes pre-coated with poly-D-lysine.

Hippocampal Cultures (Mennerick Lab). Hippocampal cells were isolated from mouse pups similar to methods described previously (Mennerick et al. 1995). Hippocampi were dissected from animals within 1 day of age, sliced into 500μm-thick transverse sections, and then digested by 20 minute immersion at 37°C in an oxygenated solution containing 1 mg/mL papain in Leibovitz L-15 medium. Hippocampi were then triturated in modified Eagle's medium containing 5% horse serum, 5% fetal calf serum, 17mm D-glucose, 400 μM glutamine, and antibiotics penicillin and strepotomycin, by passage through a flame-polished glass pipette. Cells were plated in the same modified Eagle's medium at a density of 1500 cells/mm^2 onto glass coverslip-bottom 35 mm dishes pre-coated with collagen microdroplets sprayed onto a layer of 0.15% agarose. Each dish was then supplemented with Insulin-Transferrin-Sodium Selenite (ITSS). Aphidicolin was added on the third day post-culture to minimize glial proliferation.

Hippocampal Cultures (Goldstein Lab). Hippocampi were dissected from animals within 1 day of age, then transferred into cold Hank's buffer solution modified to include D-glucose, HEPES, and antibiotics. Hippocampi were digested in PBS containing 10U/mL papain solution, for 10 min at 37°C. 0.05% DNAseI was added to stop digestion. Hippocampi were shaken at 100rpm at 37°C for 20 min, washed twice with Dulbecco's Modified Eagle Medium (DMEM), then triturated in the same DMEM using a plastic 1 mL pipette tip. Cells were allowed to settle to the bottom of the tube for 3 minutes and supernatant was transferred to collect only single-cell suspension. Cells were plated at 200,000/cells per well onto coverslips within a 24-well dish. Coverslips

had been pre-sterilized with acetone, ethanol, and sterile ddH$_2$O washes, followed by coating with poly-L-lysine. Three hours post-plating, media was replaced with Neurobasal-A/B27 supplemented with 0.5 μM L-glutamine.

Dorsal Root Ganglia (DRG) Cultures. Embryonic day 13 pups were removed from the maternal uterus, then cleaned in DMEM. Pups were decapitated, and DRGs were obtained by first isolating the spinal cord, then plucking DRGs directly from the spinal cord. For explant cultures, DRGs were placed directly into 24-well plates pre-coated with poly-D-lysine and laminin at 1-2 DRG explants/well, in media containing DMEM supplemented with 10% fetal bovine serum, 50 ng/mL nerve growth factor, and penicillin & streptomycin. For dissociated cultures, DRGs were dissociated by a 25 minute incubation with trypsin at 37°C, then triturated using a 1 mL pipette tip. Cells were plated onto 24-well dishes pre-coated with matrigel, using Neurobasal media supplemented with 1:50 B27 and 50ng/mL nerve growth factor. For both explant and dissociated cultures, aphidicolin was added at 24 hours to prevent glial cell proliferation.

Transfection. Lipofectamine 2000 (Invitrogen) was used to transfect primary neuronal cultures with PrP-EGFP and EGFP-PrP constructs within the pCDNA3.1(+) Hygro plasmid, as per protocol provided by the manufacturer.

Lentiviral Preparation & Transduction. Construction of N-terminally tagged EGFP-WT PrP and EGFP-PG14 has been described previously (Medrano et al. 2008). Constructs were subcloned into lentiviral plasmid pRRLsinCMV by PCR and restriction enzyme digest. HEK293 cells were transfected with this plasmid, along with viral plasmids pMD-G, pMD-LG, and REV, using Lipofectamine 2000 (Invitrogen) as per

187

protocol supplied by the manufacturer. Cells were incubated for 48 hours, after which supernatant was collected and used to transduce DRG dissociated cultures.

Microscopy and image analysis. Primary neurons were imaged in the living state using a Zeiss LSM 510 inverted confocal microscope with an Axiovert 200 laser scanning system using LSM Image Browser software. For kymograph analysis, we used a Nikon TE-2000E inverted fluorescence microscope, and images were captured and analyzed with Metamorph imaging software.

A3.3 Results

Primary Cultures from Transgenic Mice. The first attempts to track EGFP-tagged PrP particles were in cerebellar granule cells cultured from Tg(WT-EGFP) line A mice and Tg(PG14-EGFP) line X mice. The protocol we use fosters neuritic extension and growth in CGNs in primary culture, but does not stimulate differentiation into axons and dendrites. Using confocal microscopy, I was able to easily observe both stationary and moving particles within or on neurites of CGNs from Tg(PG14-EGFP) primary cultures (Figure 1). In contrast, WT-EGFP was much more difficult to image. On one (and only one) rare case was I able to track what was presumably a moving WT-EGFP particle in CGN neurites (Figure 1). This movie was obtained only after dozens of hours on the confocal and days/weeks spent culturing CGNs.

Movies were obtained by capturing images at regular intervals over the course of 3 to 5 minutes. CGNs were able to survive at room temperature without CO_2 regulation for approximately 10 min, after which they began to visibly deteriorate. Several attempts to use heating stages and a microscope-fitted apparatus for CO_2 regulation were unsuccessful at extending CGN culture longevity.

188
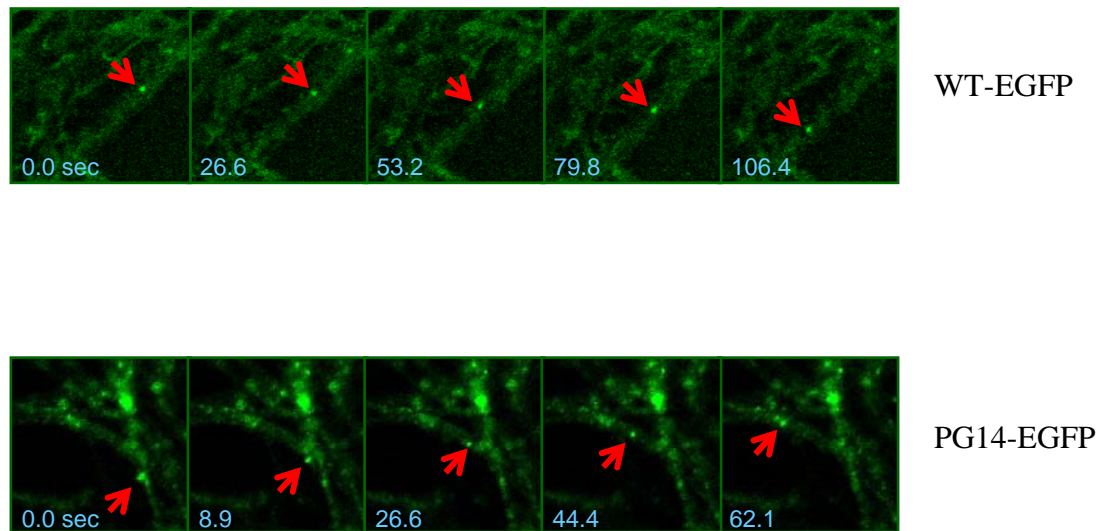
WT-EGFP

PG14-EGFP

Figure 1. Axonal Transport in CGNs. Mobile fluorescent particles (red arrows), presumably corresponding to PrP-EGFP traveling in vesicles, were observed in CGNs cultured from WT-EGFP (top panels) and PG14-EGFP (bottom panels). Images of the same field were recorded at different time points (indicated in blue, seconds)

Upon capturing movies, several difficulties were at once evident. First, WT-EGFP molecules coated the surface of CGN neurites, thus making visualization of any distinct particles within the extensions near impossible. This continued to be one of the main difficulties encountered throughout this project. Attempts to clear peripheral WT-EGFP by PIPLC cleavage was unsuccessful. Enzymatic cleavage seemed incomplete, leaving many fluorescent puncta on the neurites which were stationary. These were presumably not intracellular vesicles being shuttled within neurites because the majority of fluorescent puncta were stationary. I was unable to distinguish between what was vesicular and what was cell surface PrP. In contrast, because PG14 does not reach the cell surface, intracellular fluorescent puncta could easily be observed, in both stationary and mobile forms.

A second technical problem came from the fact that the CGN cultures had to be grown at high densities in order to survive *ex vivo*. This led to a dense meshwork of overlapping neurites crisscrossing at wildly variable angles, making particle tracking extremely difficult. Neurites were packed so tightly that they could not easily be defined even by phase contrast. I attempted to troubleshoot this difficulty by 1) culturing CGNs at lower densities, and 2) diluting transgene-positive CGNs with non-fluorescent transgene-negative CGNs at 1:10, 1:100, and 1:1000. Culturing CGNs at lower density led to poor cell survival and overall neuronal health. Diluting fluorescent cells onto non-fluorescent cells resulted in healthy cultures, but no detectable fluorescence. The reason for loss of fluorescence may be due in part to the fact that C-terminally tagged PrP-EGFP constructs are very dim (leading to lower signal to noise ratios), or because overlapping from non-fluorescent neurites prevented excitation of hidden GFP-laden neurites.

Given the relative dimness of constructs and over-crowding of neurites, we decided to explore other cell culture systems to use as models of axon-specific transport. I tried culturing hippocampal neurons first, which have the ability to differentiate into dendrites and axons in culture, and can be grown at low enough densities for imaging and particle tracking. The two main protocols I worked with came from the labs of Steve Mennerick and Larry Goldstein. These procedures were accomplished with post-natal pups, and were easier to work with compared with protocols that required pre-natal pups, because no mothers had to be sacrificed.

A technician named Ann Benz from Steve Mennerick's lab was able to help me culture hippocampal cells derived from Tg(WT-EGFP) and Tg(PG14-EGFP) mice. The result was that WT-EGFP, but not PG14-EGFP molecules, were detectable above background (Figure 2A). The protocol from postdoc Sandra Encalada in Larry Goldstein's lab was high maintenance, with very finicky outcomes in terms of culture survival. I was unable to culture neurons reliably using this protocol, and Sandra herself admitted to the same.

Dorsal root ganglia (DRGs) are pseudo-monopolar cells that extend a single bifurcated axon both *in vivo* and in cell culture. With the help of MSTP student Craig Press from Jeff Milbrandt's lab, I was able to successfully culture DRGs from E13 pups routinely, as both explants and dissociated cultures. Because DRGs extend only one forked axon, neuritic meshwork is not a problem, and the cultures could be grown at low enough densities that each axon could be traced to a cell body for retrograde/anterograde orientation. However, DRG explants harvested from Tg(PrP-EGFP) mice demonstrated that WT-EGFP was only dimly fluorescent, and that PG14-EGFP was not detectable over

background (data not shown). Inability to detect PG14-EGFP in hippocampal neurons and DRGs from Tg(PG14-EGFP) animals is likely due to the low expression level in these mice.

Cell Transfection & Transduction of PrP-EGFP and EGFP-PrP. Because neurons obtained from the Tg(PrP-EGFP) mice did not express high enough levels of fluorescent protein for detection in these cell systems, I tried introducing EGFP-tagged PrP into primary neurons cultured from non-transgenic animals via transfection. This method had been initially used by the Goldstein lab in their efforts to determine whether kinesin I was the main motor responsible for PrP axonal transport. Preliminary findings from their lab were shared at a conference in 2005 (Encalada *et al.* 2008), but more complete findings have yet to be published.

In these experiments, I used N-terminally-tagged EGFP-PrP constructs driven by a CMV promoter to increase protein expression for better fluorescence detection. N-terminally-tagged constructs are, in general, brighter than the C-terminally tagged PrP-EGFP molecules used in the transgenic mice. However, it was also discovered at the time that significant fractions of EGFP-PrP are cleaved at the junction connecting the fluorescent tag and the PrP protein. Because large pools of EGFP molecules were separate from their PrP substrates, it became unreliable to use this construct to accurately track fluorescent PrP particles without confusing them for cleaved GFP particles. To add injury to insult, neurons had very poor survival outcomes post-transfection.

I then generated lentiviral constructs carrying WT-EGFP and PG14-EGFP fusion proteins and transduced these into DRGs. I had concurrently made lentivirus carrying

A. Hippocampal Neurons
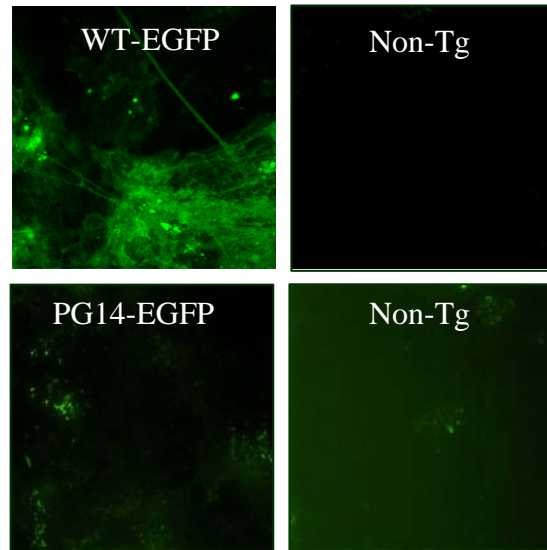
B. DRGs
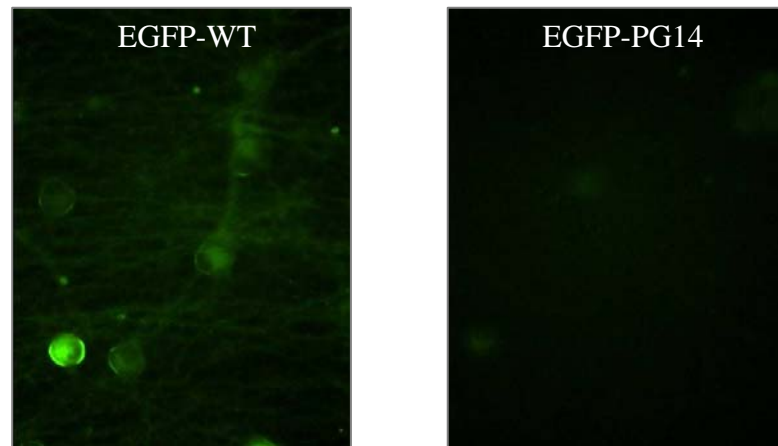
Figure 2. EGFP-tagged PrPs in hippocampal cells and DRGs. (A) Hippocampal neurons derived from transgenic mice expressing WT-EGFP(top left panel), PG14-EGFP (bottom left panel), or from non-transgenic littermates (right panels) were cultured, then analyzed by fluorescence microscopy. Fluorescent signal above background could be detected in cells expressing WT-EGFP, but not PG14-EGFP. (B) DRGs were transduced with lentivirus carrying N-terminally tagged EGFP-WT (left panel) or EGFP-PG14 (right panel). Expression of EGFP-WT could be detected mainly in the soma of DRGs, but EGFP-PG14 expression was not detected.

DNA encoding only cytosolic GFP as a positive control. I exposed dissociated DRG

cultures to several serial dilutions of low-titer lentivirus (from supernatant of packaging

HEK293 cells) and found that DRGs expressed cytosolic GFP very well. At high titers,

WT-EGFP expressed well enough to detect a dim fluorescence over background, but

PG14-EGFP could not be detected with fluorescence microscopy (Figure 2B). Part of the

reason is likely due to the repeated observation that PG14 constructs in general are

expressed at lower levels than WT PrP constructs.

A3.4 Discussion

Several large technical difficulties hinder the progress of this project. The first

and most formidable difficulty is establishing a suitable assay in which to measure axonal

transport. Multiple obstacles include: 1) the fluorescence intensity of C-terminally

tagged PrP-EGFP fusion proteins are extremely dim and can be difficult to detect and

measure; 2) WT PrP coats the surface of the neurites, obstructing the view of any moving

intracellular particles; 3) anterograde and retrograde directions are difficult to distinguish

in some cultures, as neurites are not easily traceable to a cell body of origin, and 4)

imaging live neurons can be difficult, as they are very sensitive to the temperature and

CO_2 levels of their environment.

Assuming successful resolutions can be found and applied to the technical

challenges of the project, there are several experiments that could test whether mutant

PrP PG14 aggregates induce axonal blockage. The first would be to measure rates of

transport of WT and PG14 protein particles, then compare the average velocity in the

anterograde and retrograde directions. Additionally, particles could be counted and

classified as moving or stationary. A decreased average particle speed, or decreased percentage of mobile particles, in PG14-expressing cells would suggest deficiencies in axonal transport. A second experiment involving measuring speeds of fluorescently-tagged synaptic vesicle proteins, i.e. synaptophysin, co-transfected with either WT PrP or PG14, would help determine whether axonal transport of non-PrP proteins is affected by mutant PrP expression as well. These investigations could be conducted at either steady-state in fully mature neurons, or in developing cells in the process of polarization. Because WT PrP has been implicated in axon development and regeneration (Sales et al. 2002; Moya et al. 2005, and see Introduction), it would be interesting to know whether expression of a PrP mutant would interfere with this process.

A3.5 References

Encalada, S. E., K. L. Moya, et al. (2008). "The role of the prion protein in the molecular basis for synaptic plasticity and nervous system development." J Mol Neurosci **34**(1): 9-15.

Medrano, A. Z., S. J. Barmada, et al. (2008). "GFP-tagged mutant prion protein forms intra-axonal aggregates in transgenic mice." Neurobiol Dis **31**(1): 20-32.

Mennerick, S., J. Que, et al. (1995). "Passive and synaptic properties of hippocampal neurons grown in microcultures and in mass cultures." J Neurophysiol **73**(1): 320-32.

Miller, T. M. and E. M. Johnson, Jr. (1996). "Metabolic and genetic analyses of apoptosis in potassium/serum-deprived rat cerebellar granule cells." J. Neurosci. **16**(23): 7487-7495.

Moya, K. L., R. Hassig, et al. (2005). "Axonal transport of the cellular prion protein is increased during axon regeneration." J Neurochem **92**(5): 1044-53.

Sales, N., R. Hassig, et al. (2002). "Developmental expression of the cellular prion protein in elongating axons." Eur J Neurosci **15**(7): 1163-77.